NASA CR-114687

THE EFFECT OF ENGINE COMPONENT NOISE ON V/STOL AIRCRAFT NOISE CONTOURS

by

R.G. FOGG

GENERAL ELECTRIC COMPANY

prepared for

NATIONAL AERONAUTICS AND SPACE ADMINISTRATION

NASA - Ames Research Center

CONTRACT NAS2-5462

1. Report No.	2. Government Accession No.	3. Recipient's Catalog No.
NASA CR-114687		

4. Title and Subtitle	5. Report Date
THE EFFECT OF ENGINE COMPONENT NOISE ON V/STOL AIRCRAFT NOISE CONTOURS	February 1974
	6. Performing Organization Code

7. Author(s)	8. Performing Organization Report No.
R. G. Fogg	R73 AEG 306
	10. Work Unit No.

9. Performing Organization Name and Address	11. Contract or Grant No.
General Electric Company Evendale, Ohio 45215	NAS2-5462
	13. Type of Report and Period Covered
12. Sponsoring Agency Name and Address	Contractor Report
National Aeronautics and Space Administration Washington, D. C. 20546	14. Sponsoring Agency Code

15. Supplementary Notes

Project Manager, D. H. Hickey, NASA Ames Research Center
Moffett Field, California 94035

16. Abstract

An analytical study of fly-over noise using noise contours to show the effects of varying airplane and path parameters. The method of approach was to synthesize engine component noise spectra and exercise these components along given flight paths to measure the individual and total fly-over effect as a function of noise footprint area.

The study was carried out in two phases. Phase I utilized a research type aircraft and Phase II used an advanced VTOL aircraft. The effect of cross flow was considered for both inlet and exhaust sections of the engine.

17. Key Words (Suggested by Author(s))	18. Distribution Statement
V/STOL Aircraft Noise Contours	

19. Security Classif. (of this report)	20. Security Classif. (of this page)	21. No. of Pages	22. Price*
Unclassified	Unclassified	116	$9.00

* For sale by the National Technical Information Service, Springfield, Virginia 22151

Table of Contents

List of Tables and Figures

List of Tables and Figures - Continued

List of Tables and Figures - Continued

List of Tables and Figures - Continued

I. SUMMARY

As instructed in Task V of NASA Ames contract NAS2-5462 an analytical study of fly-over noise was carried out using noise contours to show the effects of varying airplane and path parameters. The method of approach was to synthesize engine component noise spectra and exercise these components along given flight paths to measure the individual and total fly-over effect as a function of noise footprint area.

The study was carried out in two phases. Engine component noise was held the same for both phases. The difference was that Phase I utilized a lift fan commercial transport aircraft operated along two different paths. Phase II used a lift-lift/cruise fan commercial transport aircraft and was restricted to only one path. The effect of cross-flow was considered for both inlet and exhaust sections of the engine.

Some significant conclusions were:

1. Fan exhaust radiated noise is the loudest noise contributor of the five components considered.
2. Total area within a contour is sensitive to the flight path and was minimized using the long vertical rise and descent.
3. Cross flow effects can increase component noise one to two PNdB.
4. Trade-off's available in flight speed, power plant exhaust vector angle, and aircraft flight trajectory can result in significant changes in noise contours.

II. INTRODUCTION

Historically the General Electric Company Flight Propulsion Division has carried out design studies, component tests, and manufacture of experimental lift fan propulsion units. A recent lift fan study designated LF460 was carried out to support an application for a small intercity transport. This work was performed for NASA Ames under contract NAS2-5462.

In addition to the engine design effort noise characteristics were predicted and an analysis carried out using these characteristics to predict fly-over noise with the lift fan installed in specific aircraft. This report presents a description and results of the fly-over noise study.

III. CALCULATION TECHNIQUES

To identify the effects of significant engine noise sources produced by operation of V/STOL aircraft during the take-off and landing configurations, a sophisticated calculation procedure was required to predict the individual noise sources and combine them in the correct sequence. Since large amounts of data in the form of noise spectra are handled and many of the calculations are repetitive, the use of computer calculation procedures was necessary. Consequently existing fly-over noise computer programs were modified to suit the needs of this study.

One revision was to prepare a mathematical model to calculate the effect of jet noise generation of a flow of air moving across the jet nozzle and perpendicular to its axis. This effect was considered to be significant in the case of the V/STOL aircraft since the lift fan exhaust was in some cases at an angle to the fuselage axis and thus subject to considerable cross-flow. Calculation of this effect was made as part of the fly-over noise calculation since a continuous evaluation of the aircraft forward motion was required. Typical corrections are shown in Figure 1. The corrections in the form of delta dB are a function of jet exhaust velocity and cross-flow velocity. The cross-flow calculation method is presented in Reference 1.

A second revision to the existing computer program, similar to the effect of cross-wind on the exhaust jet noise, was to adjust for flow across the lift fan inlet. The adjustment took the form of an incremental change to the fan fundamental as a function of fan tip speed and aircraft forward speed. Test data was used as the basis of identifying this adjustment factor. A typical adjustment schedule is shown in Figure 2. The details as to how this adjustment schedule was generated are presented in Reference 2.

A third necessary revision to the computer program was to increase the capacity of the fly-over noise calculation routines. Due to the presence of several noise sources such as lift fans, cruise fans, and gas generator, a variety of different noise producing components are present. These components also have the capability of varying their thrust axis with respect to the fuselage centerline as well as increasing or decreasing power on an individual basis.

Consequently the computer program was expanded to accommodate the necessary variables. Computer subroutines used to calculate the noise contour coordinates were adapted for use with the expanded program.

Computer techniques for handling component noise prediction were generally available. However, some specialized options and methods of mechanically handling large amounts of information were instituted for this study. Consequently the computer program was expanded to accommodate the necessary variables. Computer subroutines used to calculate the noise contour coordinates were adapted for use with the expanded program.

Computer techniques for handling component noise prediction were generally available. However some specialized options and methods of mechanically handling large amounts of information were instituted for this study.

The noise contour coordinates were prepared using an interitative technique. From a specific runway centerline position an initial approximation of the contour sideline coordinate was made using a sideline distance - EPNL schedule based on previous experience with noise contour calculations. Spreading out from this initial point, fly-over calculations were performed until sufficient calculations were made at listening (microphone) locations which bracketed the desired contours. The exact contour coordinate was then calculated by interpolating between the known points.

The fly-over noise calculation is made by placing the listening microphone at a specific location on the ground plane. The engine noise source mounted on the aircraft traverses a given trajectory such as the climb or approach path. The noise is then predicted at the microphone at specific time intervals based on separation distance and angle orientation. Noise is attenuated by a distance correction; the spherical divergence, an atmospheric correction factor, and an EGA factor applied over that portion of the separation distance that lies within a 100 foot boundary layer from the ground.

It was also assumed that the full volume of noise from all engines is heard by the ground microphone and that no noise reduction occurs from fuselage shielding.

IV. ENGINE COMPONENT NOISE

The basic propulsion unit used for this study is the LF460 lift fan. A comprehensive design study was carried out on this power plant and is described in Reference 3. The engine design study provided mechanical design, aero-thermal analysis, performance data, and a noise analysis. The noise analysis described general noise characteristics, noise generating mechanisms and suggestions for noise suppression. The engine study was not limited to a lift fan configuration but also included analysis of the engine components configured as a cruise fan with a swiveled nozzle for additional vertical lift at take-off.

In order to carry out the detailed analysis for the contour study it was necessary to predict noise spectra for the various engine components. Five specific components were chosen and are listed below:

1. Fan inlet radiated noise.
2. Fan exhaust radiated noise
3. Compressor inlet radiated noise
4. The combined jet noise from the fan exhaust and tip turbine exhaust.
5. Tip turbine turbomachinery noise.

Existing General Electric, acoustic engineering prediction techniques were utilized to prepare the component noise spectrum using aero-thermodynamic data from the engine design study.

It is noted that some size scaling was accomplished from the original LF460 design. The designated aircraft take-off gross weight of the original or Phase I research aircraft was 51,500 lbs. This aircraft had four lift fans installed. It was also assumed that for safe operation an excess of thrust to weight of ten percent was required. Consequently, at lift-off an individual engine thrust of 14,200 lbs. is needed. In addition to the required lift-off thrust a 20% increment is required for safety considerations and engine out control. The noise rating point, however, was referred to the "most used" or "working" lift-off thrust value of 14,200 lbs. and this value is referenced to the lift fan as 80 percent of maximum available thrust. The component noise then is based on the LF460 reference design scaled in the ratio of 14,200/12,200 = 1.165. Scaled engine thermodynamic cycle parameters are presented as Table I.

Since the power plant components used in both the Phase I and Phase II sections of this contour study are from the same family of power plants the basic noise spectra are applicable for both phases of the study.

V. AIRCRAFT CHARACTERISTICS

A. Lift Fan Aircraft

The aircraft used in Phase I of this study was a vehicle representing the pure lift fan approach to commercial VTOL. The vehicle incorporates four lift fans with exit louvers and mounted in large pods on the wing with their respective gas generators. A plan view of the aircraft is shown on Figure 3. Figure 4 defines the thrust vector angle. Take-off gross weight for this Phase I aircraft was assigned as 51,500 pounds. The power plants were sized using the rule that 20% of the thrust must be reserved for emergency control purposes and a 10% excess of thrust over take-off gross weight is required at lift-off. Consequently the nominal take-off operating power required is 80% of full power. This 80% power point was specifiedas the noise rating point and is therefore defined for purposes of our noise analysis as a power setting of unity.

To exercise the noise characteristics of the Phase I aircraft two flight paths were selected. The first was a short vertical rise with a shallow climb and gradually increasing speed. The second was a long vertical rise, a horizontal sprint for rapid acceleration, and nominal climb out. Two compatible landing paths were also considered. The first path utilized a short vertical descent and the second followed a long vertical descent. Each path had its own unique speed schedule, lift fan exhaust louver schedule, aircraft attitude schedule, and engine power setting schedule. These schedules are presented on Figures 5 through 24.

B. Lift-Cruise Fan Aircraft

For Phase II of the study an aircraft with lift cruise fans installed as well as lift fans was chosen for examination. A general arrangement of the aircraft is shown on Figure 25. Four lift fans, two mounted on the wings and two mounted on the fuselage are installed. Two lift cruise fans are mounted on the aft fuselage location replacing the conventional power plants and are capable of supplementing vertical lift during the take-off and landing operation. The cruise fans have swivel nozzles with a fixed inlet oriented along the fuselage centerline. The cruise fan gas generators are mounted close to the cruise fans along the fuselage axis. Since the cruise power plant inlets

have a horizontal orientation it was assumed no distortion occurred due to crossflow. The lift fans are mounted so that the inlet is oriented perpendicular to the fuselage centerline. The lift fan exhaust is directed through a set of louvers. The lift fan gas generators are mounted such that their inlets are somewhat shielded from the ground. Consequently, the assumption was made that they do not contribute to the overall noise. A detail schedule of engine component operations is presented on Table II.

The aircraft flight path characteristics are presented on Figures 26 through 35. Both take-off and approach have a 500 foot vertical trajectory at the brake release and touch-down point with a gradually increasing climb or descent from the 500 foot altitude point.

The engines used on the second aircraft in Phase II of the study are assumed to be the same family used on the Phase I aircraft so that no new noise spectra calculations were required. Since the Phase II aircraft is assisted in vertical thrust with two swivel nozzle cruise engines it was assumed that the take-off gross weight was 42 percent greater than the Phase I aircraft.

VI. AIRCRAFT NOISE CONTOURS

A. Phase I Aircraft

In Phase I of the study, calculations were performed for two path trajectories with corresponding schedules for changes of aircraft and engine characteristics. The primary difference in the paths was the length of the vertical rise or descent. These differences produced the most significant changes when comparing the noise contours calculated from the two paths. Both PNL and EPNL contours have been prepared and the take-off plots are shown on Figures 36 through 39. Both the PNL and EPNL contours show similar characteristics. When the aircraft is flown along the path with the high vertical rise more area is enclosed for a given noise level in the vicinity of the brake release point than for the flight with the short vertical rise. As the aircraft continues along the flight path the noise contours move out and uncover additional noise area for both the high rise and low rise trajectories. Continuing to monitor the noise effect as the aircraft continues its flight, the contours resulting from the high rise path start to close early. For example, the 95 and 100 PNL take-off contours show a sideline distance reduction starting at the 2000 foot mark due primarily to power reduction and the increased separation distance from the ground. The low rise path in contrast shows steadily increasing contour coordinates from the combined effects of the aircraft rising out of the attenuation from ground effect, rear angles of the component noise spectra are uncovered, and the added increment from cross-flow effect due to increased velocity. For this low rise path, the contour shows a rapid closing trend when power cutback is initiated and the climb path steepens. The net result is considerably more area enclosed by the low rise path in contrast to the high rise path for a given PNL or EPNL value. A second significant conclusion is that the maximum sideline value of the noise contour is about the same for either path. However this maximum point occurs at different locations along the projected flight track.

To highlight the comparison of contour area calculated for the low rise and high rise take-off paths figure 40 presents the 95 PNL contours replotted on the same graph. The graph visually confirms the previous discussion.

The approach contours are presented on figures 41 through 44. Corresponding to the high and low vertical rise take-off paths two approach paths were examined

considering a high and low vertical descent. The noise contours show that with the shorter separation distances experienced during the low vertical descent path the contours are elongated in shape and cover considerably more area than the contours resulting from the high vertical descent.

Figure 45 presents a comparison of the 95 EPNL contours replotted on the same graph. This comparison dramatically shows the concentrated noise pattern for the long descent path.

B. Phase II Aircraft

Due to the many variables in the noise generation the location in three-dimensional space of the aircraft or noise source is important when a specific noise is generated that determines an important contour location. Figure 46 qualitatively shows these aircraft space locations and is presented as a reference in the following contour discussion.

Figure 47 presents the take-off PNL contour for three PNL values. The maximum sideline distance for the 95 PNL contour is 1330 feet and is determined while the aircraft is at the top of the vertical ascent made with the engines at maximum VTOL allowable power. The controlling noise component is from the wing lift fan exhaust radiated noise which presents an acoustic angle of 111 degrees. Note that the aircraft has reached an altitude where the acoustic angle for maximum PNL has been exposed. This effect coupled with increased speed produces the maximum noise value. Further travel along the flight track increases the range and attenuates the noise for a reduction in PNL.

The 95 PNL closure point occurs at a point 2100 feet down the runway. The controlling noise component is still the fan exhaust radiated noise component. As the aircraft moves along the flight track, the path parameters have stabilized and the controlling factor is range which is steadily increasing with resulting contour closure.

Figure 48 presents the approach contour for three PNL valves. In the approach operation, the lift fan exhaust noise component has the largest single value and thus the greatest effect on overall noise. The maximum sideline value of the 95 PNL contour occurs at 1240 feet. The aircraft is still about 250 feet from the vertical descent point with the engines at a power setting less than 0.7.

The apparent inconsistency of maximum sideline noise occurring when the separation distance is larger and power setting less than other aircraft-microphone combinations is explained by examining the cross flow adjustment factors. As the aircraft approaches the vertical descent point, the speed is reduced and the effect of cross-flow on noise also reduces allowing a PNL reduction.

The PNL closure point occurs at a point 3250 feet outbound from the touchdown point. All path parameters have stabilized and the closure represents the effect of increasing range.

C. Phase I and Phase II Comparison

Figure 49 presents a comparison of the contour area for the Phase I and Phase II take-off operation on the basis of PNL. The full lines show the comparison on the as calculated basis using aircraft with different gross weights. The dotted line presents an approximation with the noise values adjusted so that the Phase II aircraft has the same gross weight as the Phase I aircraft. The difference between Phase I results and the adjusted Phase II results is primarily due to the difference in flight paths. Secondary differences in the noise contours can be traced to variations in speed, vector angles, and engine component combinations which show that the parameters available in VTOL aircraft operation may be used to influence the noise signature.

Figure 50 presents a similar comparison for the approach operation. In this case the flight paths show very little difference and the adjusted Phase II schedule of area is coincident with the Phase I except for the lower noise values.

VII. NOISE COMPONENT ANALYSIS

The location of a particular contour coordinate is the result of interaction between a number of parameters such as spectra directivity, range, altitude, vector schedule, velocity, airplane attitude, power setting, and relative strength of the individual noise components. Consequently, description of the noise at a particular location is a complex analysis. The following discussion is presented to help understand the interaction of the parameters.

The total engine noise was separated into five distinct components. These components are inlet oriented fan noise, exhaust oriented fan noise, combined jet noise from the hot fan tip turbine exhaust and cooler fan exhaust, the core engine inlet radiated compressor noise, and the tip turbine turbomachinery noise.

The predicted static spectra for these five components form the basic building blocks used to calculate fly-over noise. In particular the directivity is of interest since the acoustic angle of the individual component is allowed to vary in arriving at the total noise. The component static noise is presented for reference on Figures 51 through 55.

To understand the impact of the components on fly-over noise we examined in detail the fly-over results from the Phase I study. In this case calculations were made for two separate aircraft paths for comparison. PNL was chosen as a fundamental measure. The variation of PNL was then examined during fly-over comparing the effects from the low vertical rise and high vertical rise paths. It was decided to examine the PNL variations as the noise source passes a fixed point. Two points were chosen. The first point was on the runway centerline and the second was on a sideline. Figures 56 through 79 present this data.

Calculations from data received at centerline microphone location produce rather rapid changes in the PNL values whereas at the sideline location the functions change more gradually. This phenomenon is really an expression of the geometry where the rate of change with velocity is different viewed from the side or along the path.

The difference in the behavior of the fly-over PNL curves exhibited by comparing the results from the high rise and low rise paths provide an additional

measure of evaluating the fly-over noise. The PNL values from the short vertical rise path show larger absolute values than the values from the high rise path. Also in general the PNL curves representing the low rise path have steeper slopes. The significance of these changes is seen when they are related to EPNL which is a function of peak PNL and duration. Thus we have a mechanism to significantly effect fly-over noise from an EPNL standpoint.

Based on absolute value considerations the noise from various engine components do not add directly but are affected by operational considerations of individual vectoring and power setting as well as the logarithmic addition rule. Nevertheless the relative strengths of the various engine components can be seen from Figures 80 and 81 which presents the PNL contours as if a single component had independently traversed the fly-over pattern.

The effect of the cross-flow operational factor is to increase the fan inlet radiated noise and the jet noise. To evaluate the cross-flow effect we choose a point 7000 feet down the take-off track which was far enough from the brake release position so the forward speed of the aircraft has created a strong cross-wind component. To illustrate the effect on the PNL values data is presented on Figures 82 through 85 showing the total effect and the effect on the individual components of PNL fly-over with an without cross-flow effect. Despite the fact that two different mechanisms caused a change in the jet noise, i.e., inlet distortion and jet plume deflection, the change in PNL was about the same for both inlet or jet. The assumption was made that cross-flow does not effect the core compressor or turbine noise components. Consequently only fan and exhaust components are plotted. The total cross-flow effect at this particular runway location and specific operational time frame is one to two PNdB.

VIII. EFFECT OF SUPPRESSION EXTERNAL TO THE ENGINE

The lift and lift cruise fan noise levels used to calculate the contours presented in Section V accounted for the application of acoustic wall treatment and splitters in the fan exhaust. In an actual aircraft installation there is the potential of increasing suppression by adding wall treatment and splitters to the wing and fuselage nacelles which contain the basic fan. Figure 86 shows the noise constituents of the basic fan with exhaust treatment. The following sources are dominant:

(1) Cruise fan exhaust
(2) Lift fan exhaust
(3) Cruise fan inlet
(4) Gas generator inlet
(5) Lift fan inlet

Sources 1 through 4 may be further suppressed by treatment of the nacelle with attendent penalties in weight and performance loss but little or no change in the lift fan nacelle depth or cruise fan nacelle length. Source 5, lift fan inlet is not easily suppressed due to the shallow inlet associated with the lift fan design. Studies to define suitable inlet treatment arrangements have shown the installation penalties to be quite severe even for small suppression levels like 3 PNdB. Source 5 thus becomes the limiting noise level if sources 1 through 4 are decreased substantially.

To establish the benefit of adding additional treatment to the wing and fuselage nacelles, the following suppression levels were assumed for sources 1 through 4.

	ΔPNdB
(1) Cruise fan exhaust	-15
(2) Lift fan exhaust	-15
(3) Cruise fan inlet	-10
(4) Gas generator inlet	-10

The lift fan inlet noise was then assumed to vary in suppression from 0 to 20 PNdB and the total system noise calculated.

Figure 87 shows the results of the suppression study. With the suppression defined above and no lift fan inlet suppression a 500 foot sideline level of 100.5 PNdB may be obtained. This is a reduction of approximately 7 PNdB. With lift

fan inlet suppression the total system noise may be reduced to a minimum of approximately 98 PNdB. With 2 to 3 PNdB inlet reduction a total system noise less than 100 PNdB can be obtained. As seen by the above results the benefits of additional suppression are severely limited due to both the lift fan inlet noise and the jet noise floor shown on Figure 82. By adding 10 to 15 PNdB suppression for source 1 through 4 only 7 PNdB system noise reduction was obtained and with the addition of up to 20 dB inlet reduction a maximum of 9 PNdB total system noise reduction is obtained.

IX. CONCLUSIONS

1. Considering the complete aircraft system and based on the noise suppression technology level assumed in the initial engine design the exhaust radiated fan noise is the loudest single noise contributor identified in this study. Projecting our suppression technology at some future time period the exhaust radiated fan noise and other components could be suppressed a sufficient amount so that the critical component would be forward radiated fan noise. Suppression of this component in turn is restricted by available space and mechanical design considerations.

   It is noted that the core compressor inlet and the forward radiated fan components produce higher PNL values than the rear radiated fan noise when considering individual static spectrum. However, power plant installation characteristics result in shielding the critical acoustic angles for these two components.

2. The phase II aircraft is quieter because a better take-off profile increases the separation distance from the source to the microphone.

3. Using enclosed area within a specific noise contour as a criteria this area is reduced by using a long vertical raise or descent path as contrasted to the larger enclosed contour area resulting from the short vertical rise or descent type of path.

4. The maximum sideline distance or width of any particular contour is the same for either the long vertical rise or short vertical rise. However, the maximum width occurs at different points along the extended runway centerline.

5. Reductions in engine power settings as well as attained altitude provide the most significant effects on shaping the closing point of the noise contour.

6. The objective of achieving a PNL noise level less than 100 PNdB on a 500 ft sideline can be achieved for the aircraft used in this study and using a suppression schedule within our predicted future technology. The critical suppression is a 5 PNdB reduction for the fan inlet oriented noise component.

7. Cross-flow effects are primarily influenced by aircraft forward velocity and consequently are more significant at listening or microphone locations farther along the runway. For example, for the short vertical rise path at 7000 feet down the runway centerline the cross-flow can be as much as a one to two increase in PNL.

X. NOMENCLATURE

TERM	DESCRIPTION	UNITS
EGA	Extra Ground Attenuation	ΔdB
EPNL	Effective Perceived Noise Level	dB EPNdB
dB	Decibel; re: .0002 dynes/cm^2	
M/S	Meters per Second	
PNL	Perceived Noise Level	dB PNdB
P.S.	Power Setting	
SPL	Sound Pressure Level	dB
TOGW	Take-Off Gross Weight	Lbs.
V	Velocity	Ft/Sec M/Sec
V/STOL	Vertical or Short Take-Off and Landing	
VTOL	Vertical Take-Off and Landing	

XI. List of References

1. TM 72-315 "Effect of VTOL Aircraft Flight Speed on Lift Fan Jet Noise Generation".

2. TM 72-151 "Effect of VTOL Aircraft Flight Speed on Lift Fan Noise Generation".

3. NASA CR-120787 "LF460 Detail Design".

TABLE I

Engine Cycle Parameters
Scaled LF460 Fan

Power Setting	V_8	V_{28}	W_8	W_{28}	V_{Tip}
1.000	675	680	80.5	658	1048
.909	620	650	77.5	635	1004
.882	595	640	76	623	992
.854	585	630	75.5	611	975
.817	565	620	74	600	964
.791	550	605	73	589	945
.745	525	585	70.5	565	920
.682	500	560	67.5	541	875
.591	460	520	63.5	501	818
.499	430	475	60.5	466	758
.409	380	420	56	419	688
.273	300	360	49	362	583

$A_8 = 4.35$

$A_{28} = 12.88$

TABLE II

Noise Component Designations
NASA AMES Contour Study Phase-II
Advanced VTOL Type Study Aircraft

Source Designator	Source Description	Source Number	Vector Schedule	Cross Flow Correction
1	Cruise Fan Inlet	2	Fixed at $\beta = 0$	No
2	Cruise Fan Exhaust	2	Variable β = Cruise	No
3	Cruise Fan Jet	2	Variable β = Cruise	Yes
4	Cruise Engine Turbine Noise	2	Variable β = Cruise	No
5	Gas Generator	2	Fixed at $\beta = 0$	No
6	Lift Engine Fan Inlet	4	Fixed at $\beta = 90°$	Yes
7	Lift Engine Fan Exhaust	4	Variable β = Lift	Yes
8	Lift Engine Jet	4	Variable β = Lift	Yes
9	Lift Engine Turbine Noise	4	Variable β = Lift	No

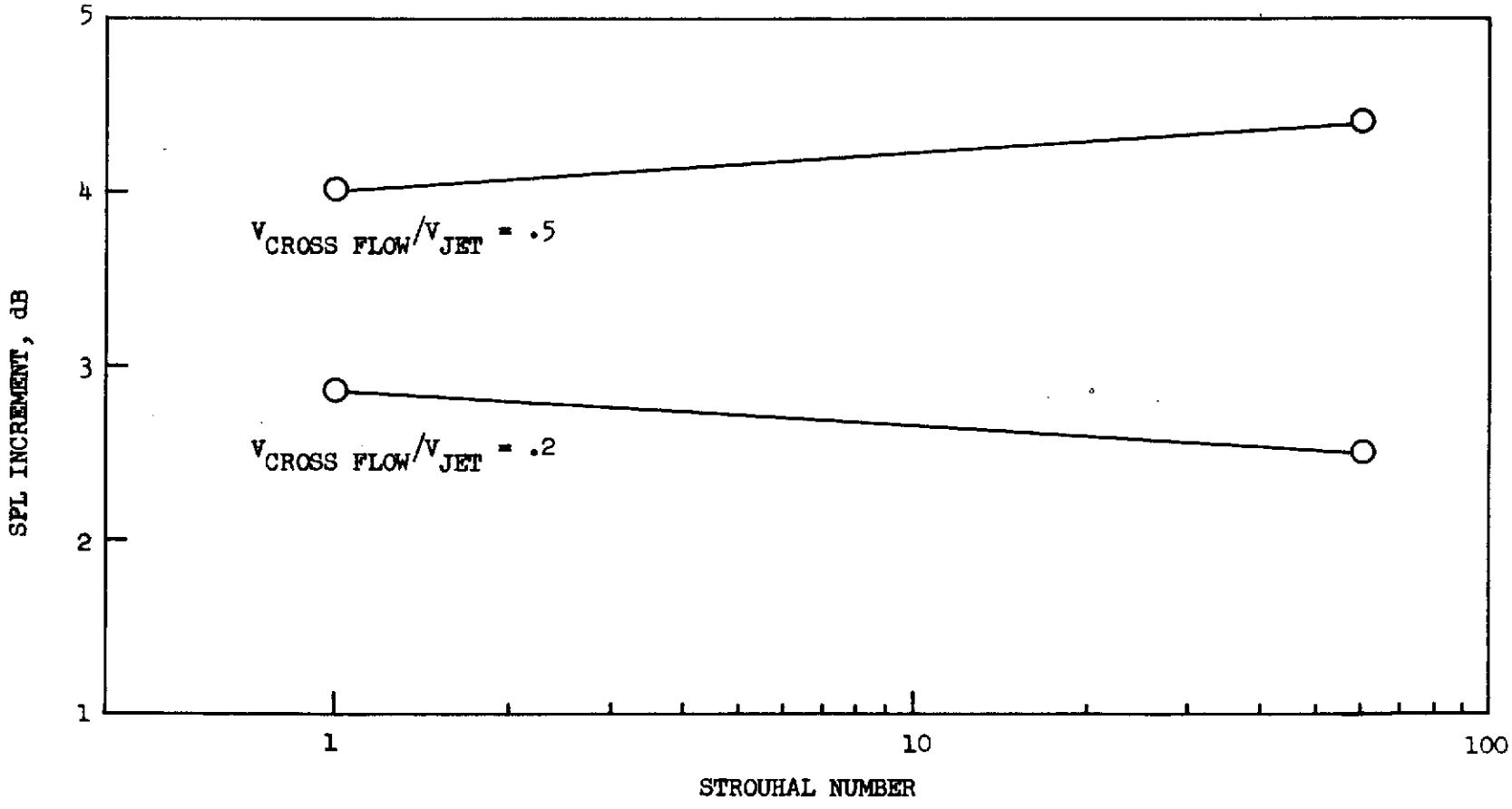

FIGURE 1 TYPICAL CROSS FLOW CORRECTIONS - EXHAUST

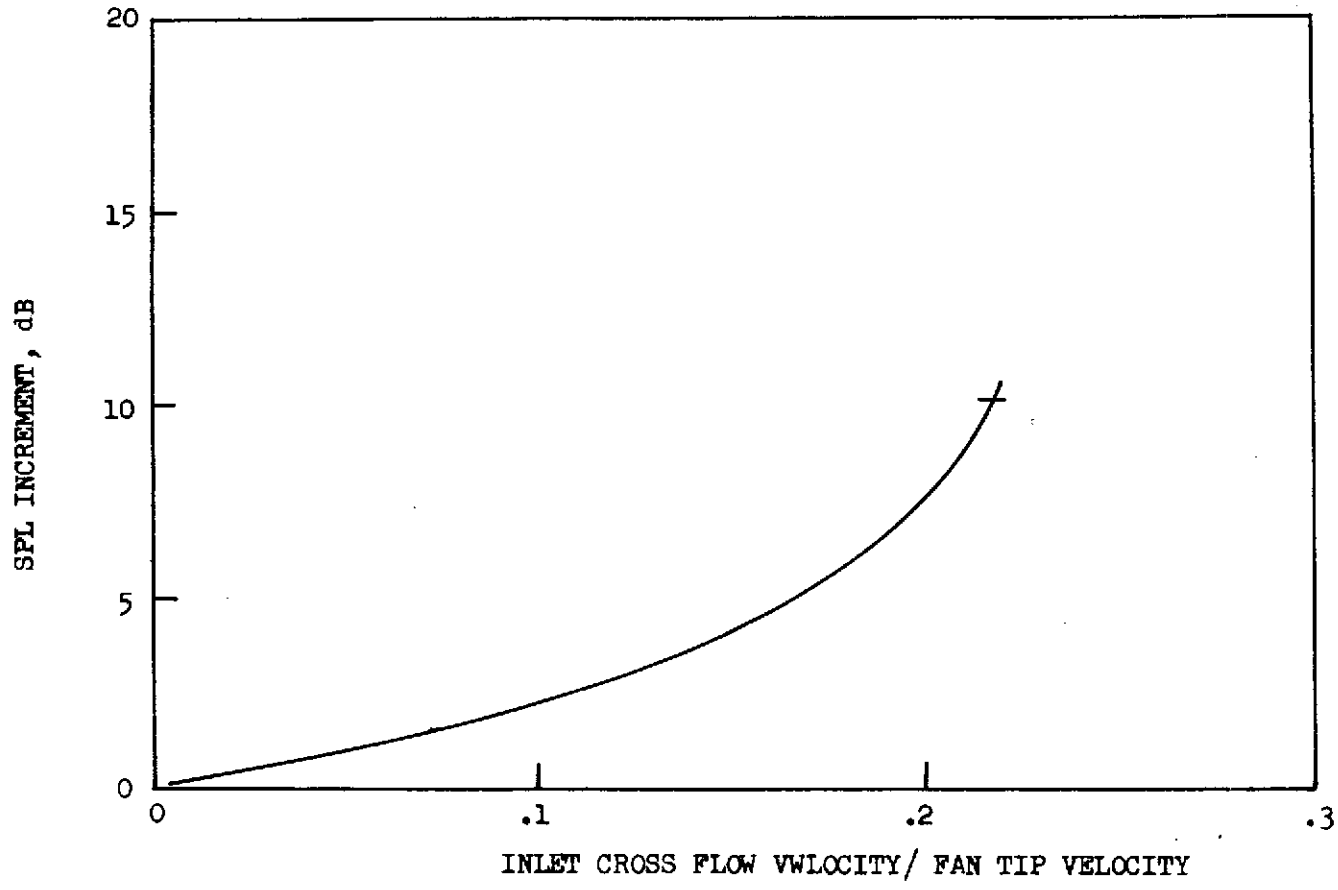

FIGURE 2 TYPICAL CROSS FLOW CORRECTIONS - INLET

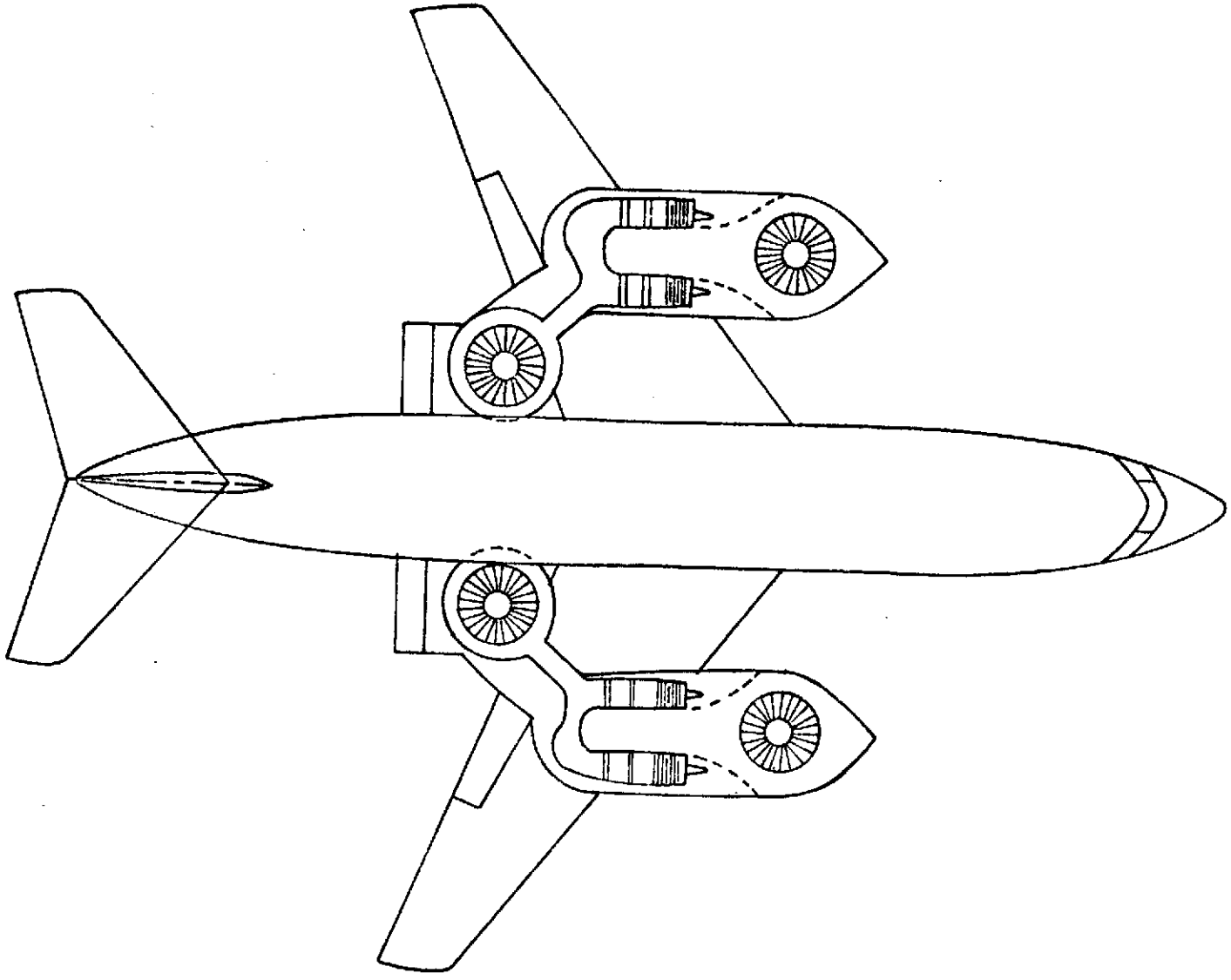

FIGURE 3 PLAN VIEW - PHASE I AIRCRAFT

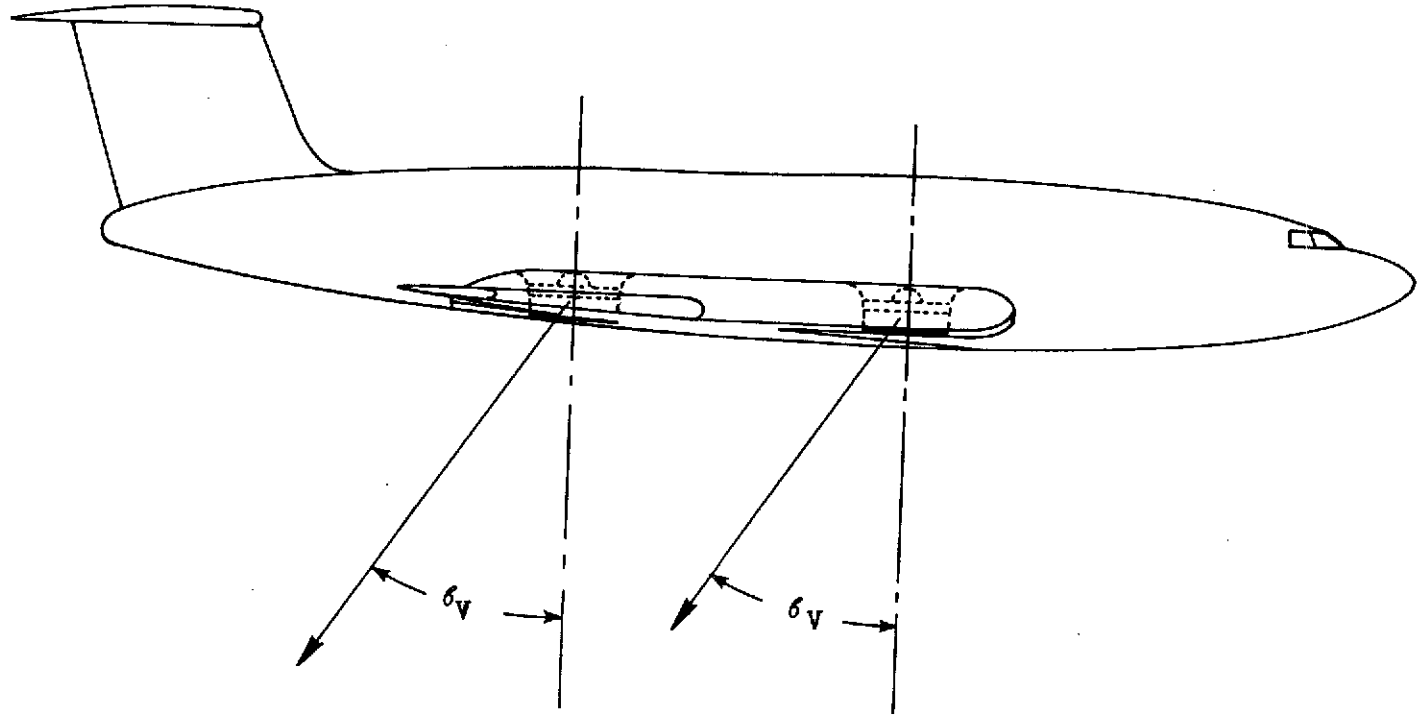

FIGURE 4 PHASE I AIRCRAFT THRUST VECTOR ANGULAR REFERENCE

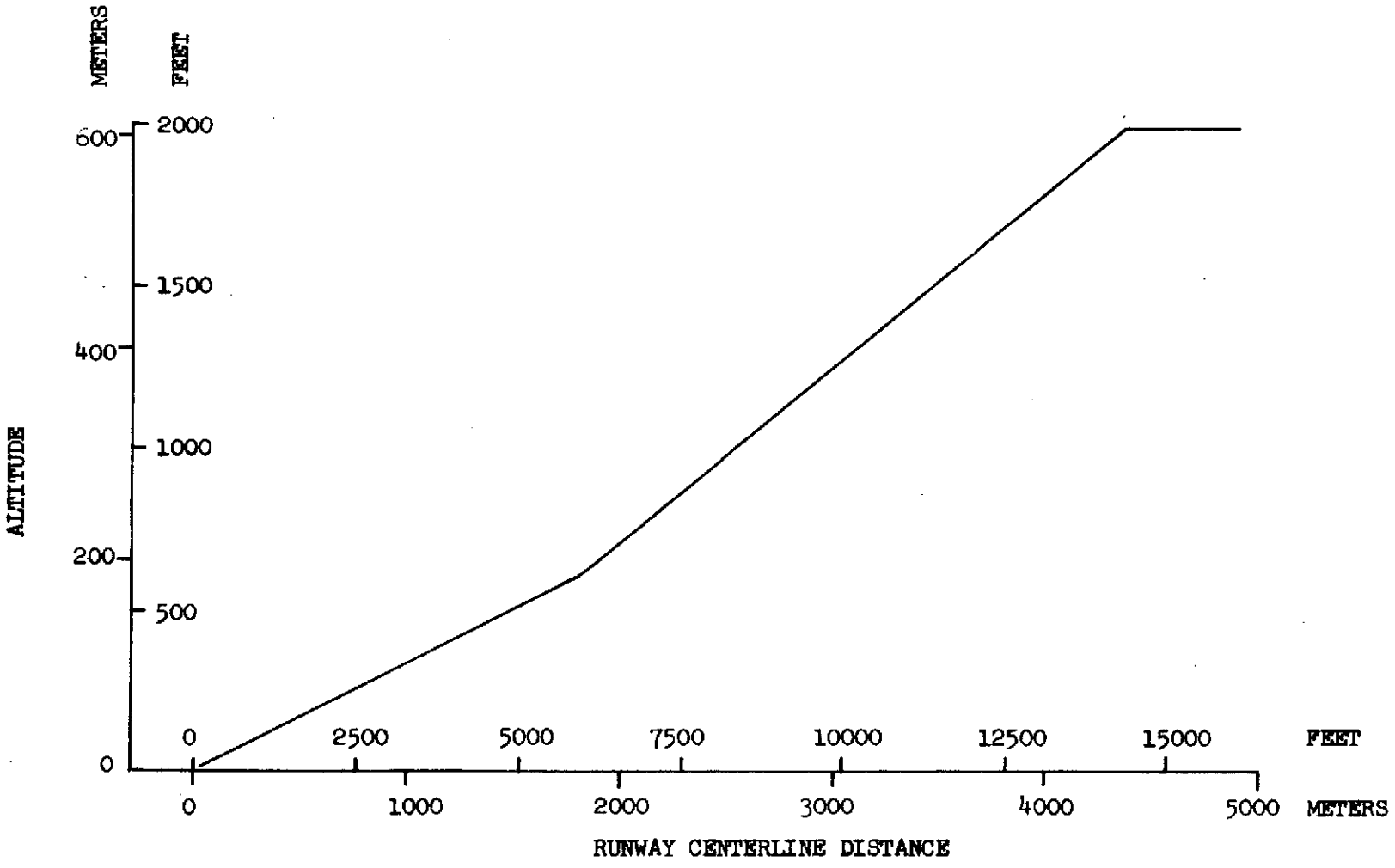

FIGURE 5 PHASE I AIRCRAFT LOW RISE TAKEOFF PATH

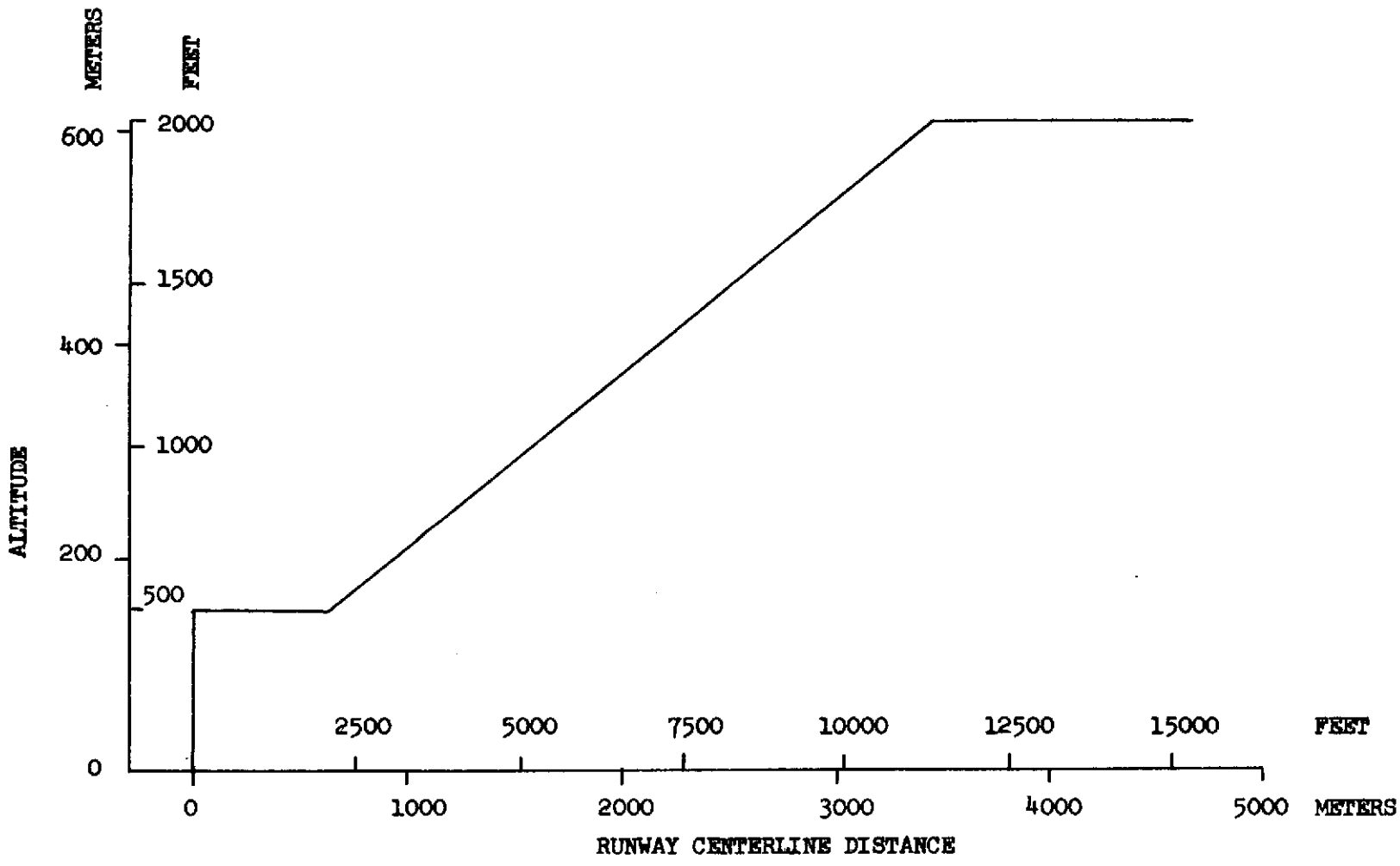

FIGURE 6 PHASE I AIRCRAFT HIGH RISE TAKEOFF PATH

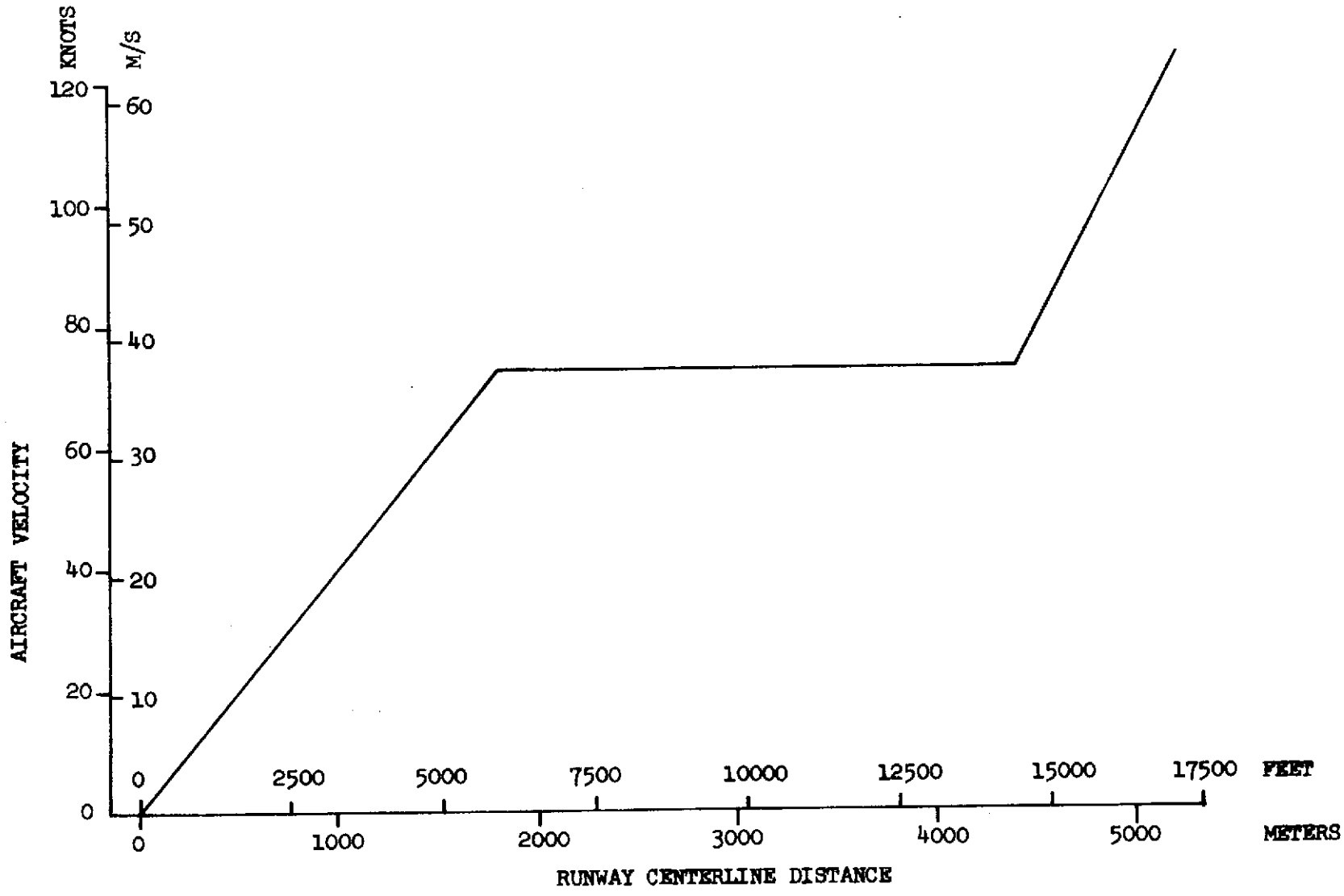

FIGURE 7 PHASE I AIRCRAFT LOW RISE TAKEOFF VELOCITY

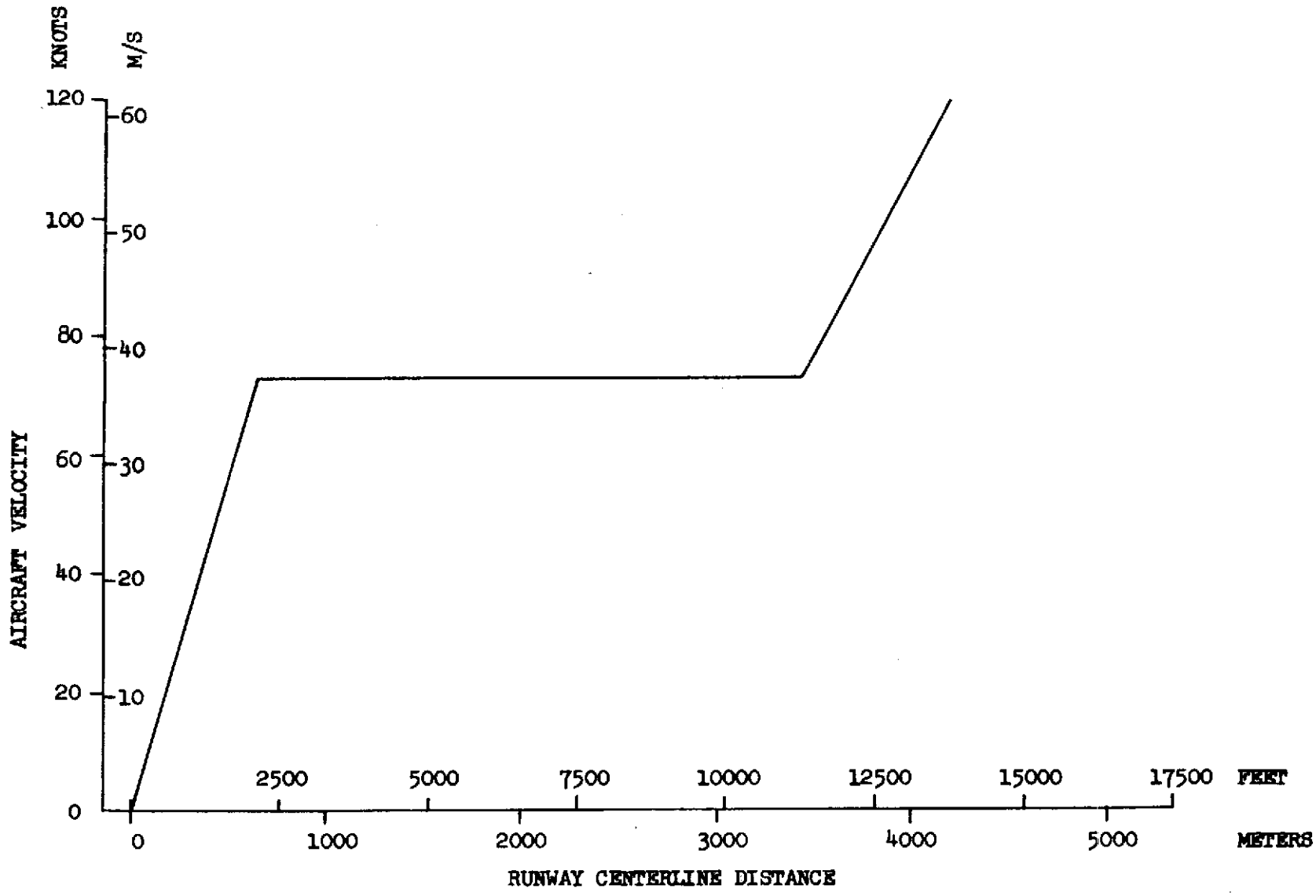

FIGURE 8 PHASE I AIRCRAFT HIGH RISE TAKEOFF VELOCITY

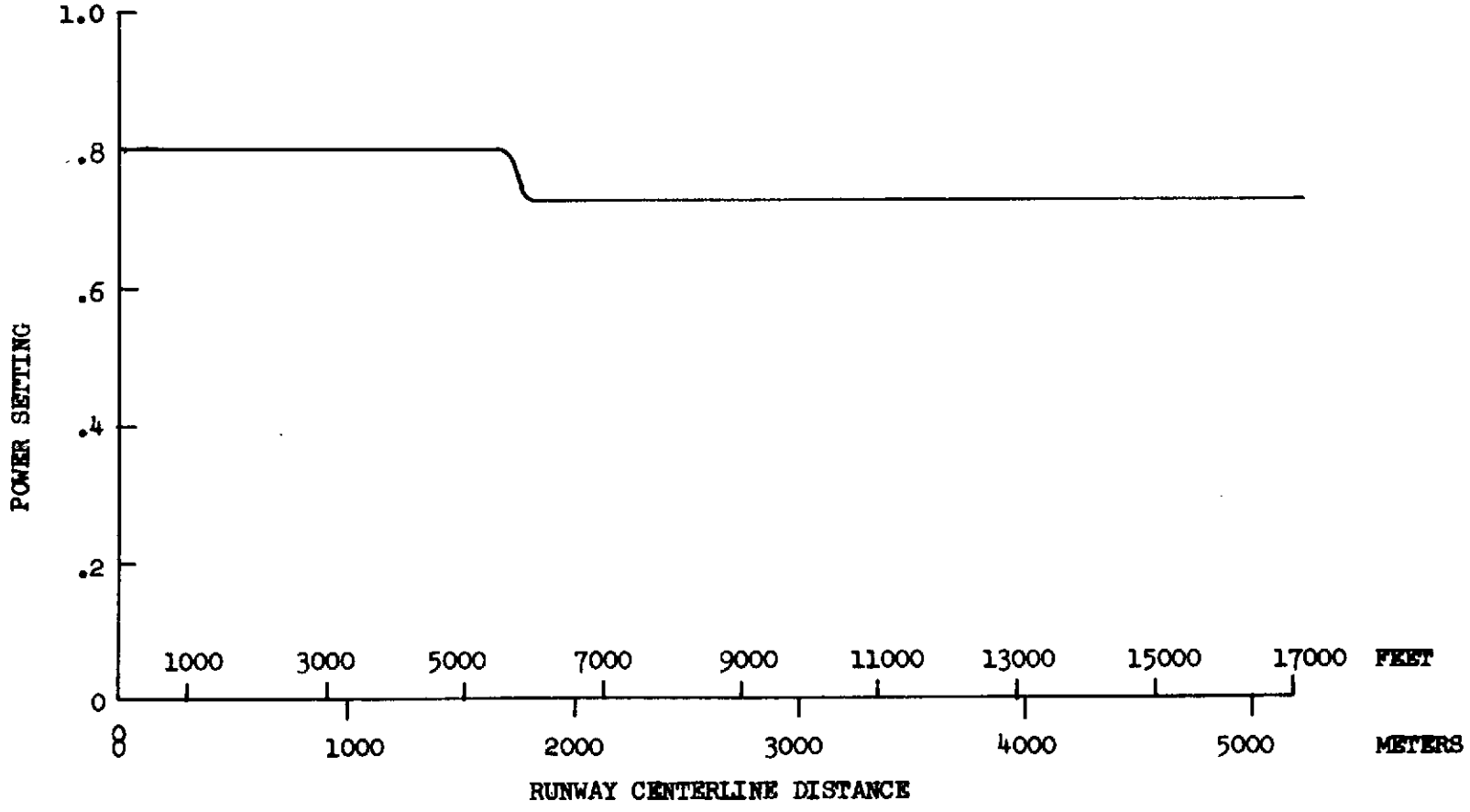

FIGURE 9 PHASE I AIRCRAFT LOW RISE TAKEOFF POWER SETTING

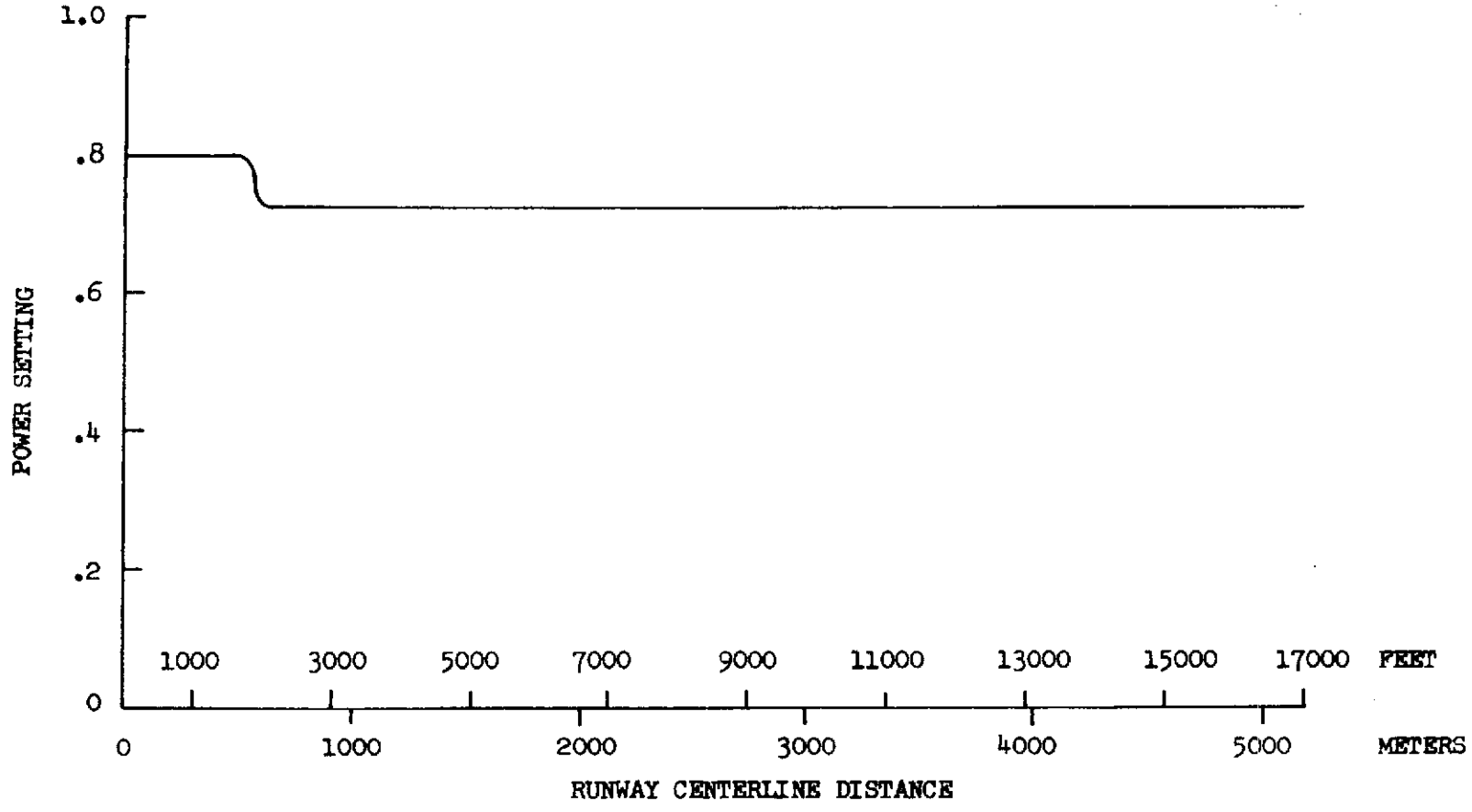

FIGURE 10 PHASE I AIRCRAFT HIGH RISE TAKEOFF POWER SETTING

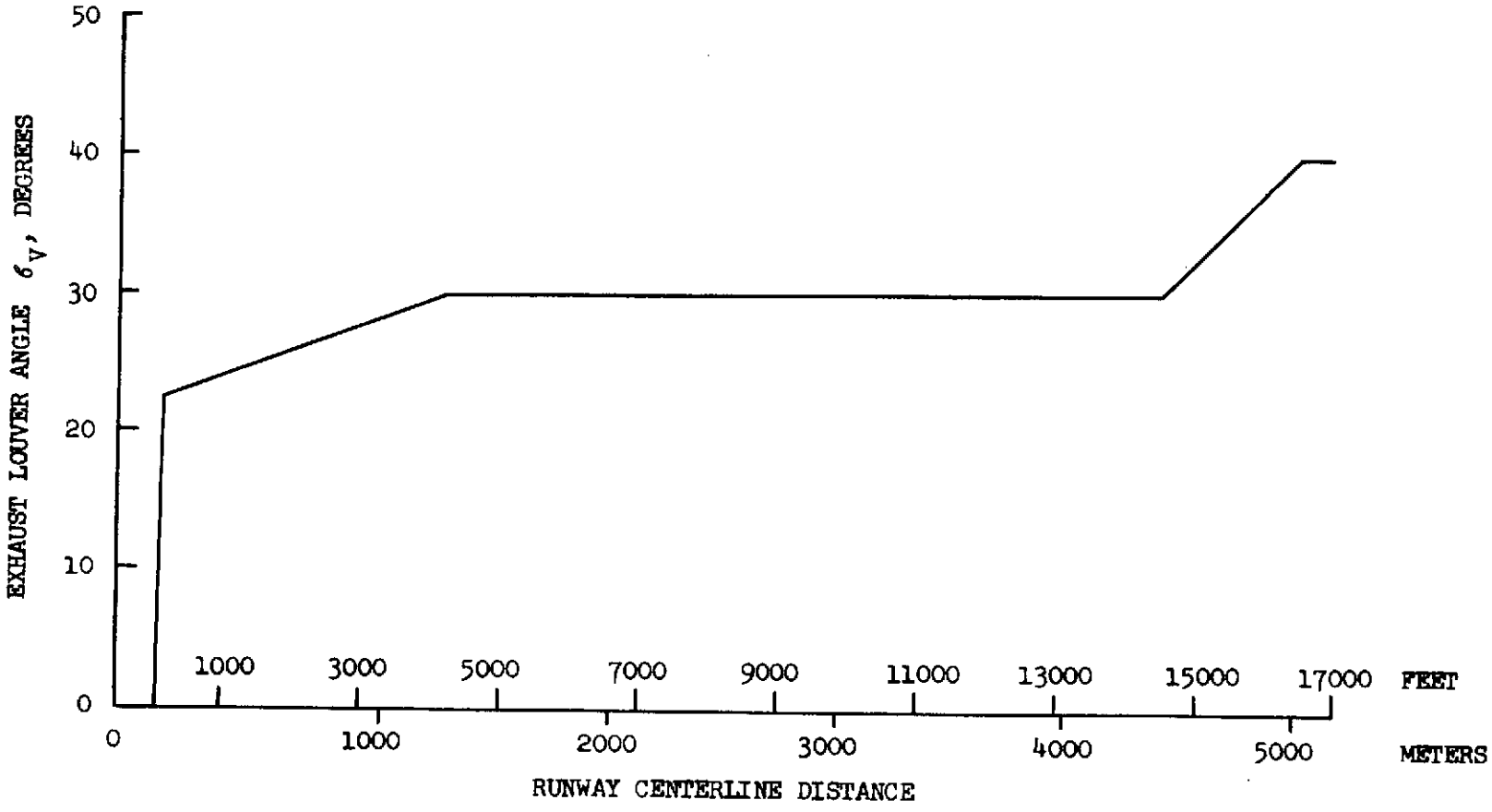

FIGURE 11 PHASE I AIRCRAFT LOW RISE TAKEOFF LOUVER SCHEDULE

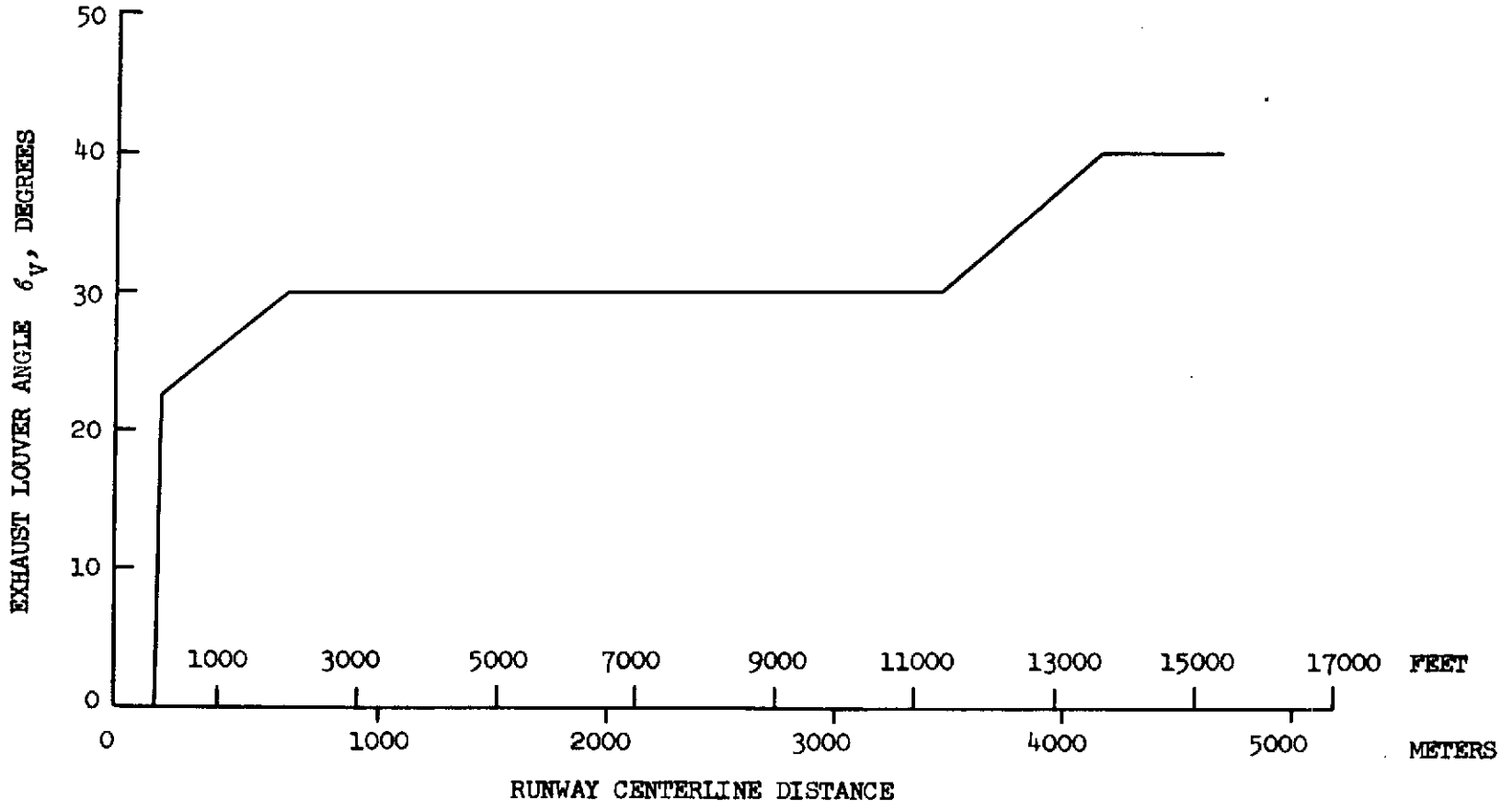

FIGURE 12 PHASE I AIRCRAFT HIGH RISE TAKEOFF LOUVER SCHEDULE

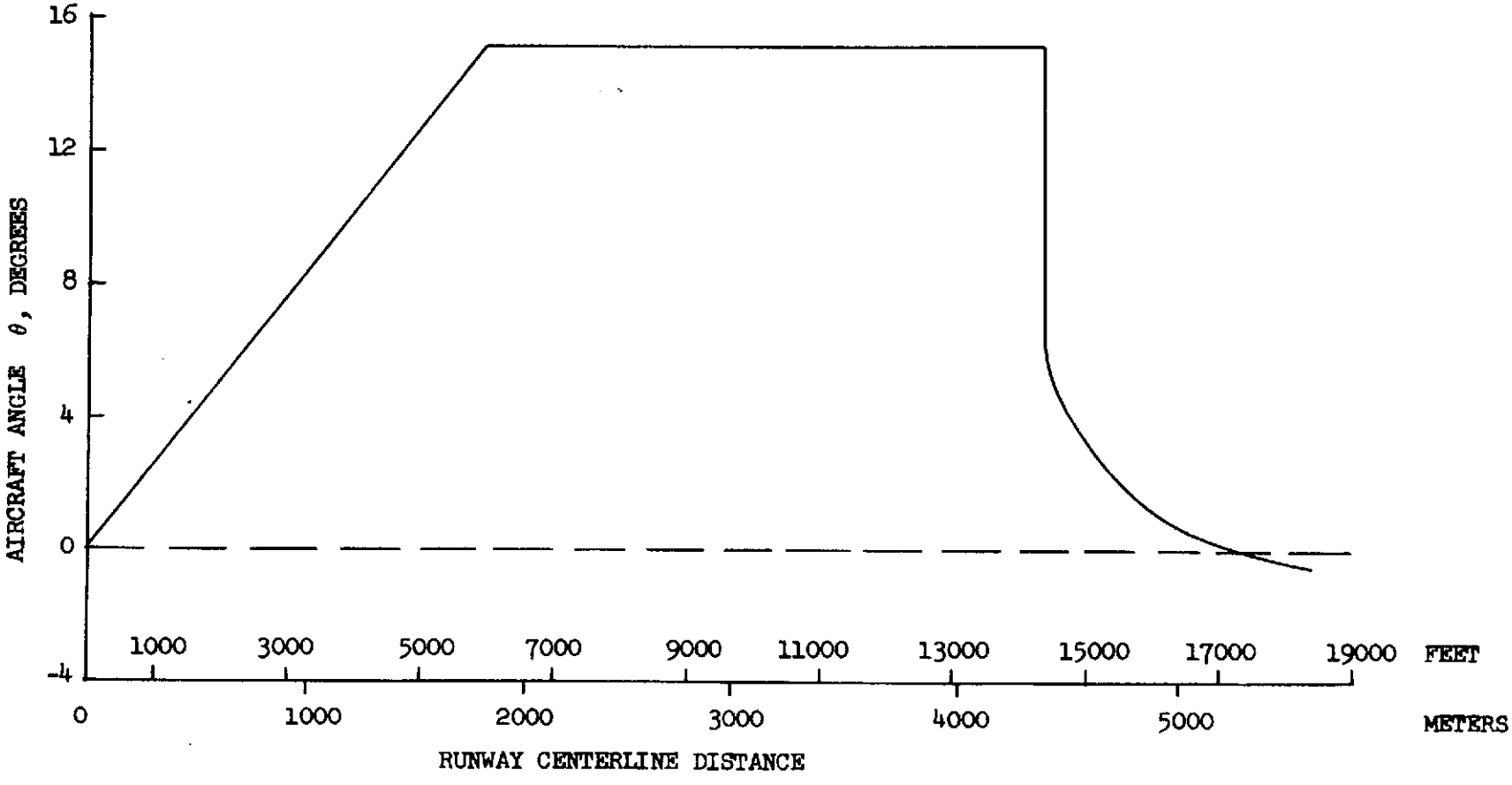

FIGURE 13 PHASE I AIRCRAFT LOW RISE TAKEOFF ATTITUDE SCHEDULE

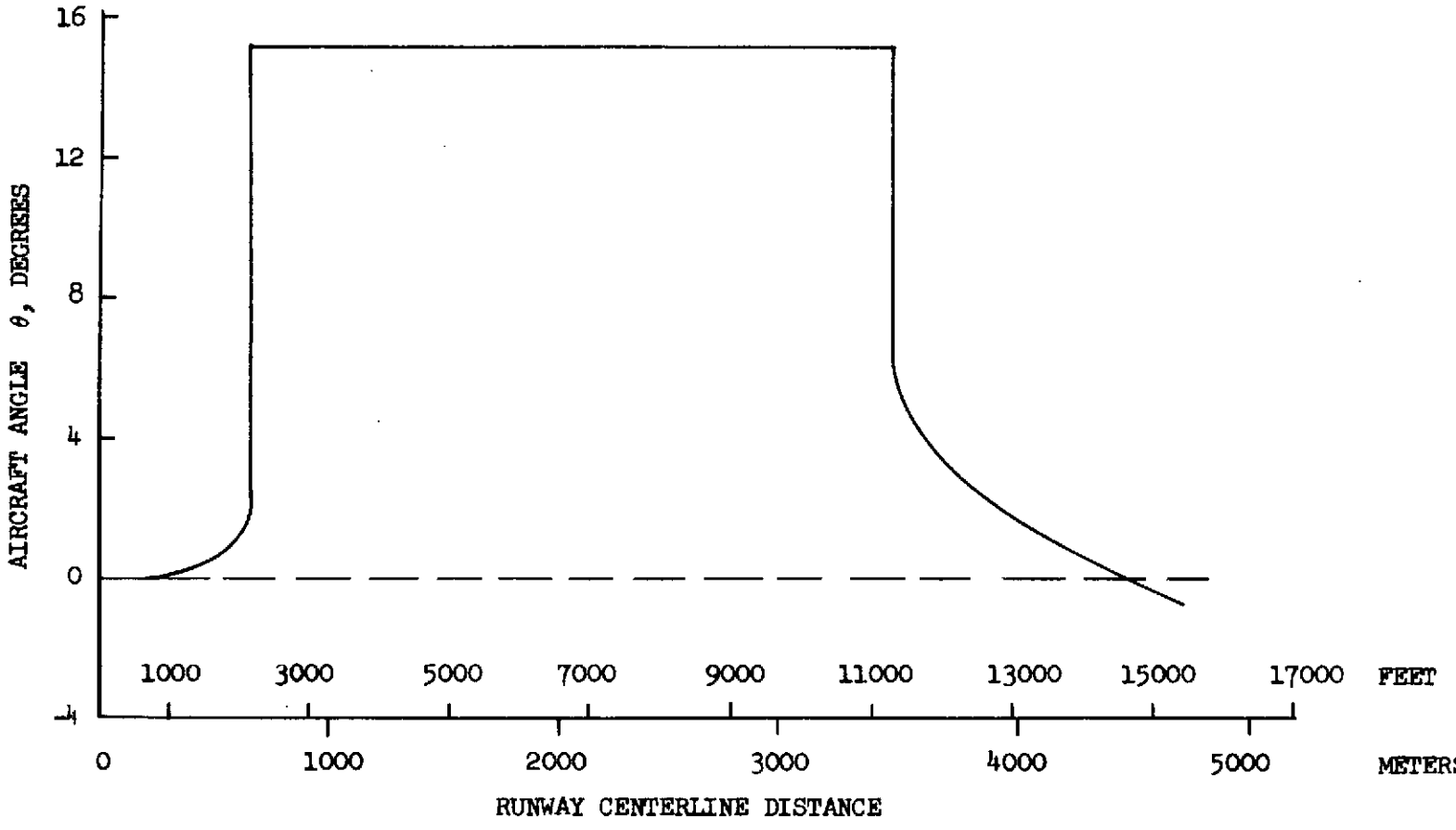

FIGURE 14 PHASE I AIRCRAFT HIGH RISE TAKEOFF ATTITUDE SCHEDULE

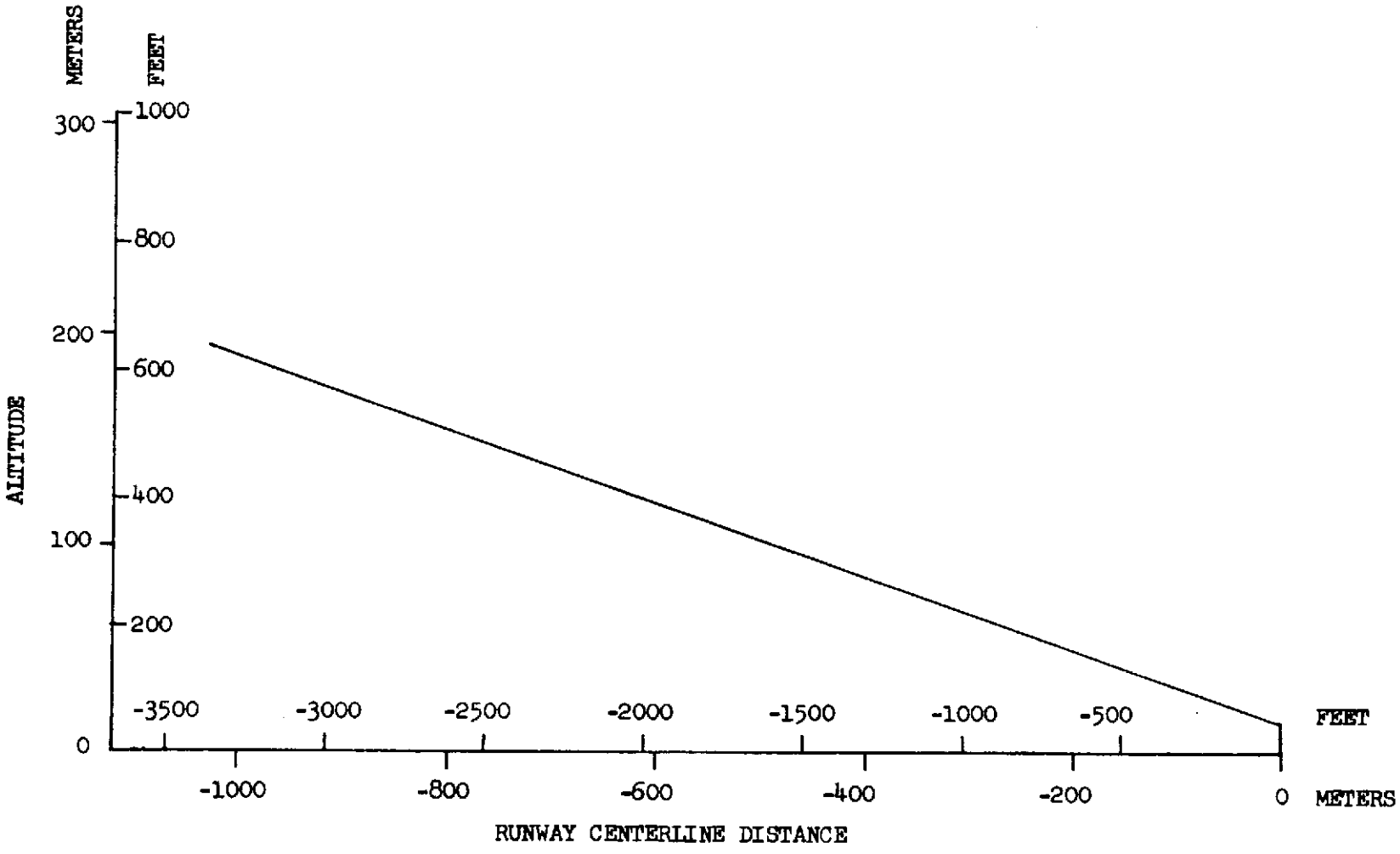

FIGURE 15 PHASE I AIRCRAFT LOW DESCENT APPROACH PATH

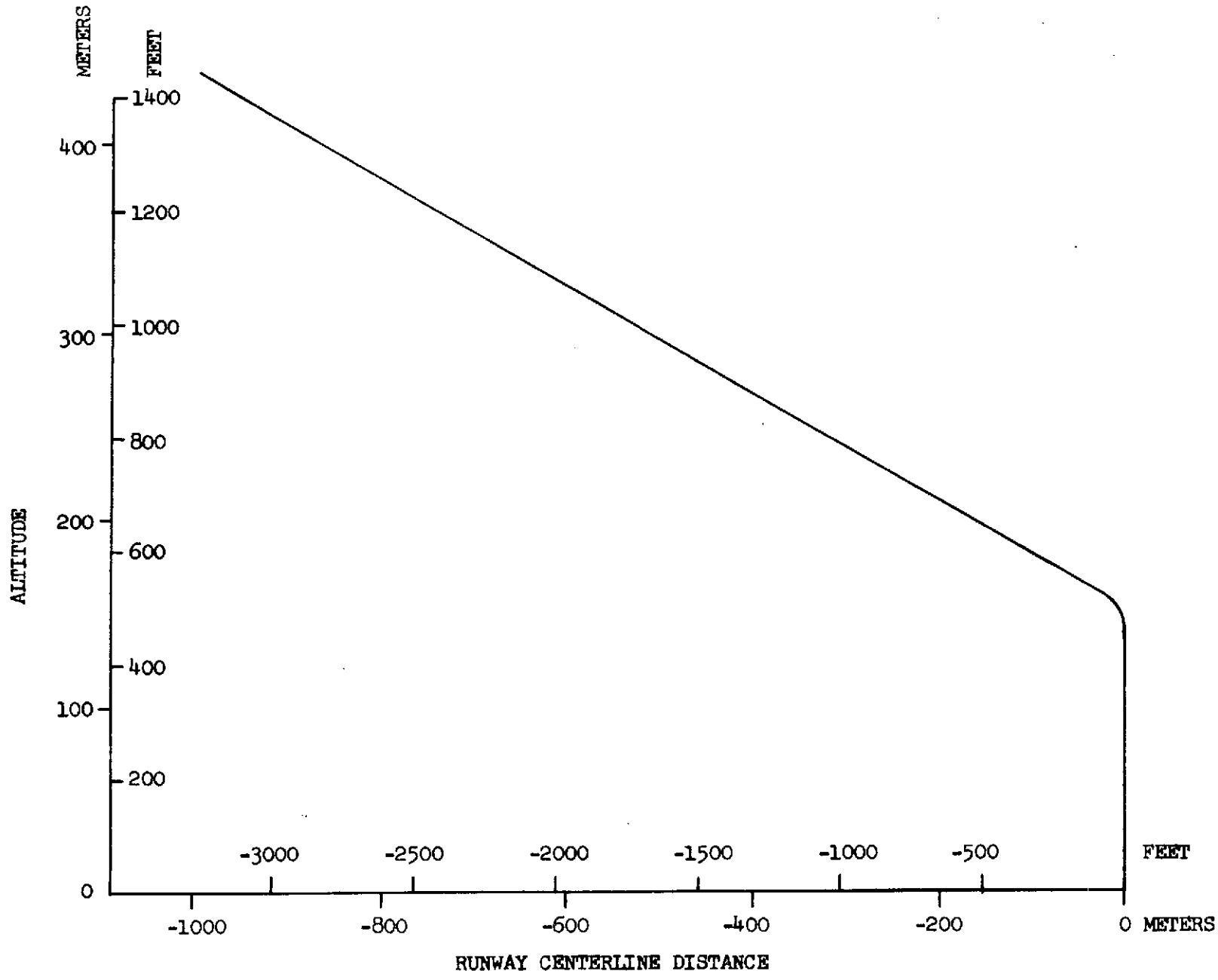

FIGURE 16 PHASE I AIRCRAFT HIGH DESCENT APPROACH PATH

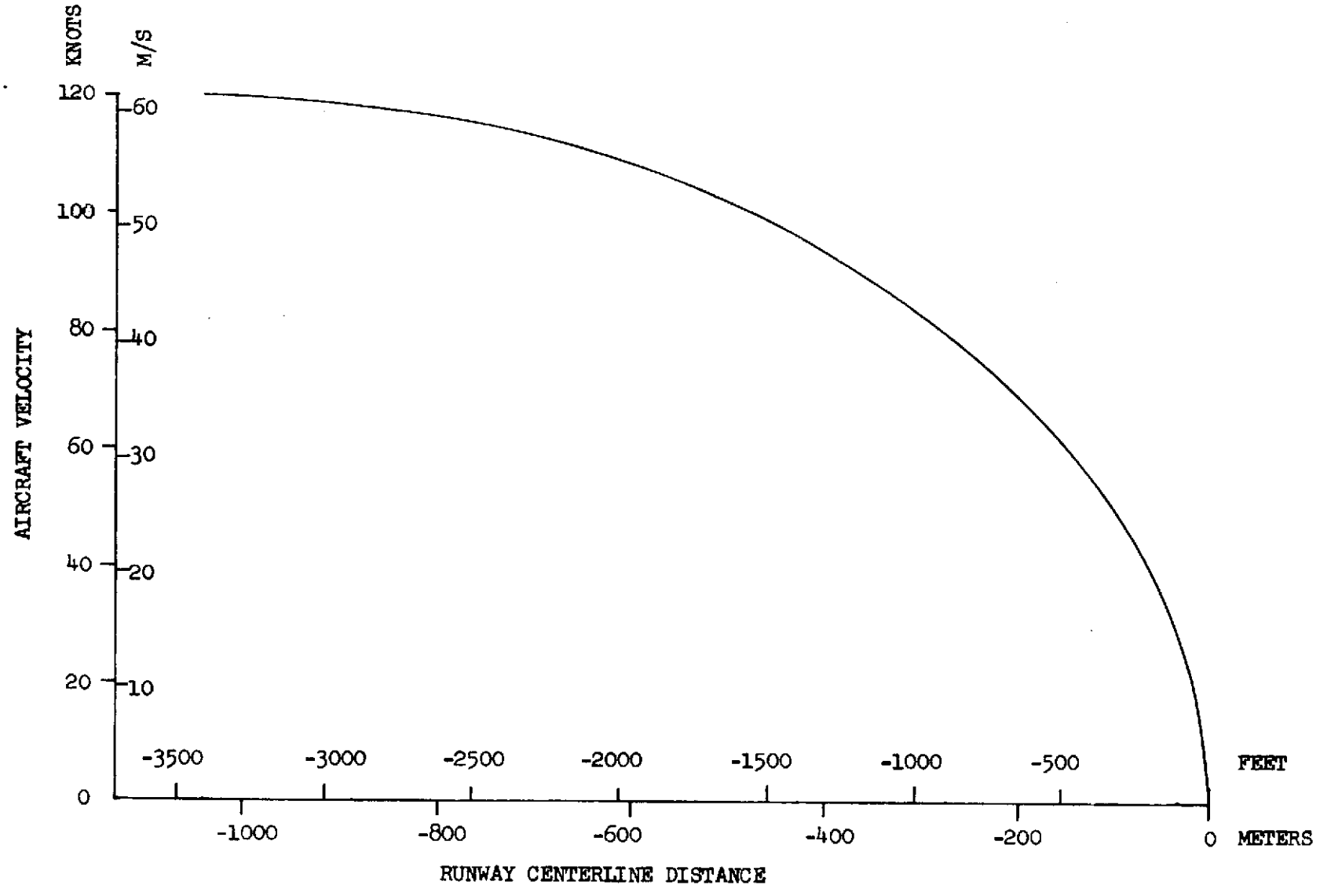

FIGURE 17 PHASE I AIRCRAFT LOW DESCENT APPROACH VELOCITY

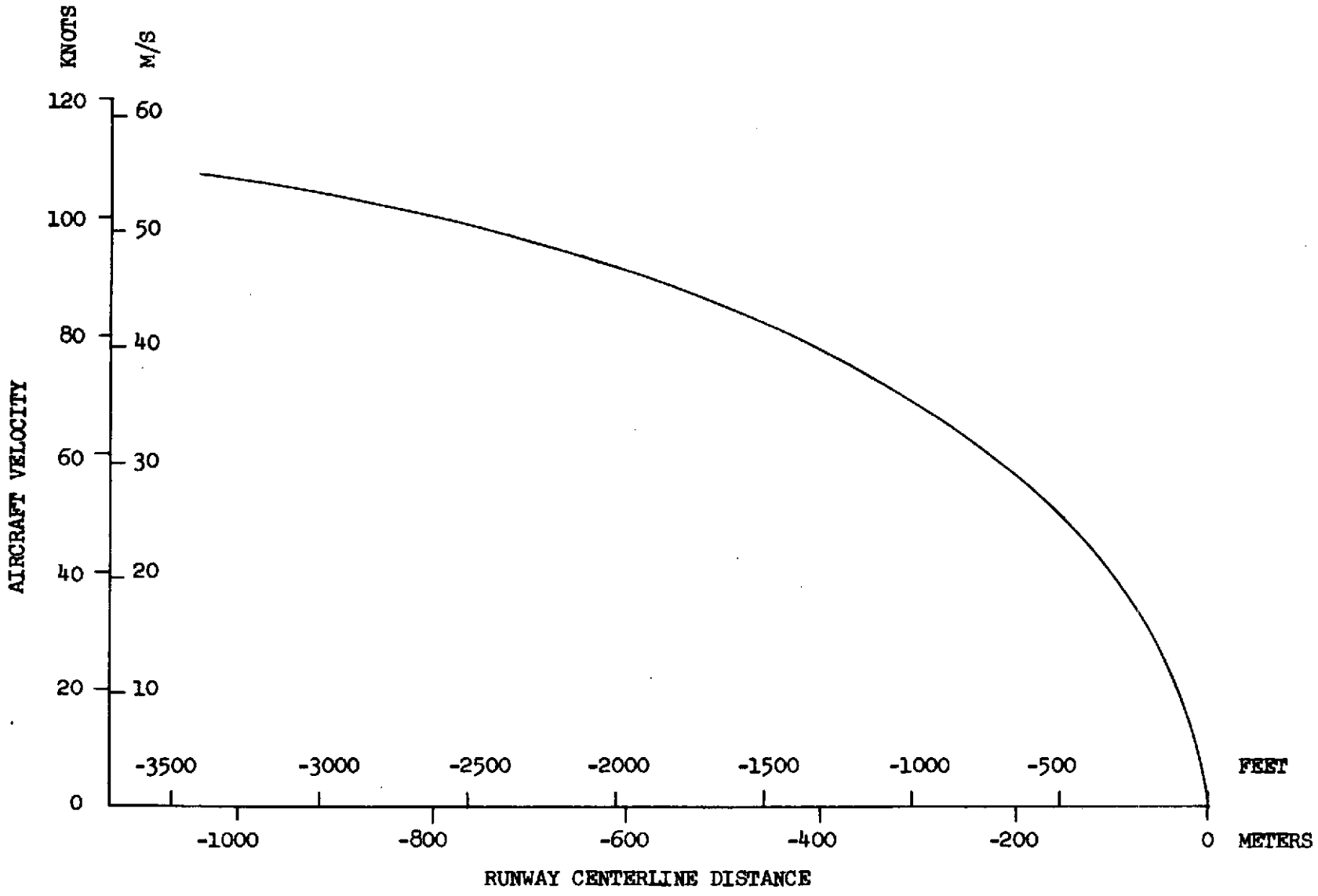

FIGURE 18 PHASE I AIRCRAFT HIGH DESCENT APPROACH VELOCITY

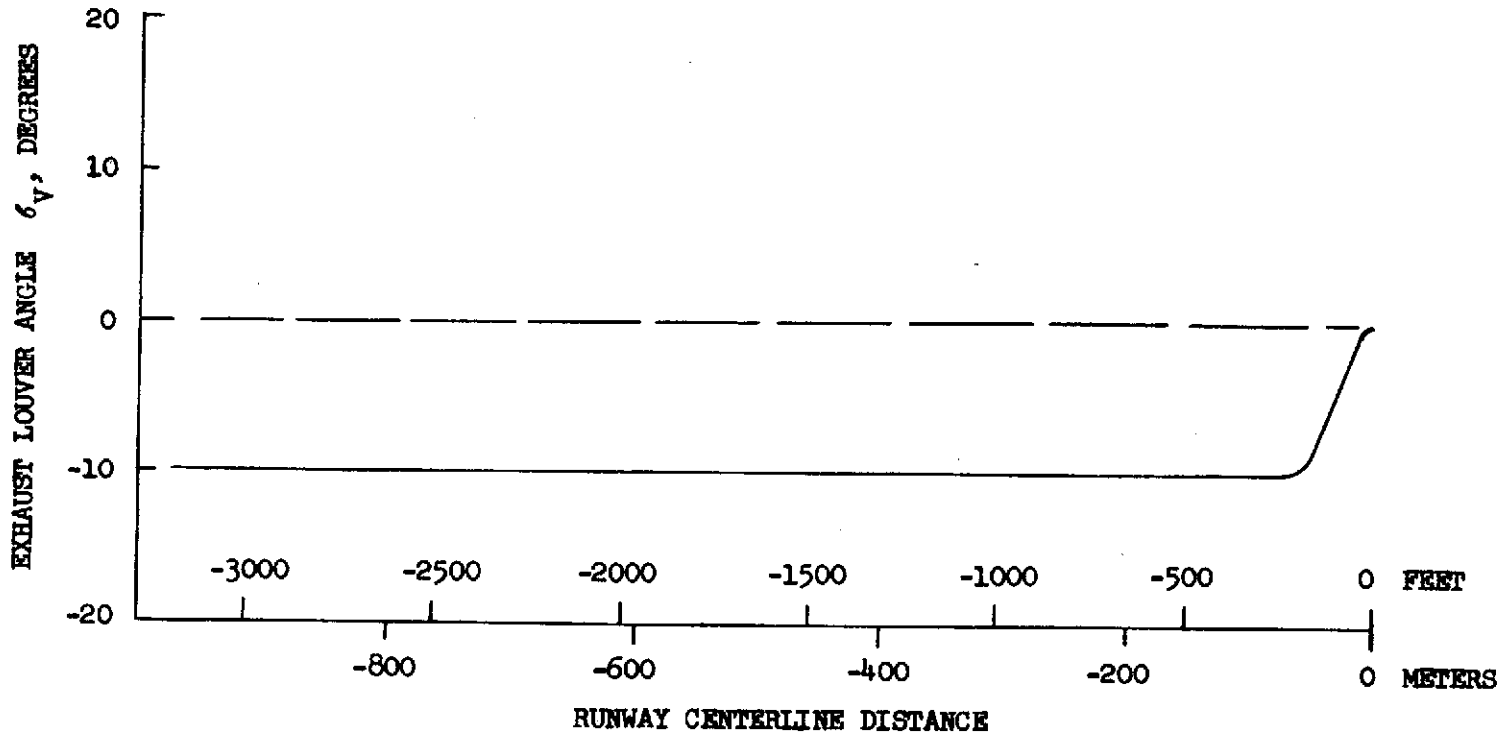

FIGURE 19 PHASE I AIRCRAFT LOW DESCENT APPROACH LOUVER SCHEDULE

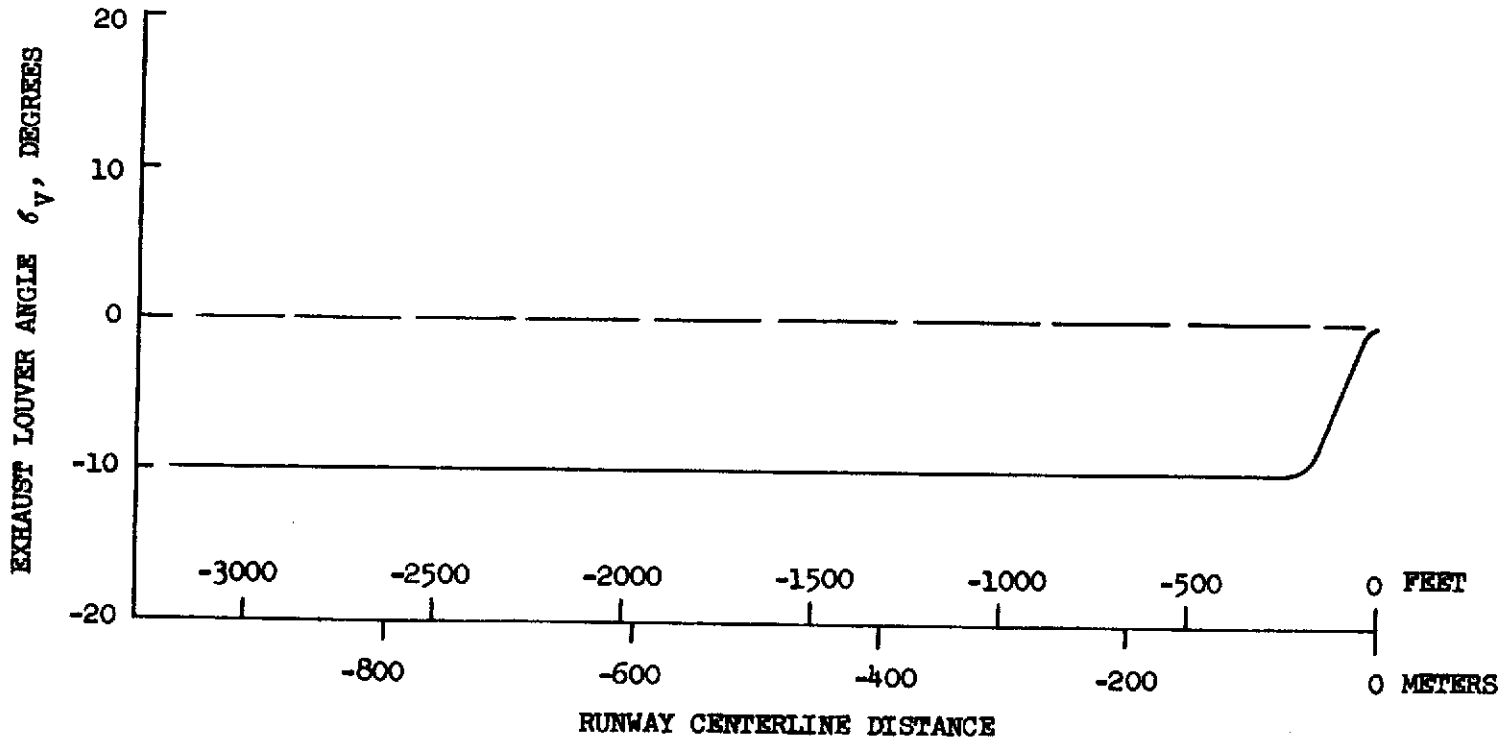

FIGURE 20 PHASE I AIRCRAFT HIGH DESCENT APPROACH LOUVER SCHEDULE

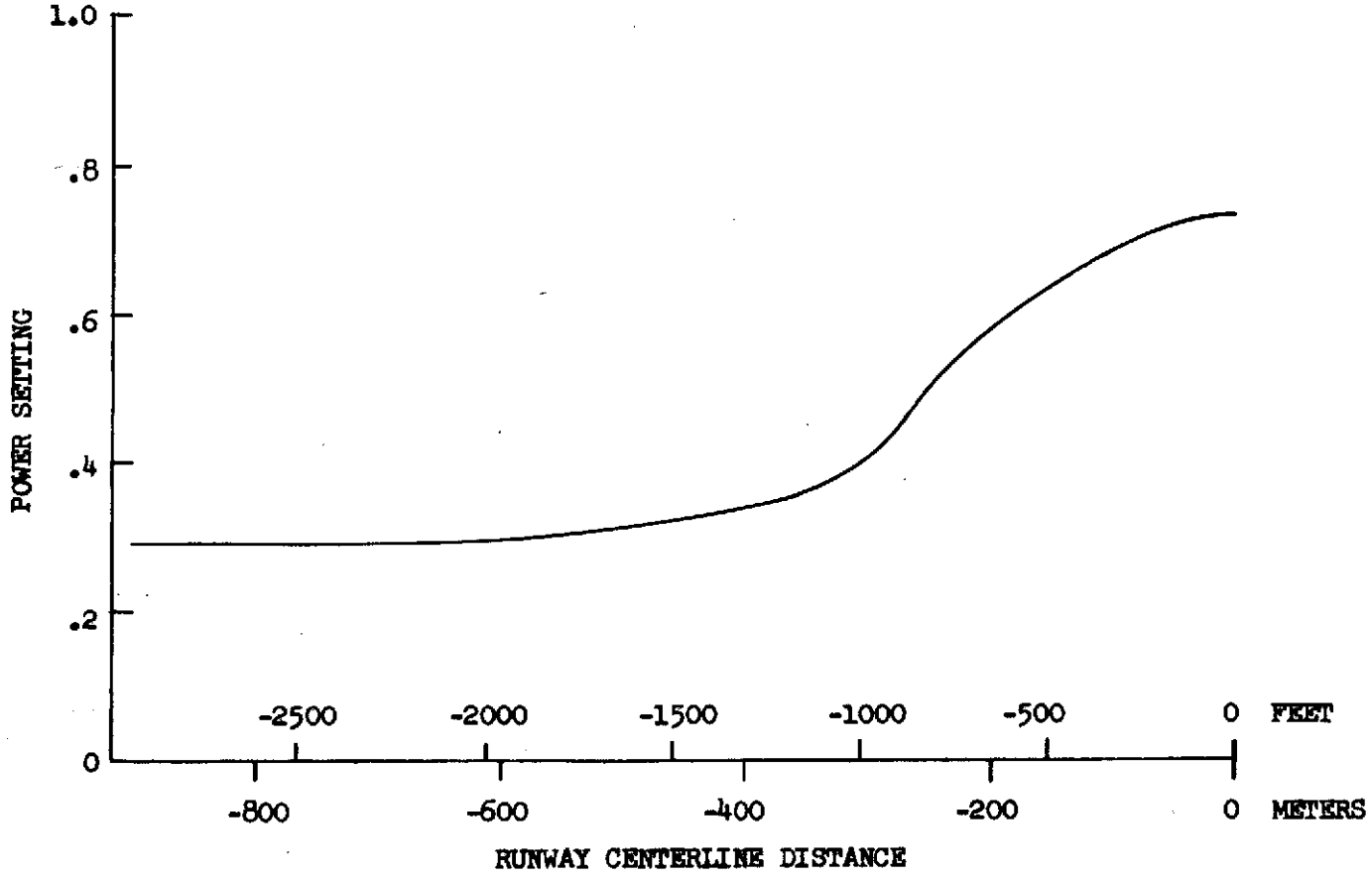

FIGURE 21 PHASE I AIRCRAFT LOW DESCENT APPROACH POWER SETTING

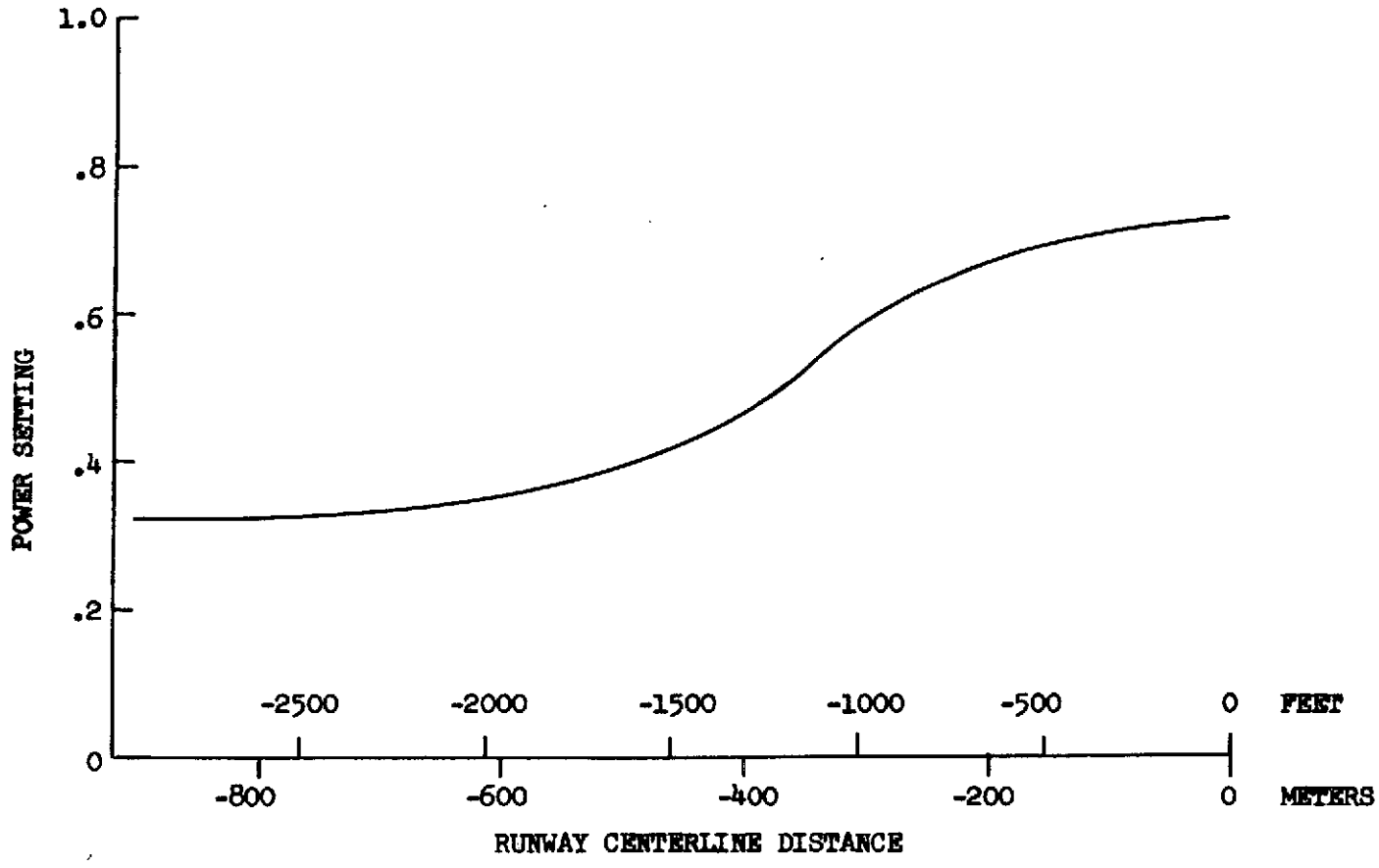

FIGURE 22 PHASE I AIRCRAFT HIGH DESCENT APPROACH POWER SETTING

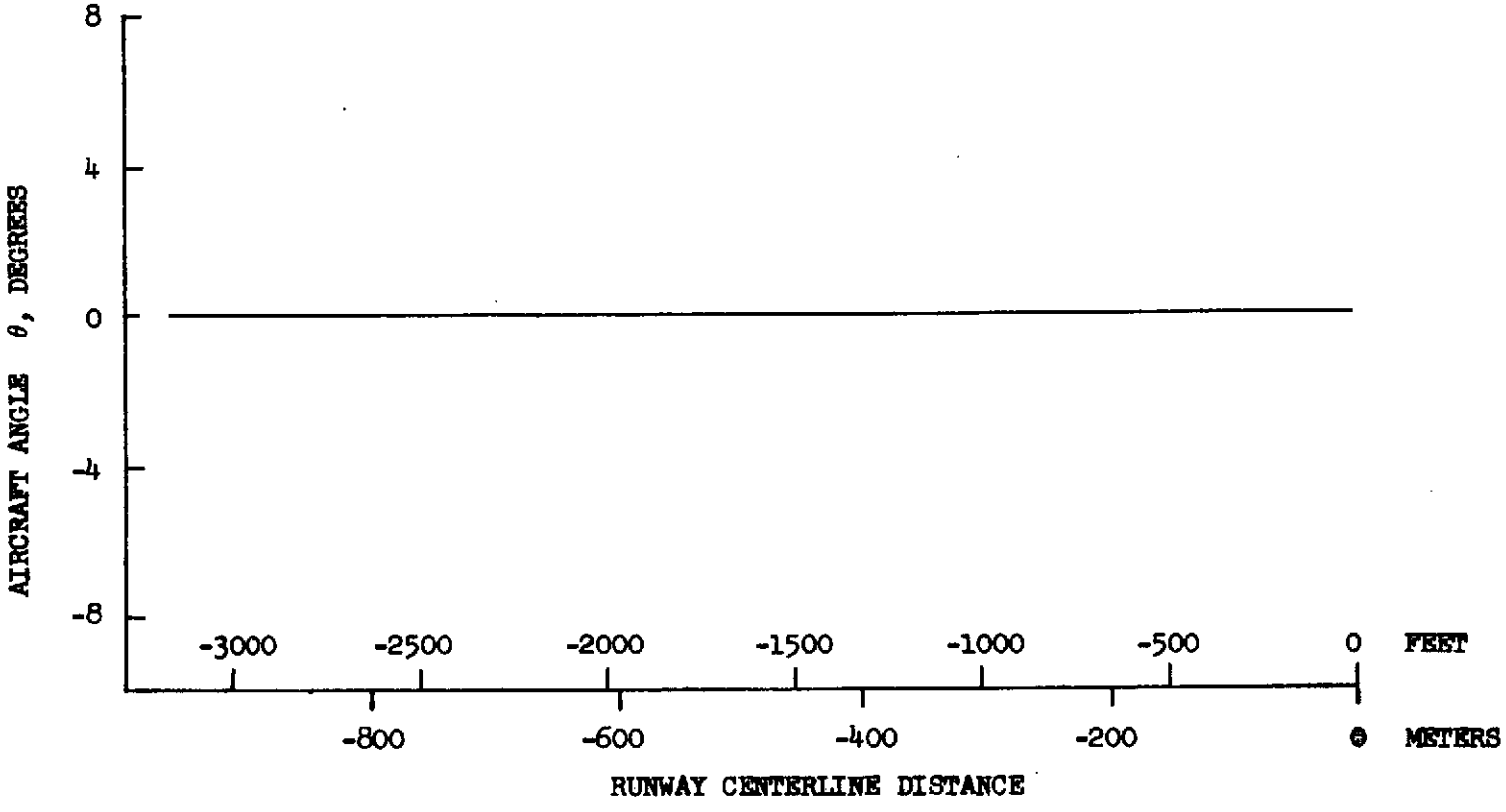

FIGURE 23 PHASE I AIRCRAFT LOW DESCENT APPROACH ATTITUDE SCHEDULE

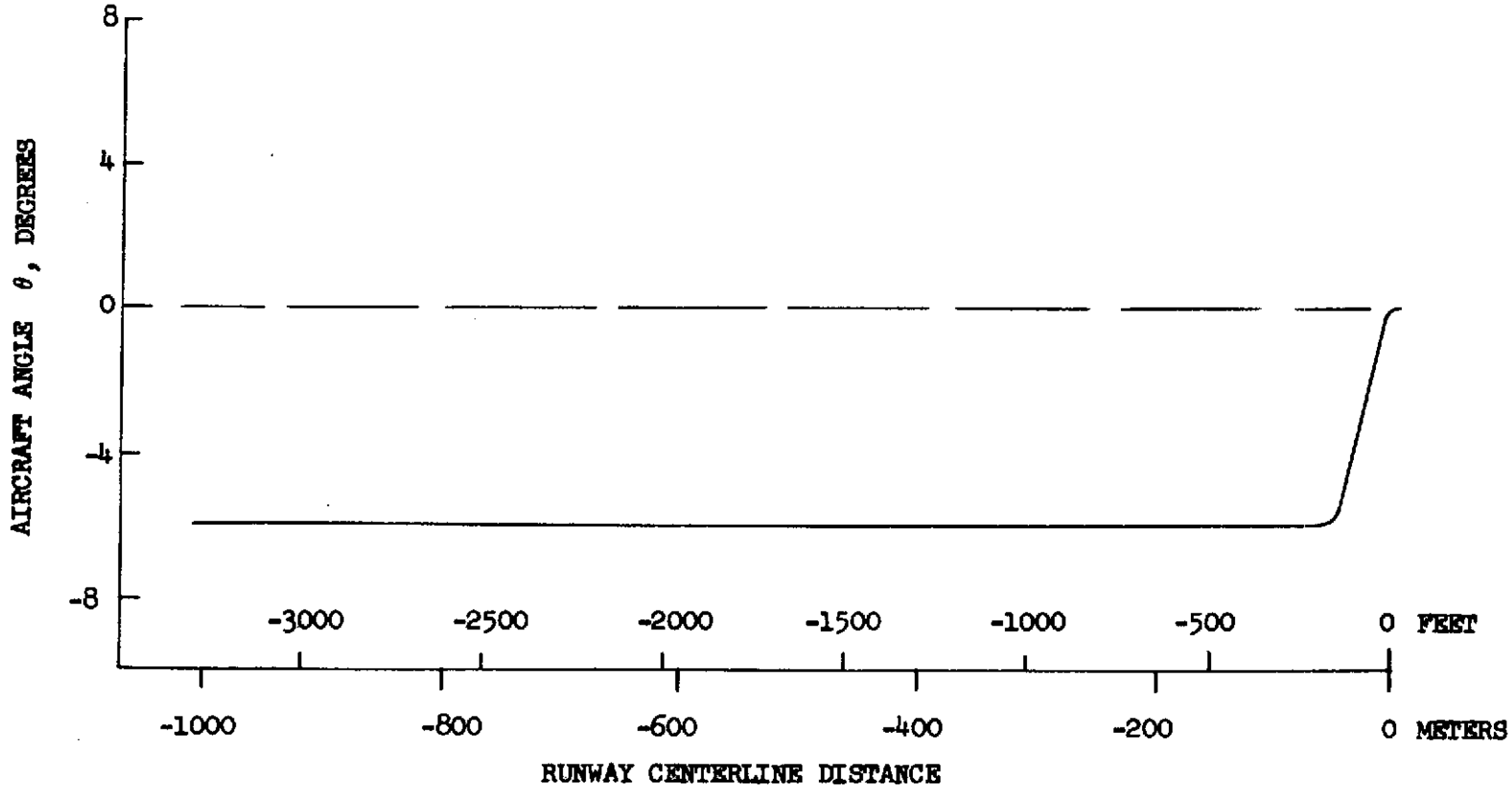

FIGURE 24 PHASE I AIRCRAFT HIGH DESCENT APPROACH ATTITUDE SCHEDULE

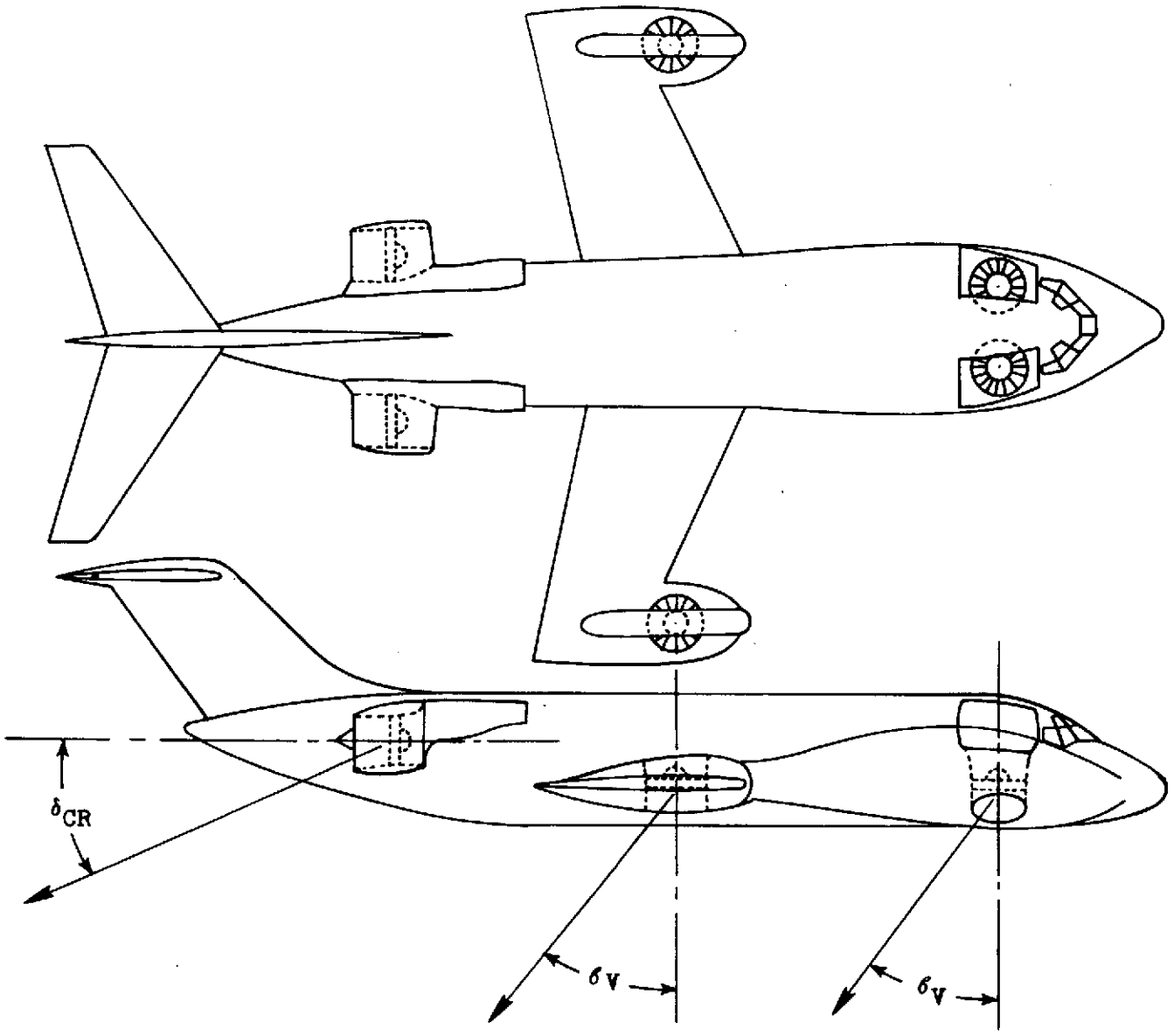

FIGURE 25 PHASE II AIRCRAFT PLAN VIEW AND THRUST VECTOR ANGULAR REFERENCE

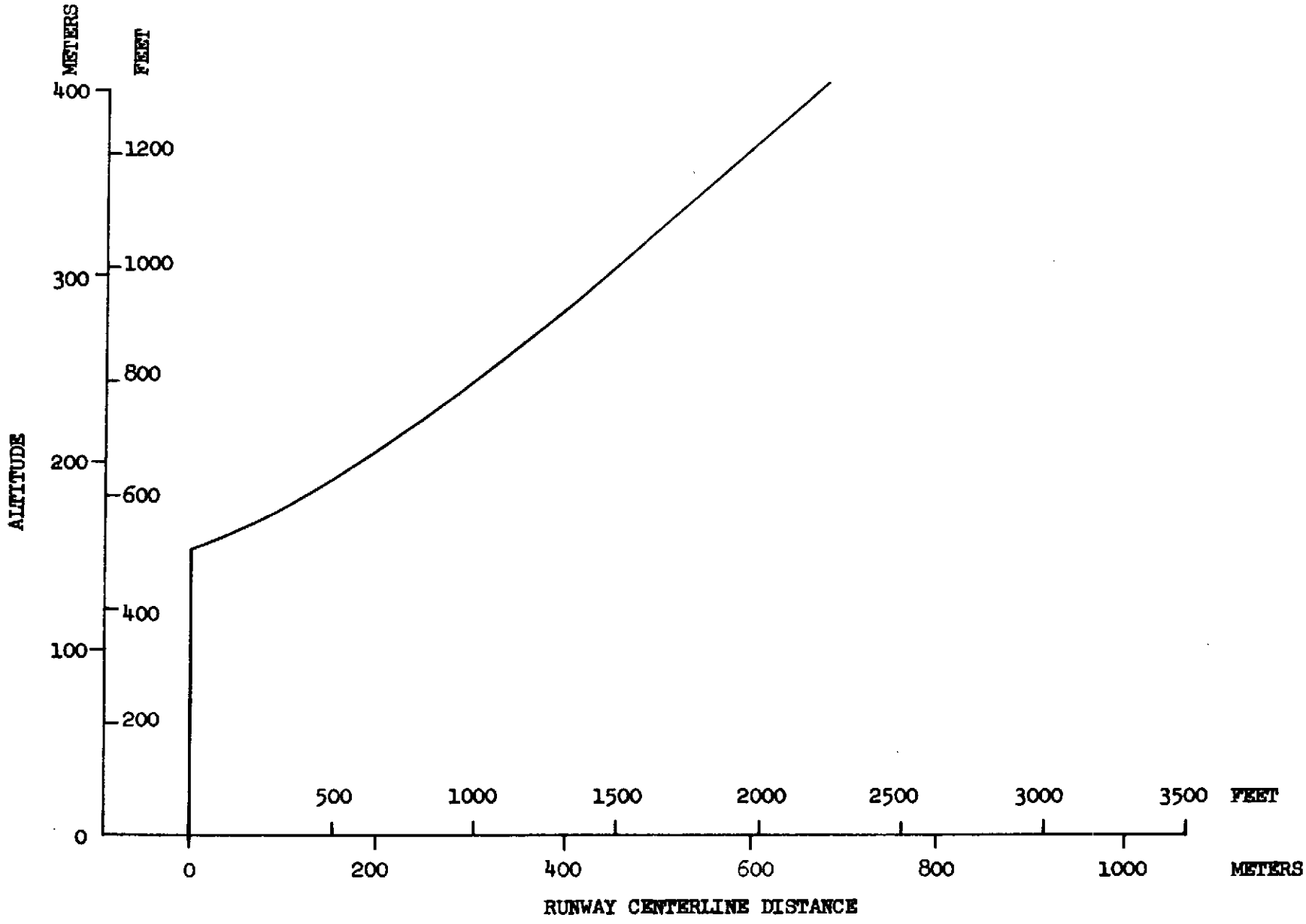

FIGURE 26 PHASE II AIRCRAFT TAKEOFF PATH

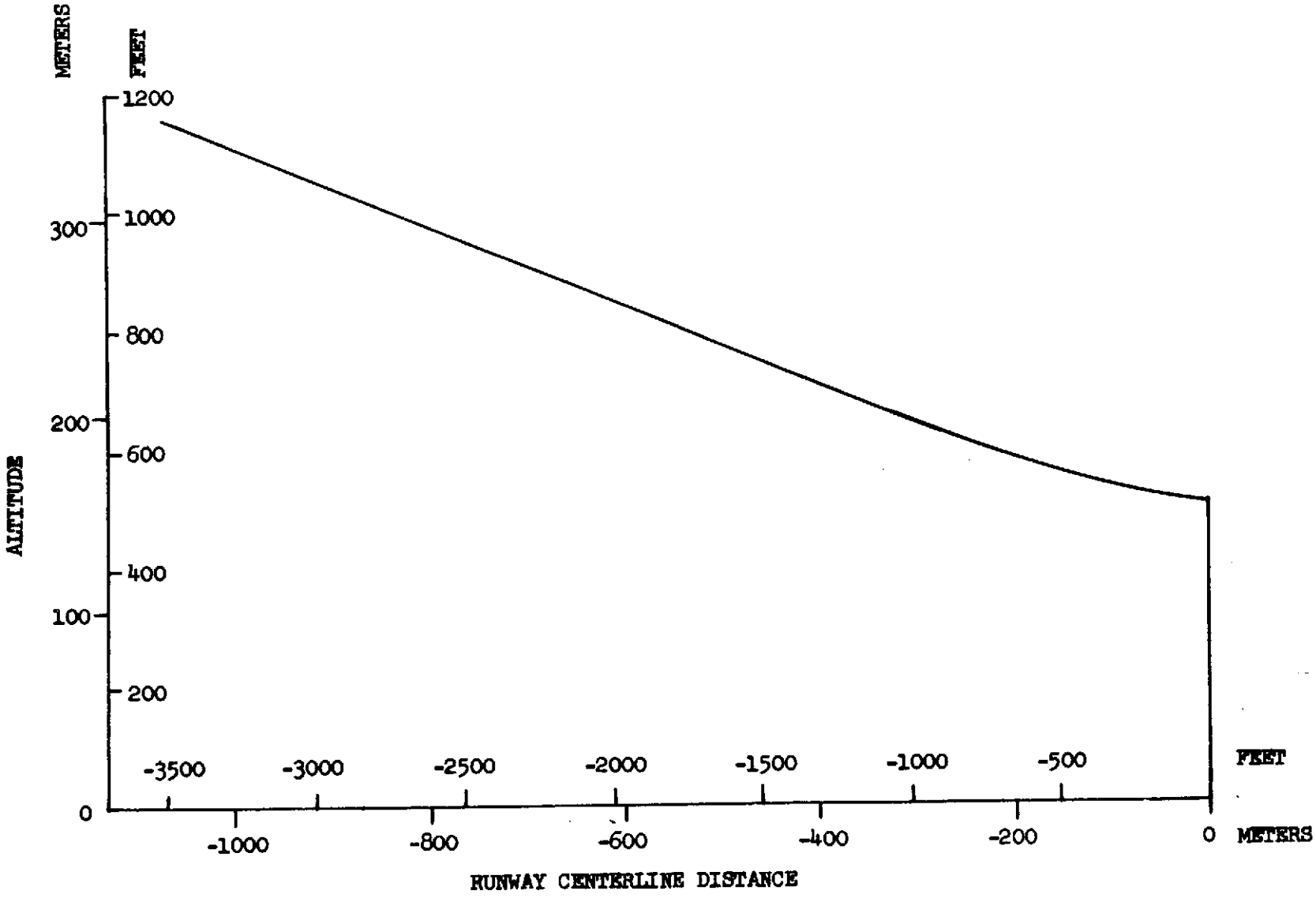

FIGURE 27 PHASE II AIRCRAFT APPROACH PATH

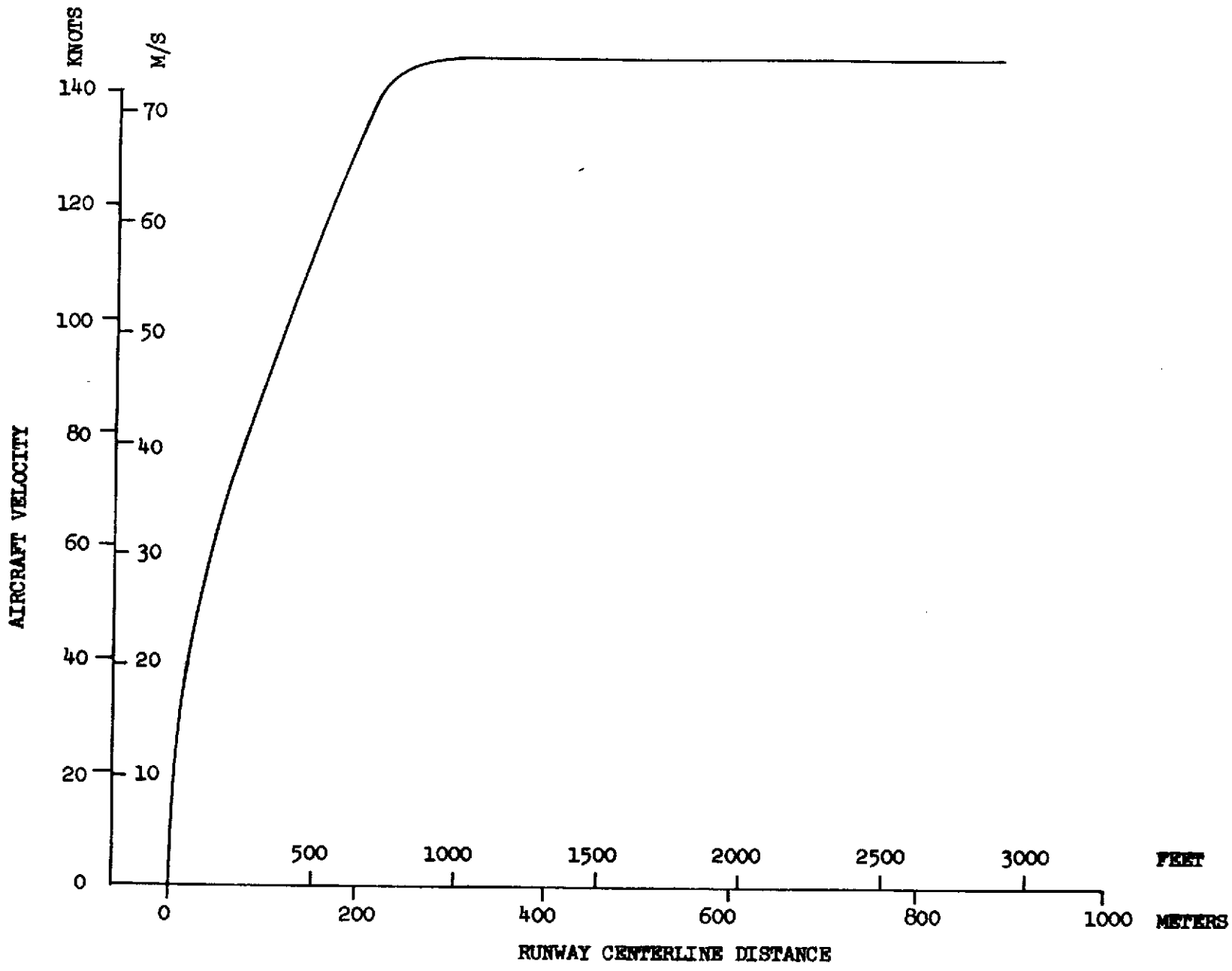

FIGURE 28 PHASE II AIRCRAFT TAKEOFF VELOCITY

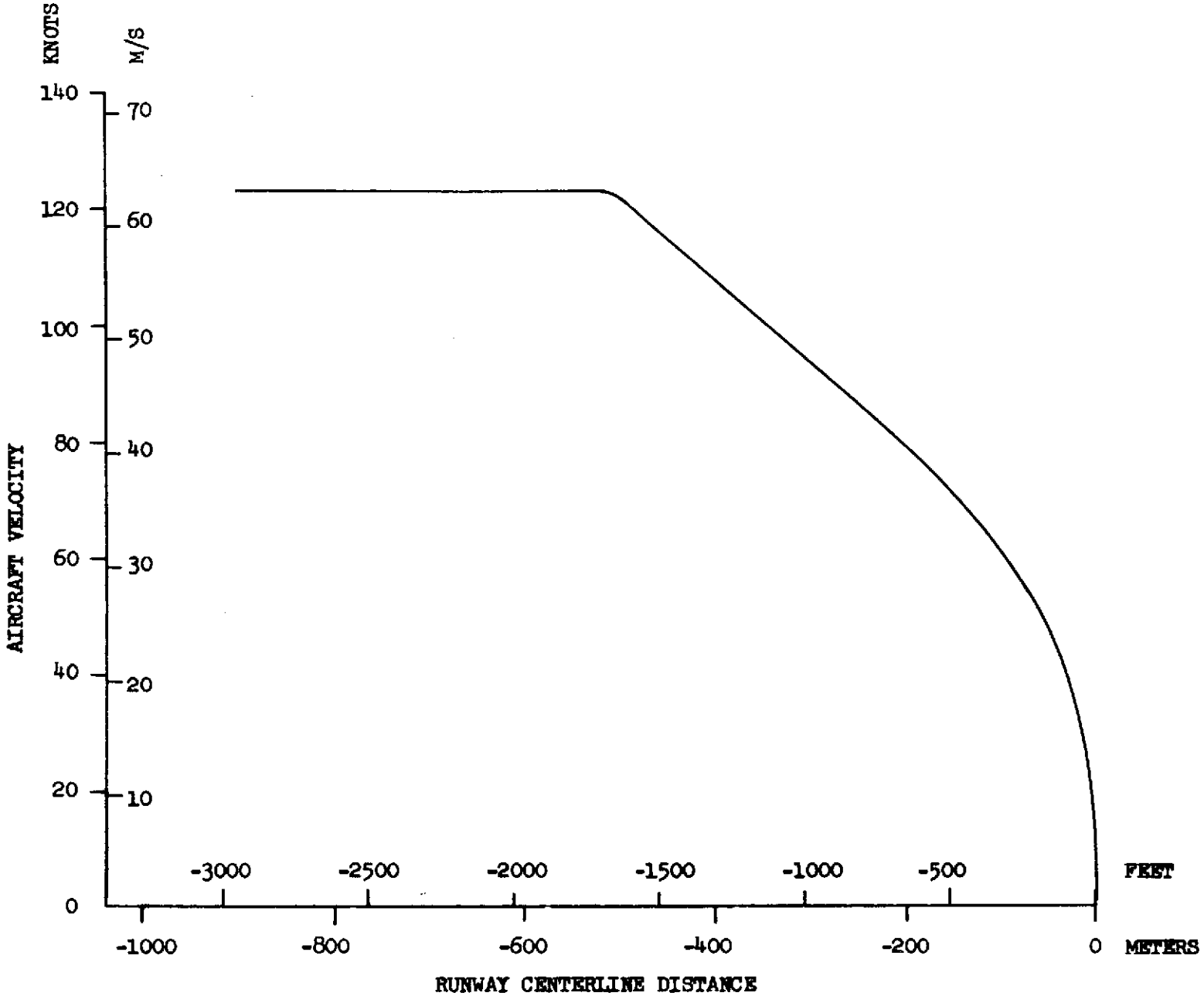

FIGURE 29 PHASE II AIRCRAFT APPROACH VELOCITY

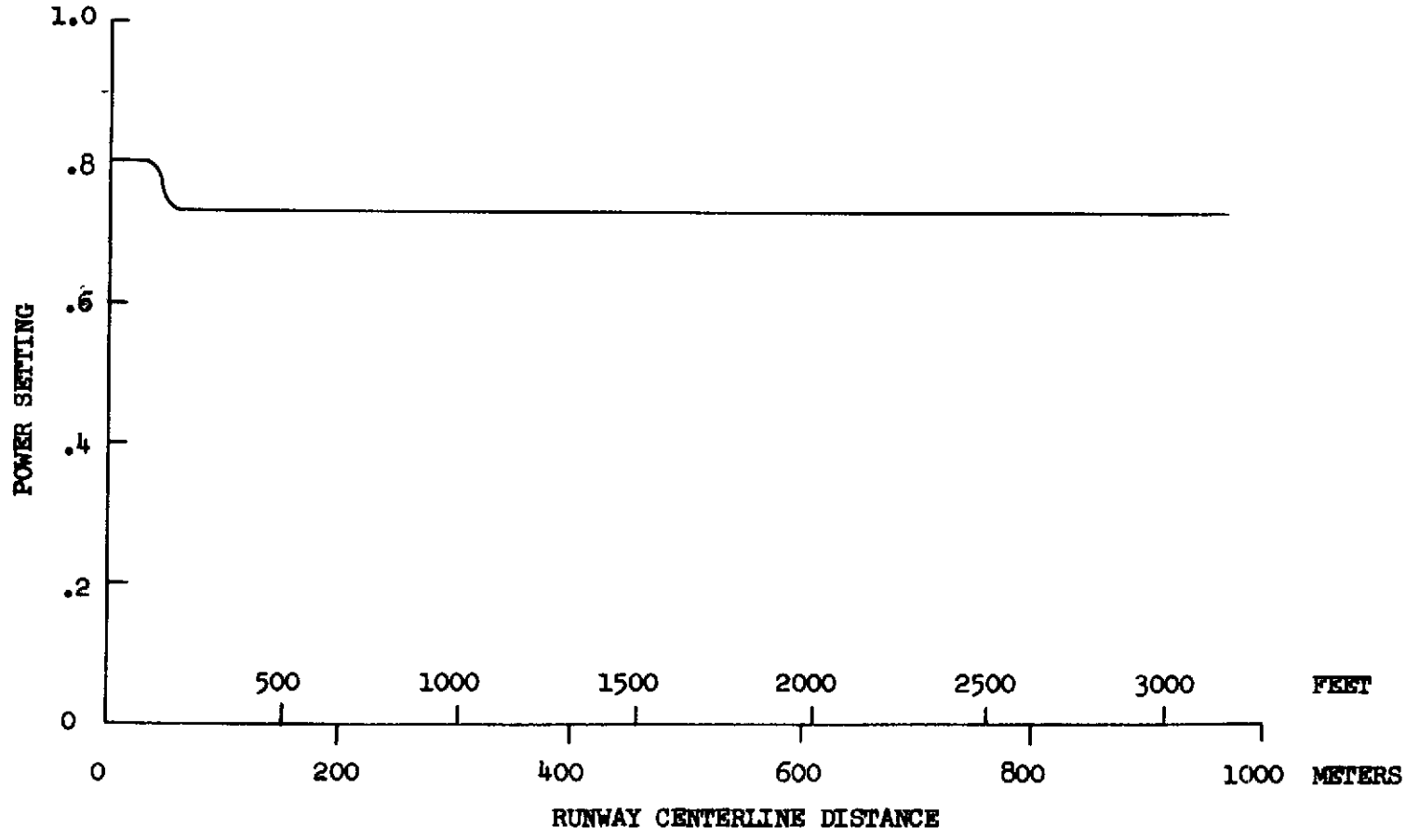

FIGURE 30 PHASE II AIRCRAFT TAKEOFF POWER SETTING

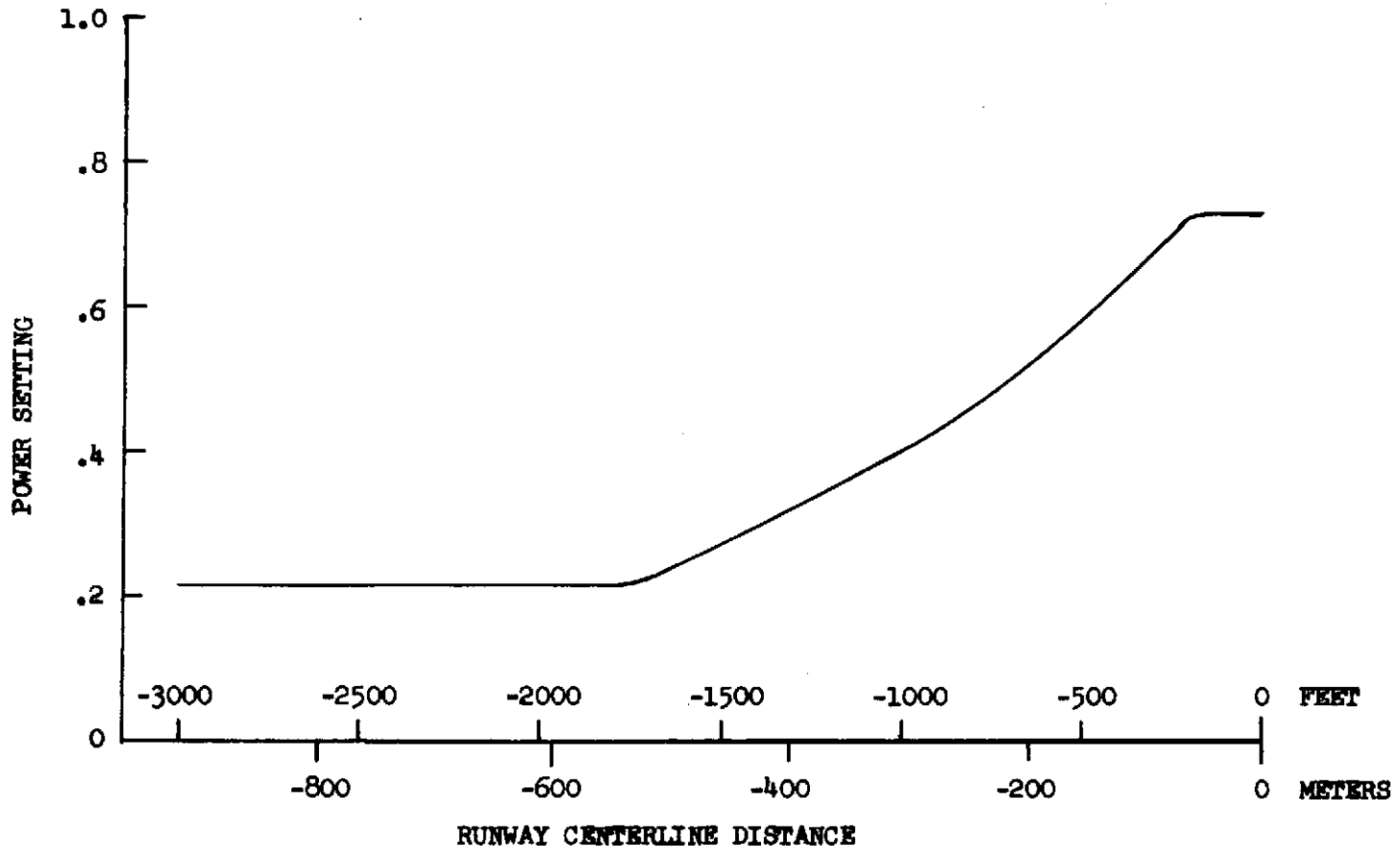

FIGURE 31 PHASE II AIRCRAFT APPROACH POWER SETTING

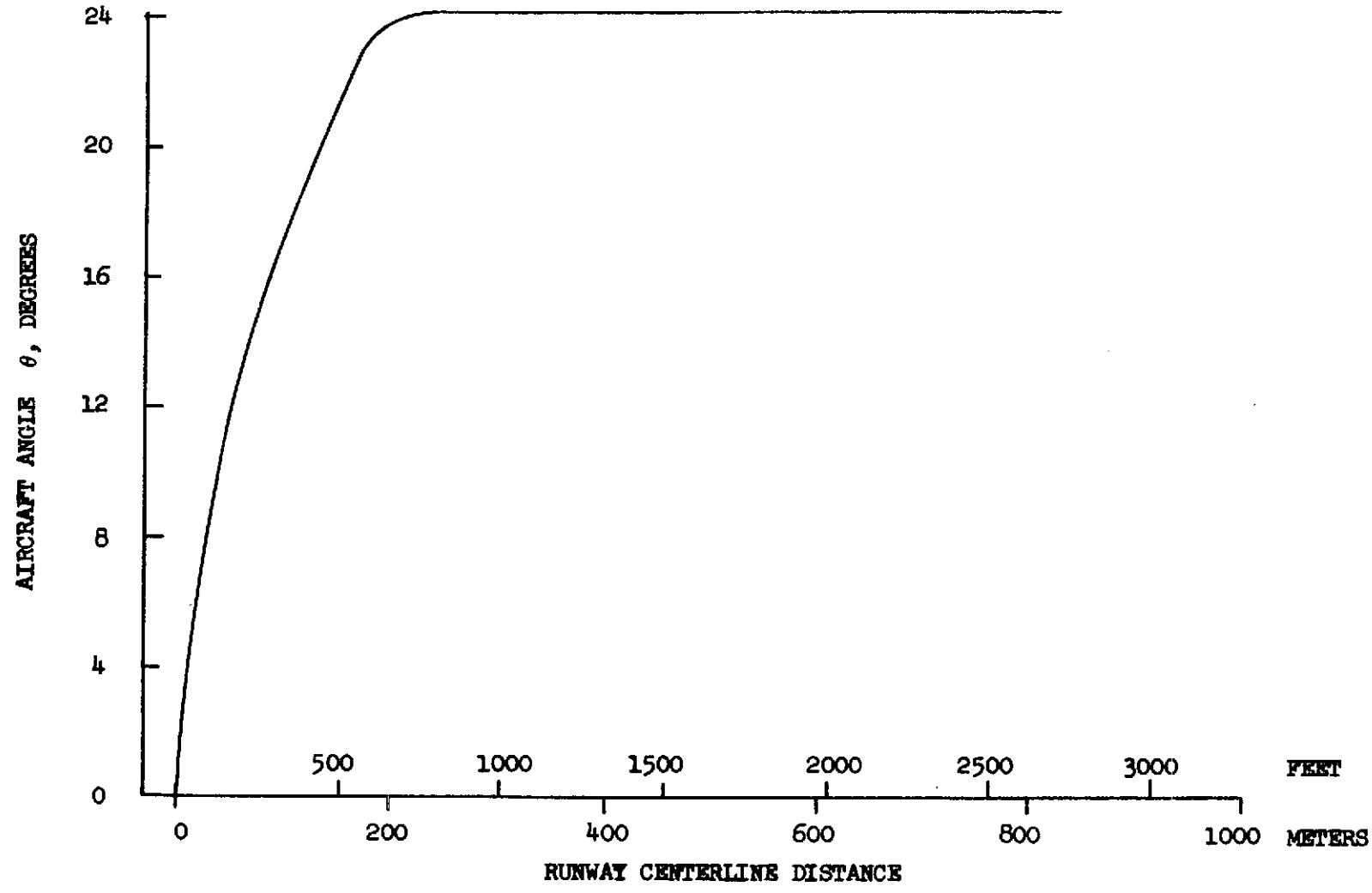

FIGURE 32 PHASE II AIRCRAFT TAKEOFF ATTITUDE SCHEDULE

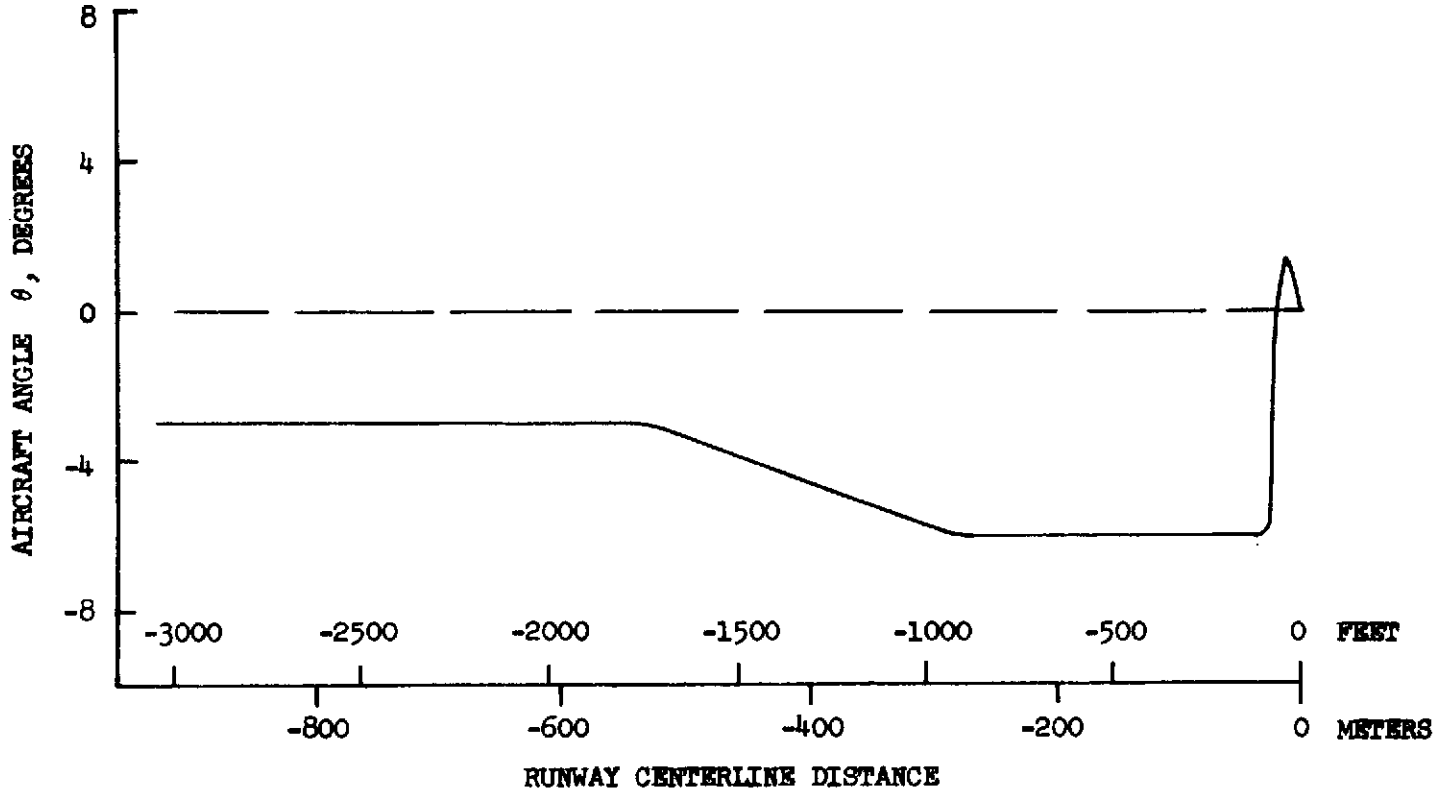

FIGURE 33 PHASE II AIRCRAFT APPROACH ATTITUDE SCHEDULE

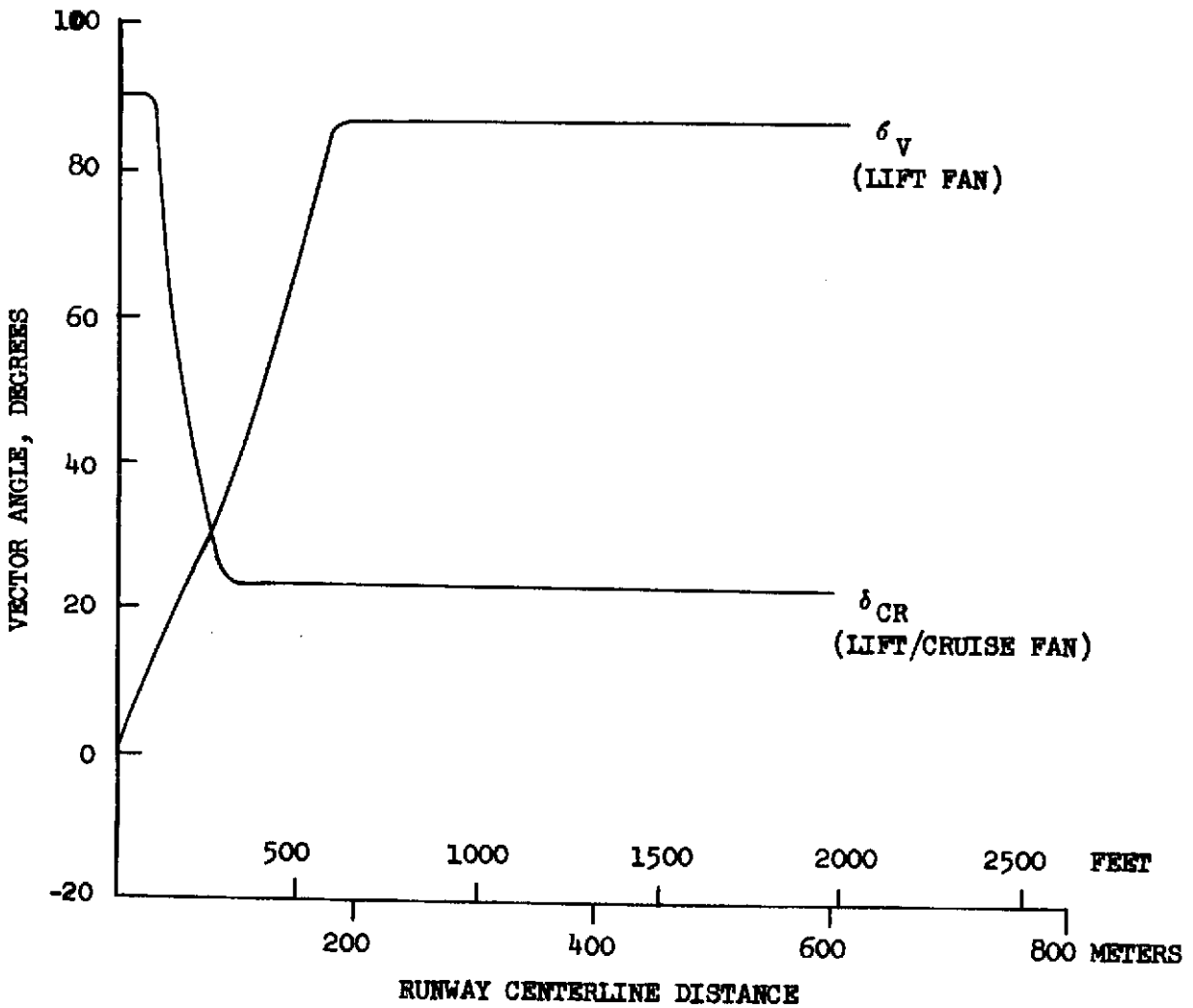

FIGURE 34 PHASE II AIRCRAFT TAKEOFF THRUST VECTOR SCHEDULES

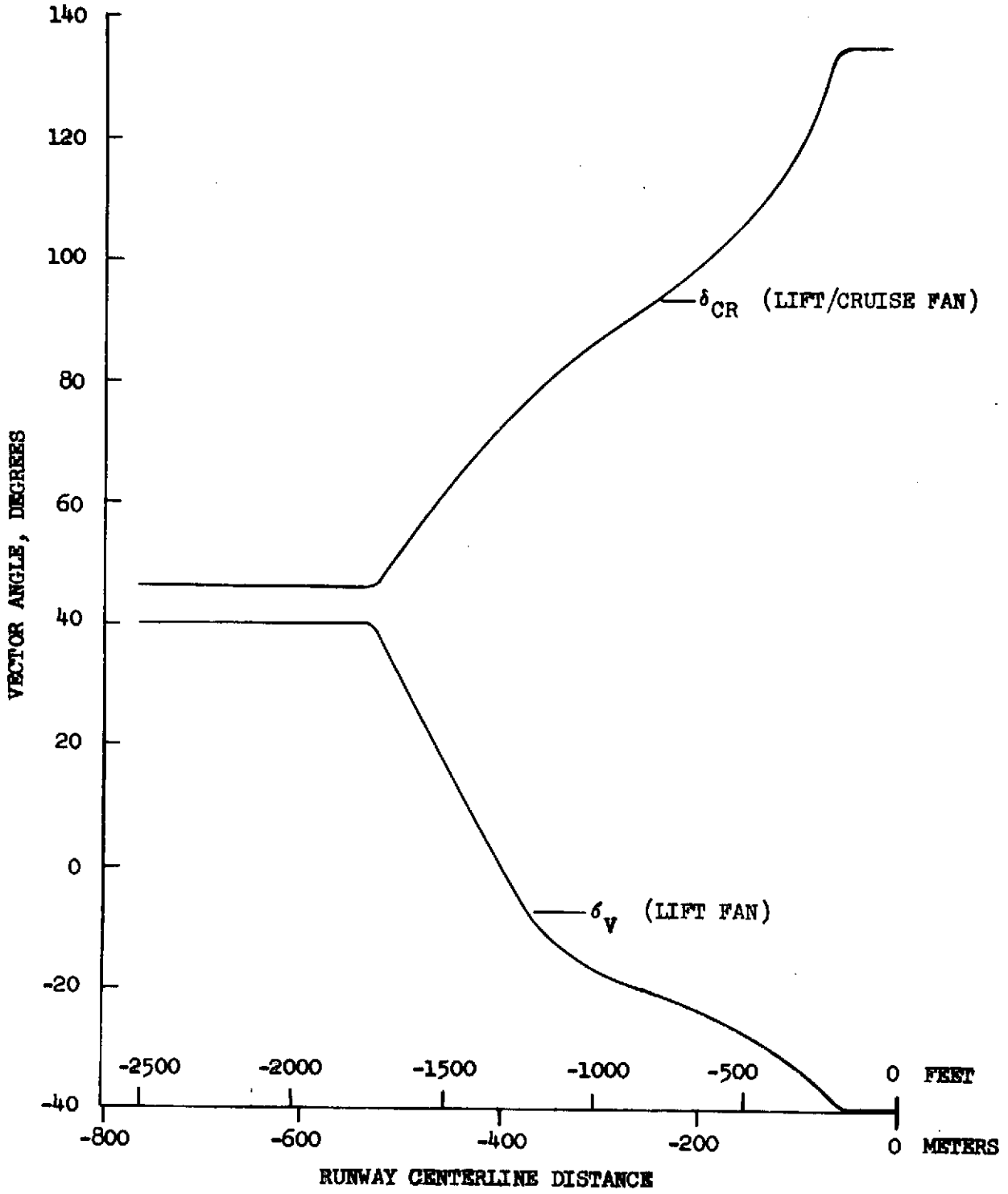

FIGURE 35 PHASE II AIRCRAFT APPROACH THRUST VECTOR SCHEDULES

AREA ENCLOSED BY CONTOUR

95 PNdB	480 ACRES
100 PNdB	255 ACRES
105 PNdB	120 ACRES

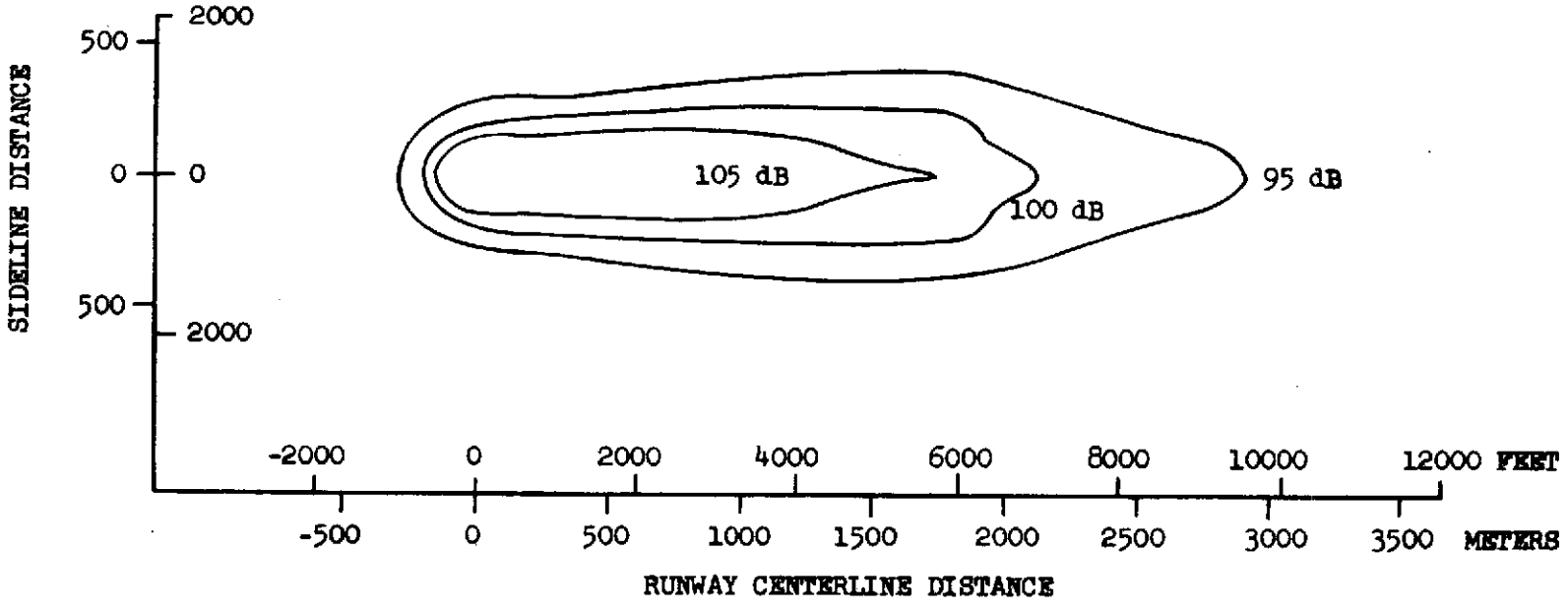

FIGURE 36 PHASE I AIRCRAFT LOW RISE TAKE-OFF PNL CONTOUR

AREA ENCLOSED BY CONTOUR

95 PNdB	315 ACRES
100 PNdB	125 ACRES
105 PNdB	37 ACRES

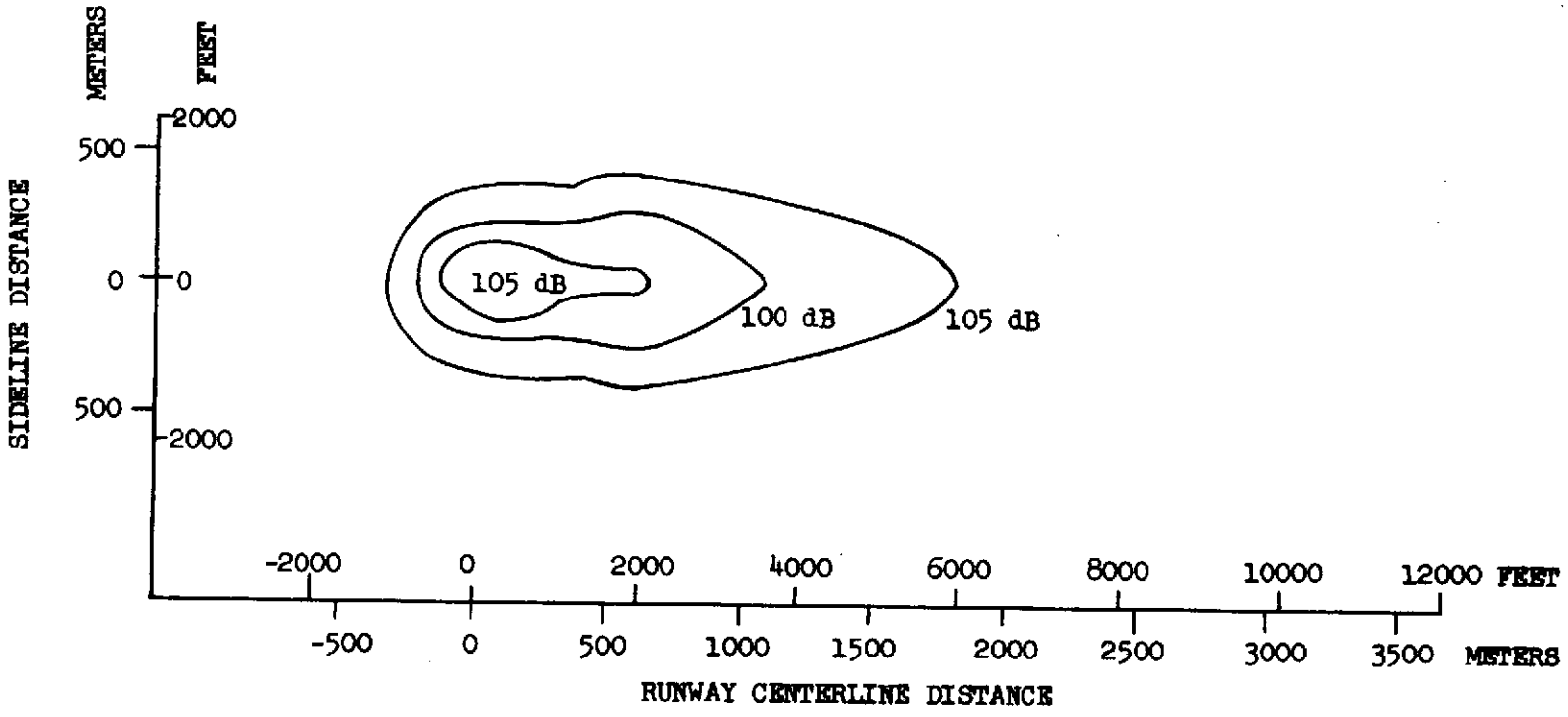

FIGURE 37 PHASE I AIRCRAFT HIGH RISE TAKE-OFF PNL CONTOUR

AREA ENCLOSED BY CONTOUR

95 EPNdB	670 ACRES
100 EPNdB	420 ACRES
105 EPNdB	225 ACRES

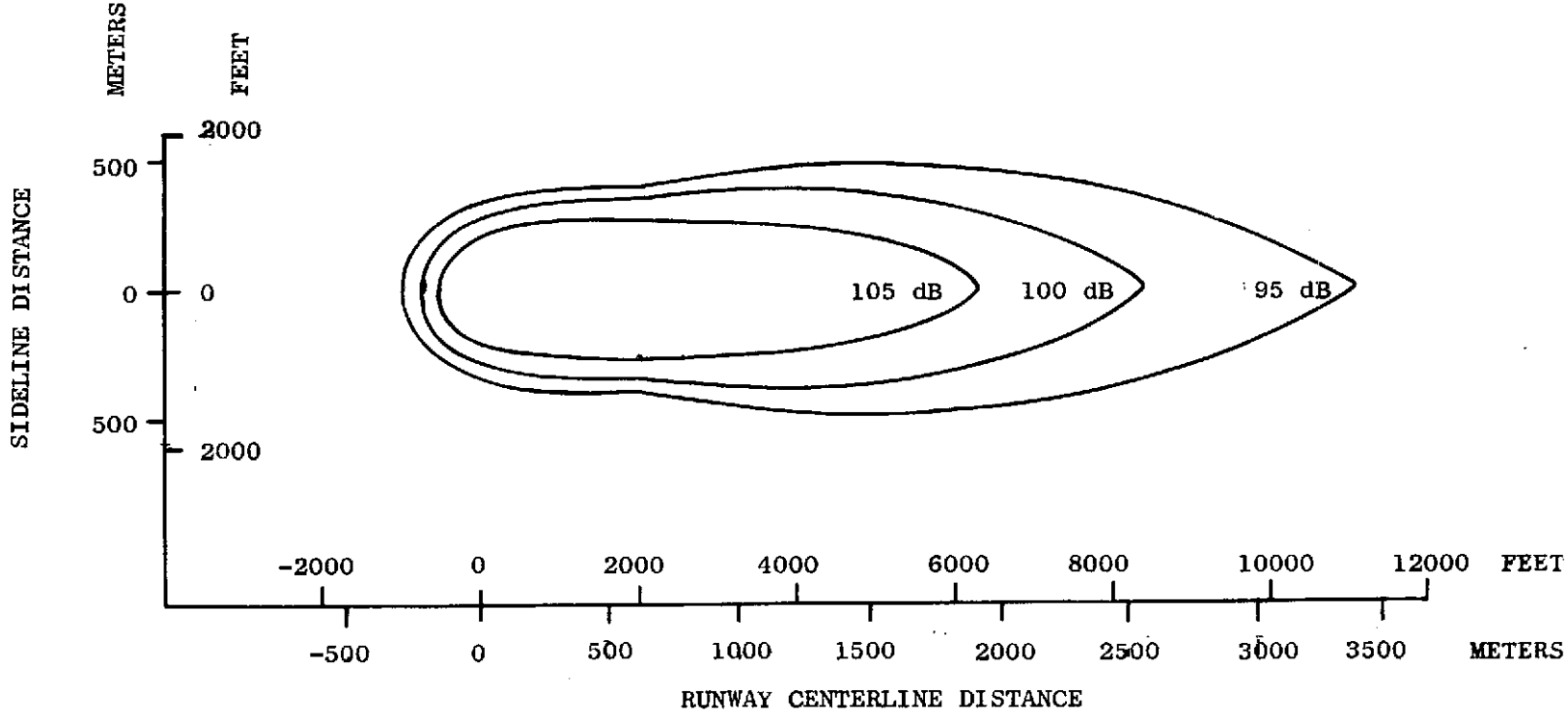

FIGURE 38 PHASE I AIRCRAFT LOW RISE TAKEOFF EPNL CONTOUR

AREA ENCLOSED BY CONTOUR

95 EPNdB	515 ACRES
100 EPNdB	295 ACRES
105 EPNdB	145 ACRES

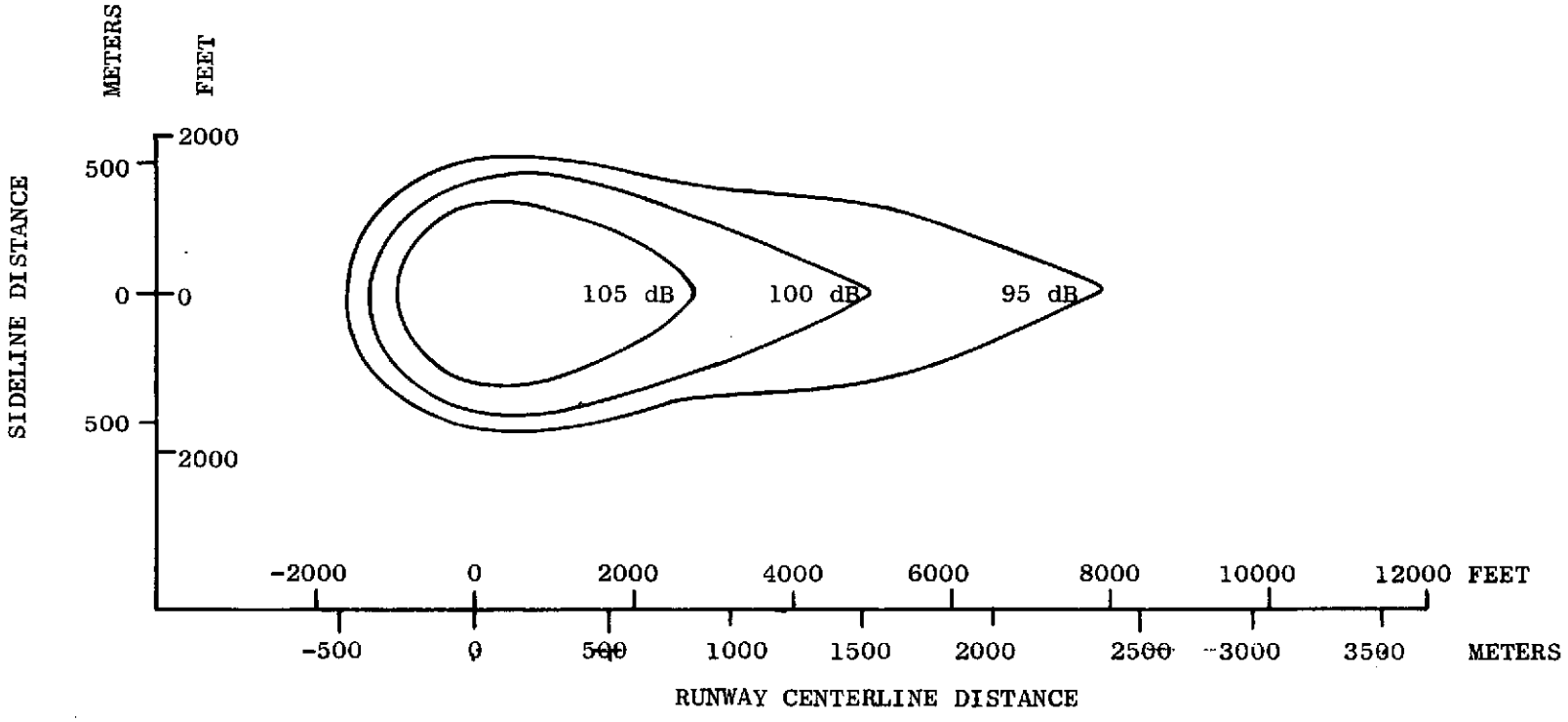

FIGURE 39 PHASE I AIRCRAFT HIGH RISE TAKEOFF EPNL CONTOUR

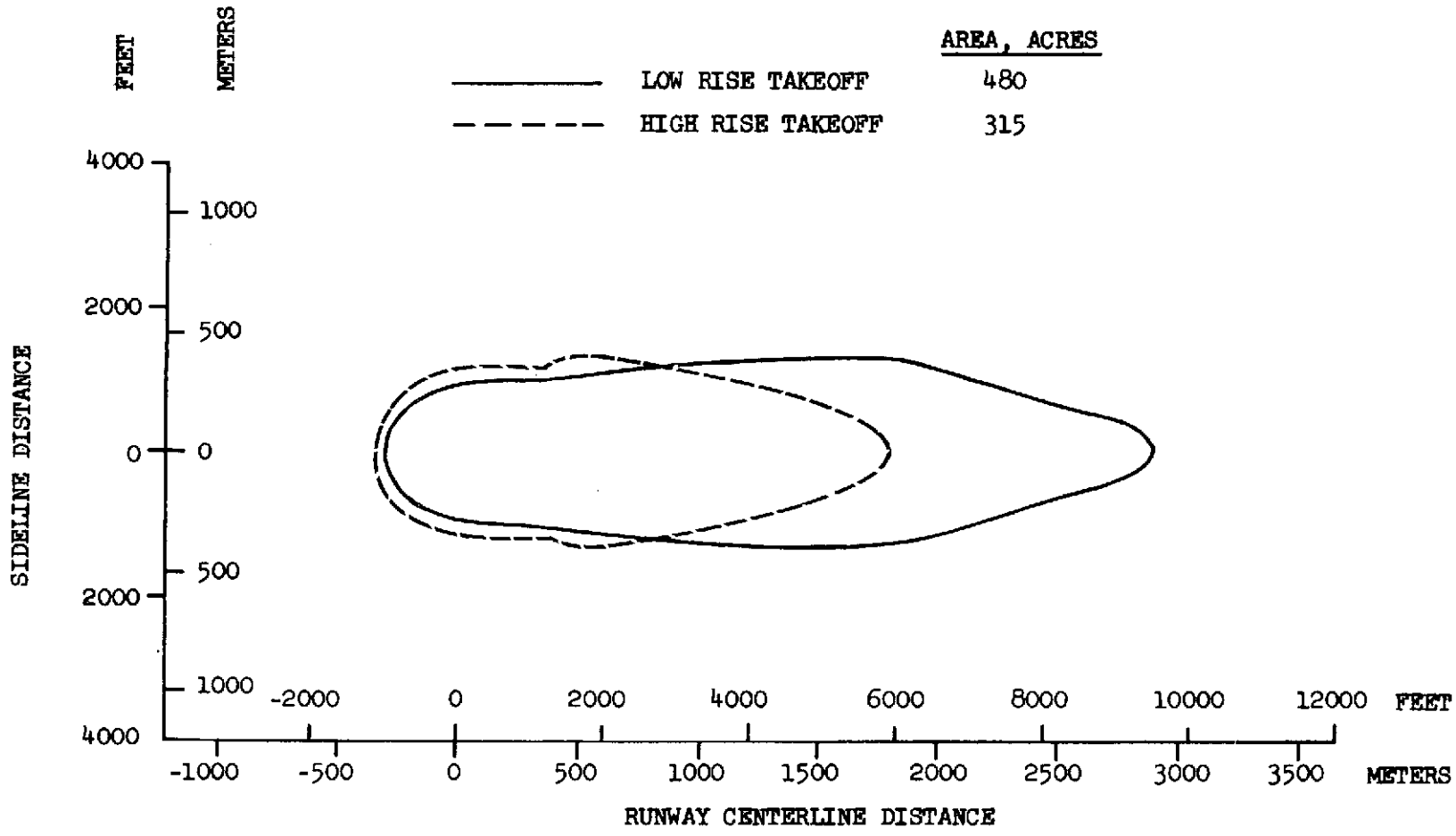

FIGURE 40 PHASE I AIRCRAFT TAKEOFF 95 PNL CONTOUR COMPARISON

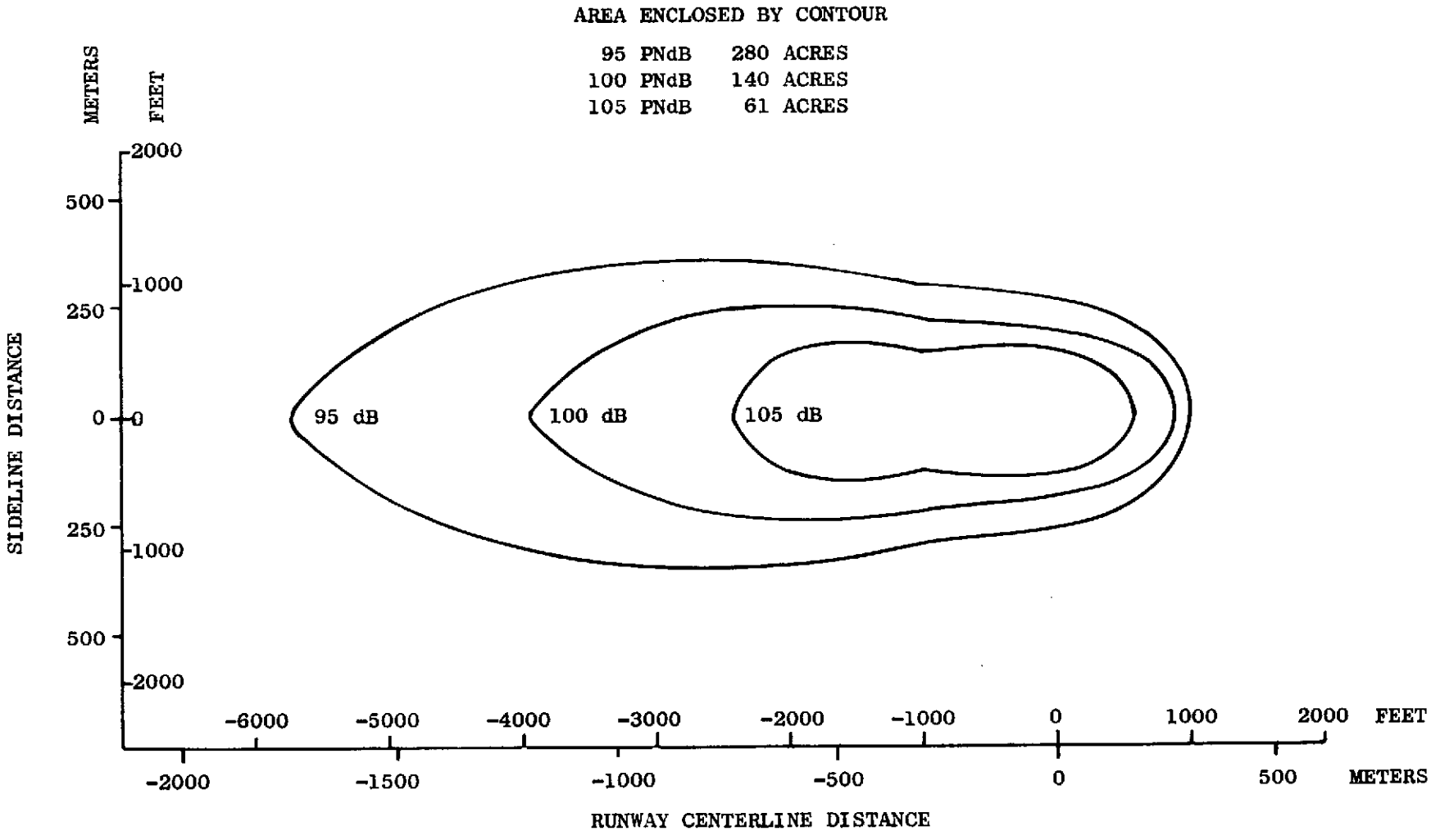

FIGURE 41 PHASE I AIRCRAFT LOW DESCENT APPROACH PNL CONTOUR

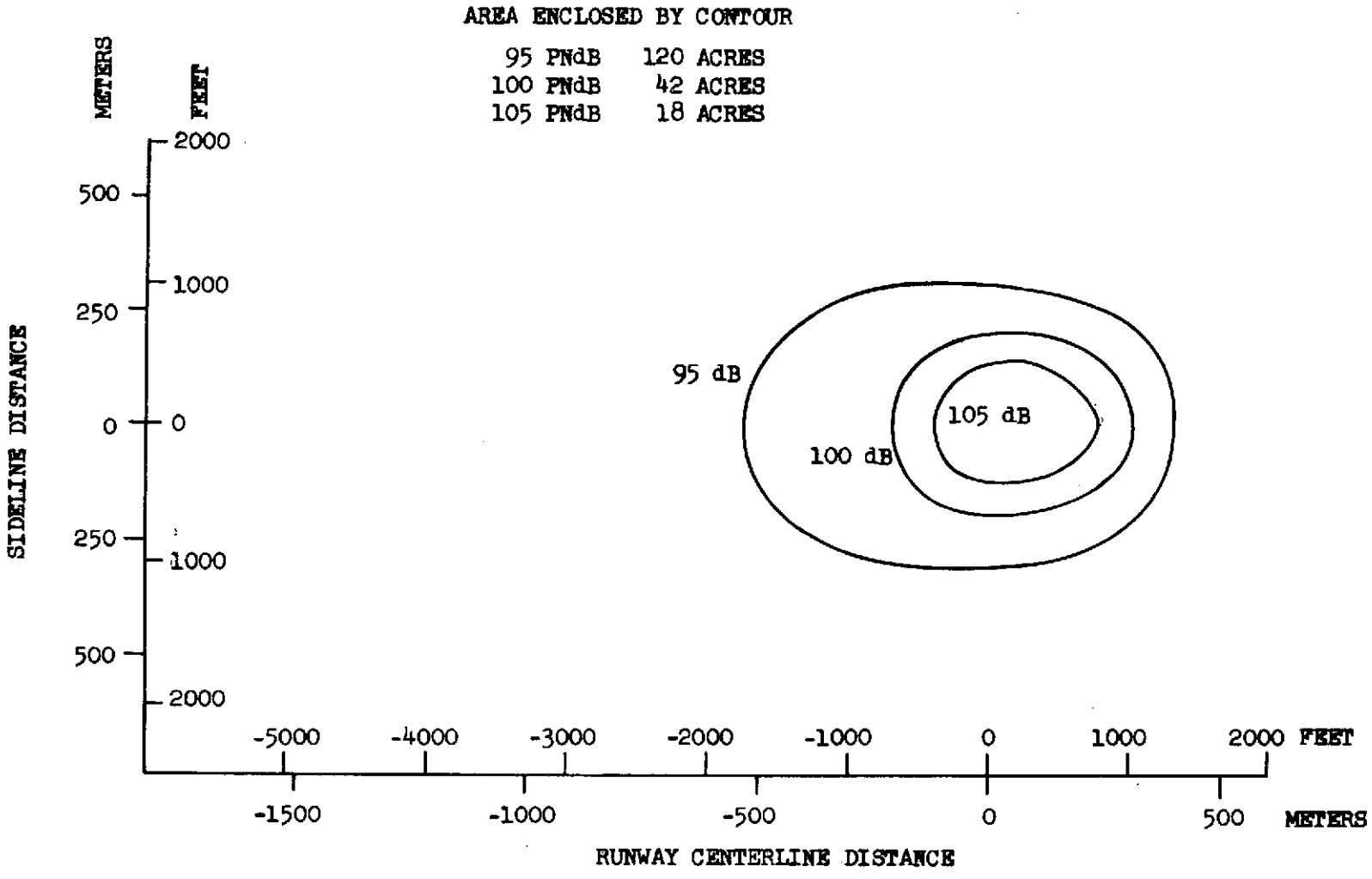

FIGURE 42 PHASE I AIRCRAFT HIGH DESCENT APPROACH PNL CONTOUR

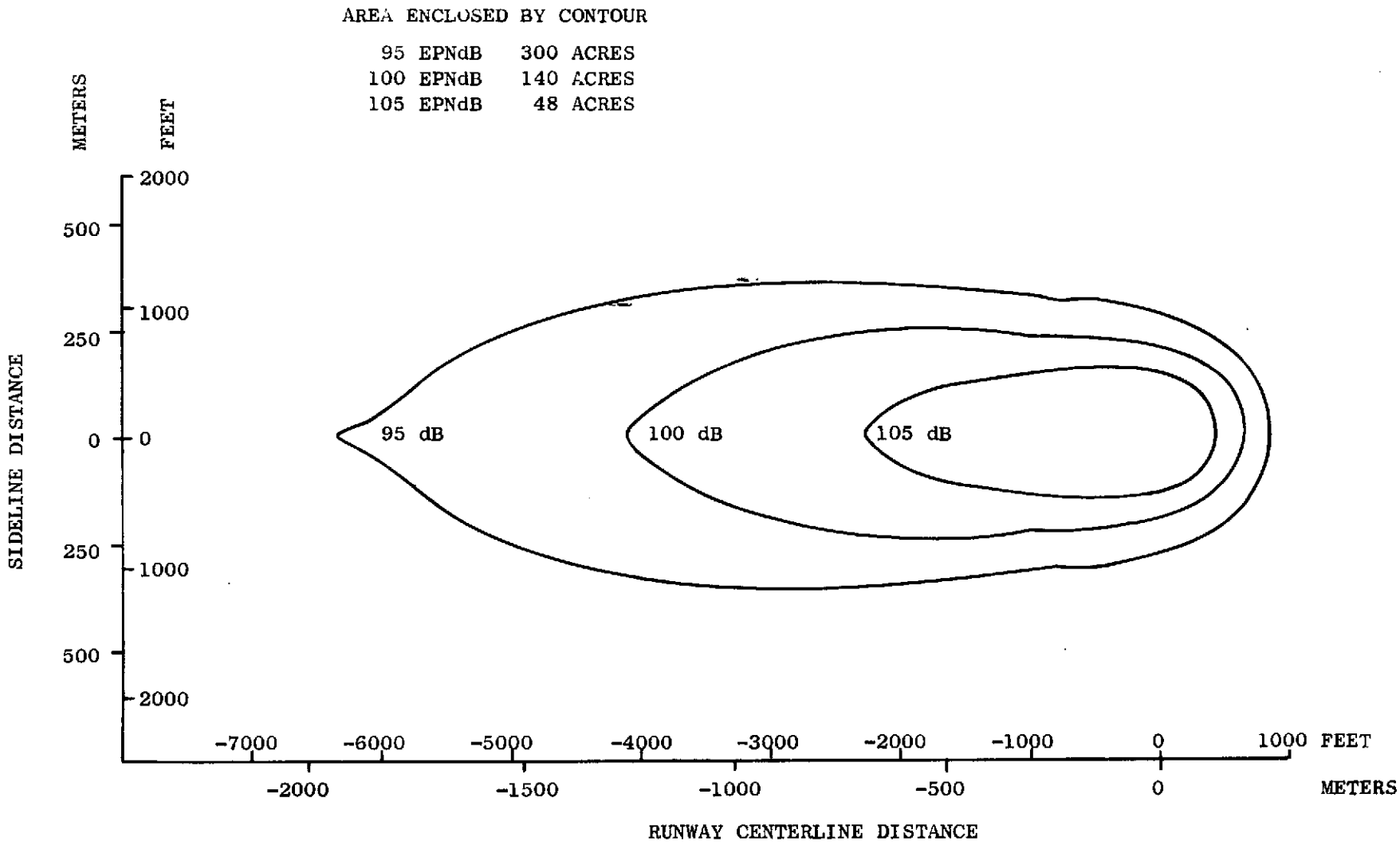

FIGURE 43 PHASE I AIRCRAFT LOW DESCENT APPROACH EPNL CONTOUR

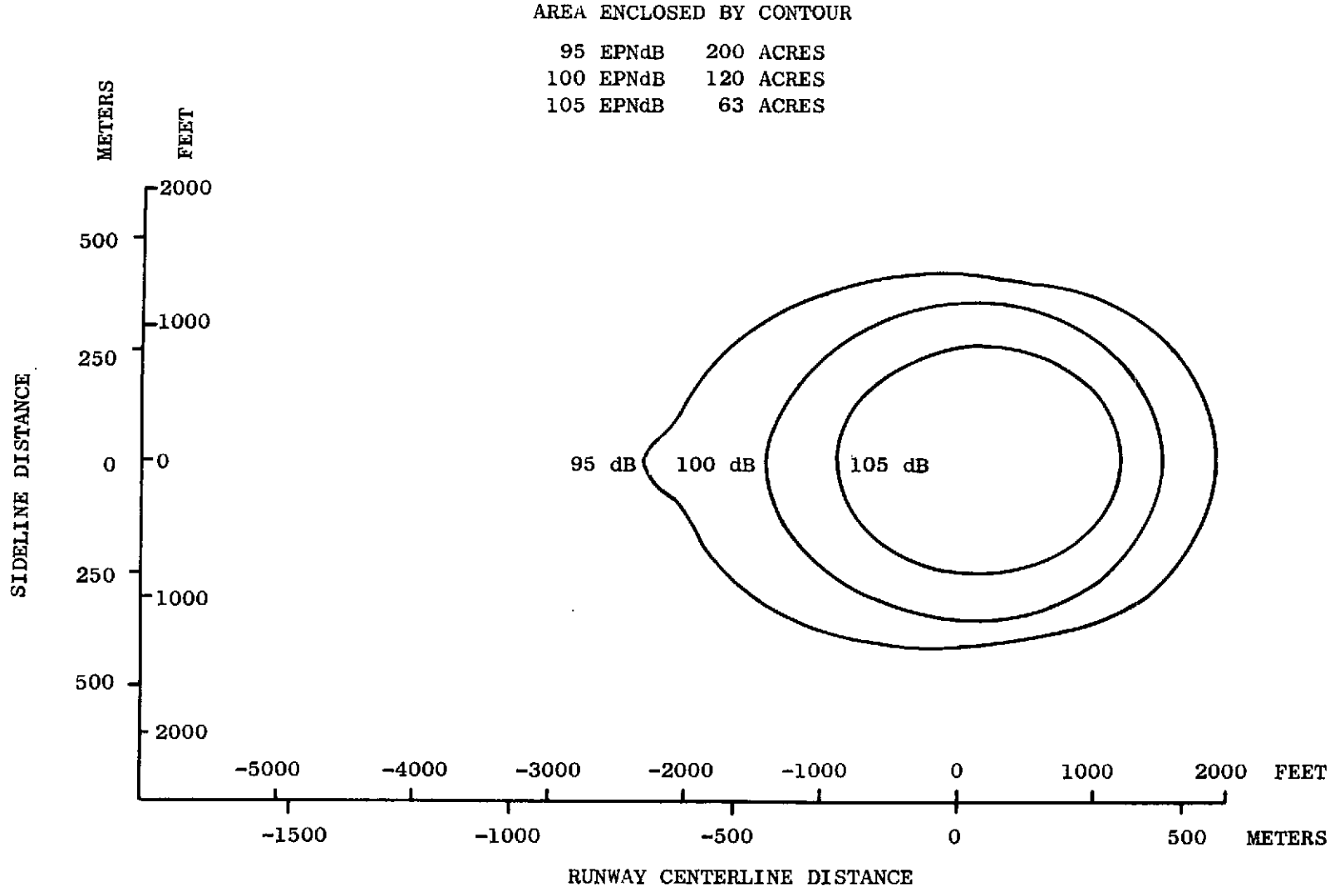

FIGURE 44 PHASE I AIRCRAFT HIGH DESCENT APPROACH EPNL CONTOUR

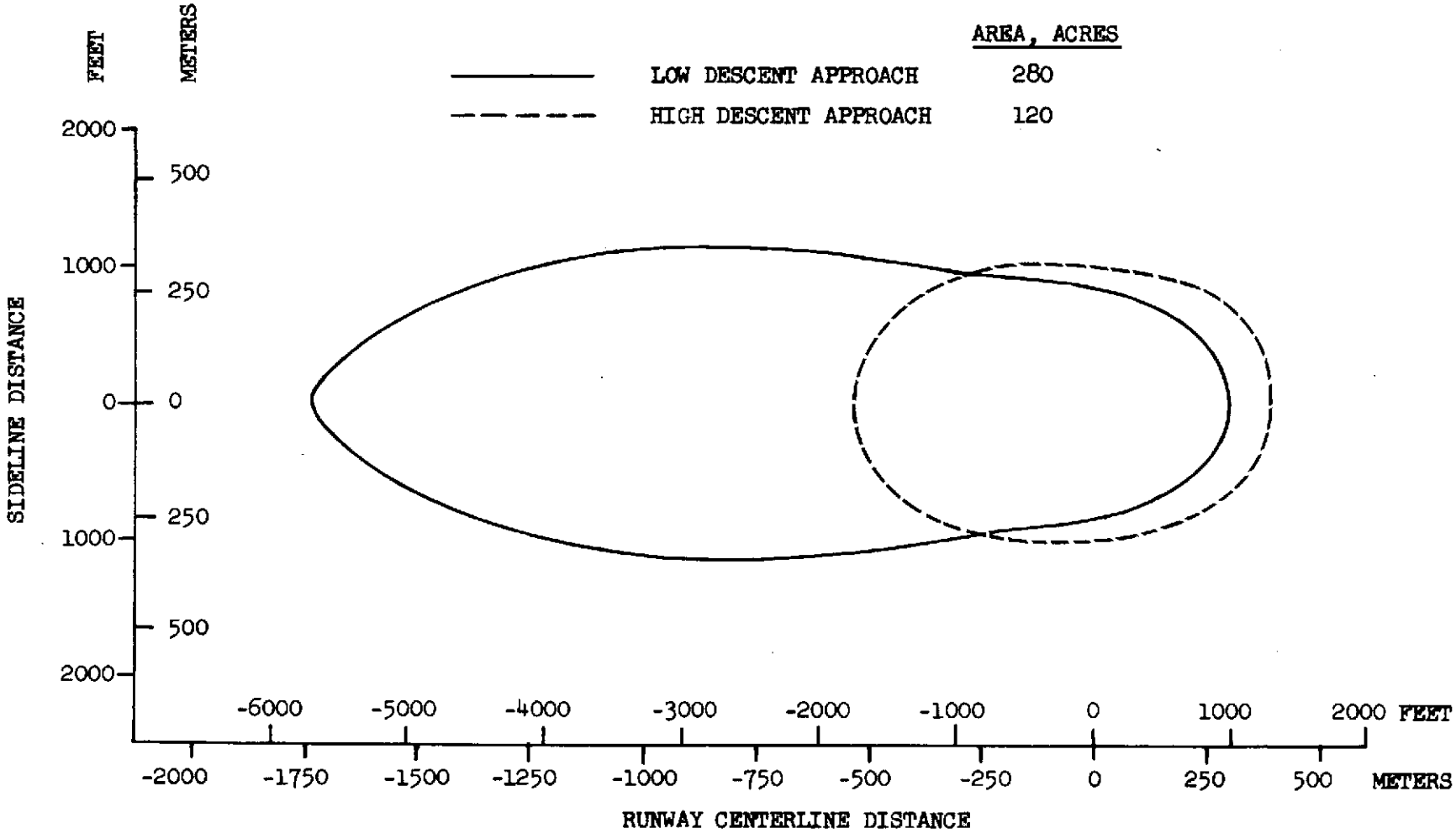

FIGURE 45. PHASE I AIRCRAFT APPROACH 95 PNL CONTOUR COMPARISON

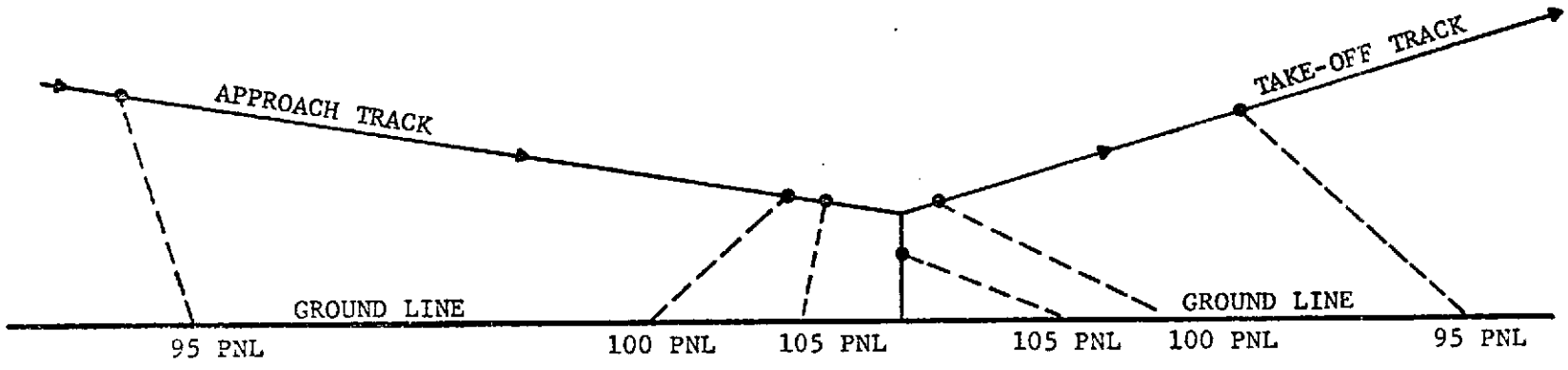

FIGURE 46 PHASE II AIRCRAFT GENERALIZED SOURCE LOCATION ON AIRCRAFT PATH

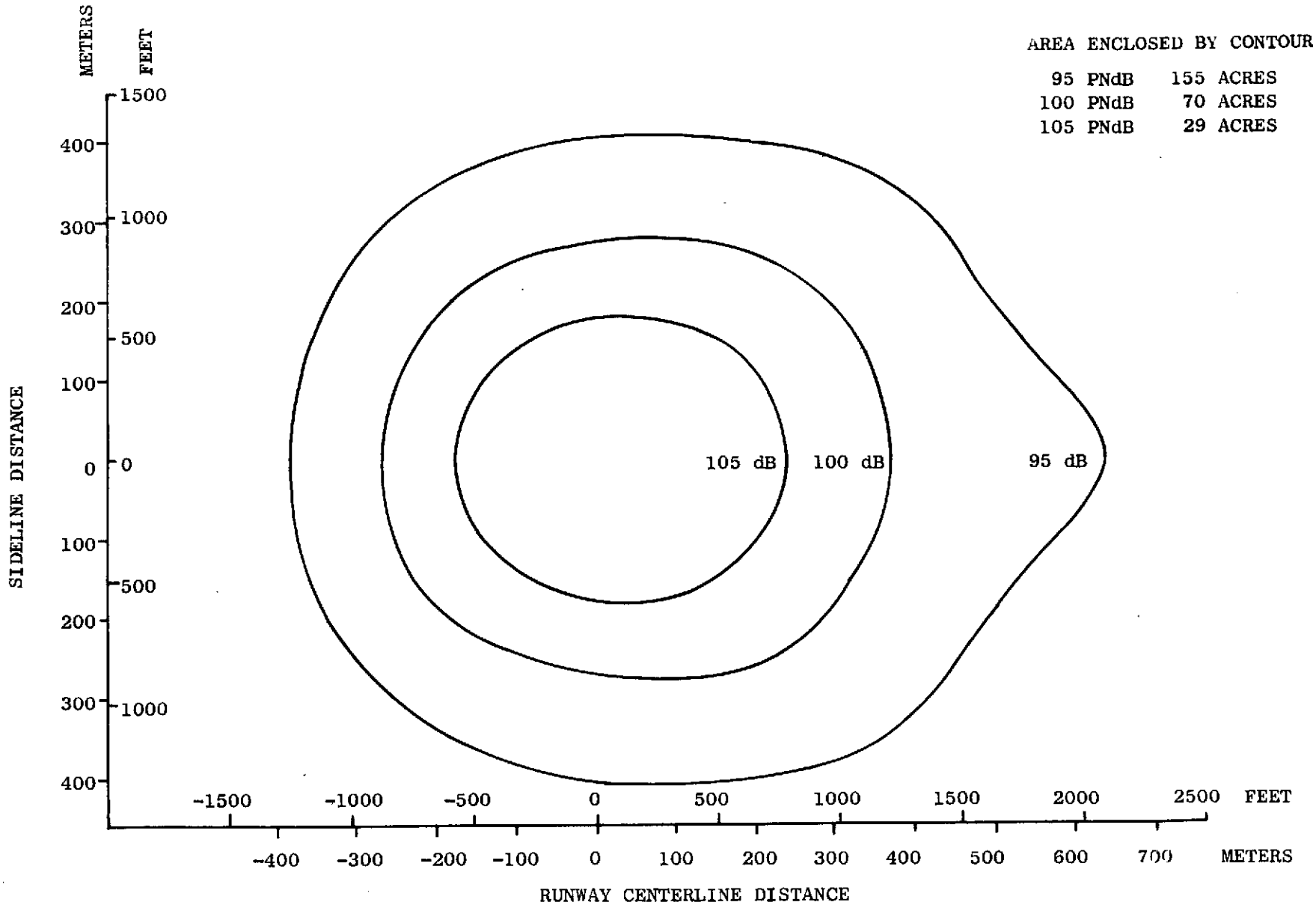

FIGURE 47 PHASE II AIRCRAFT TAKEOFF PNL CONTOUR

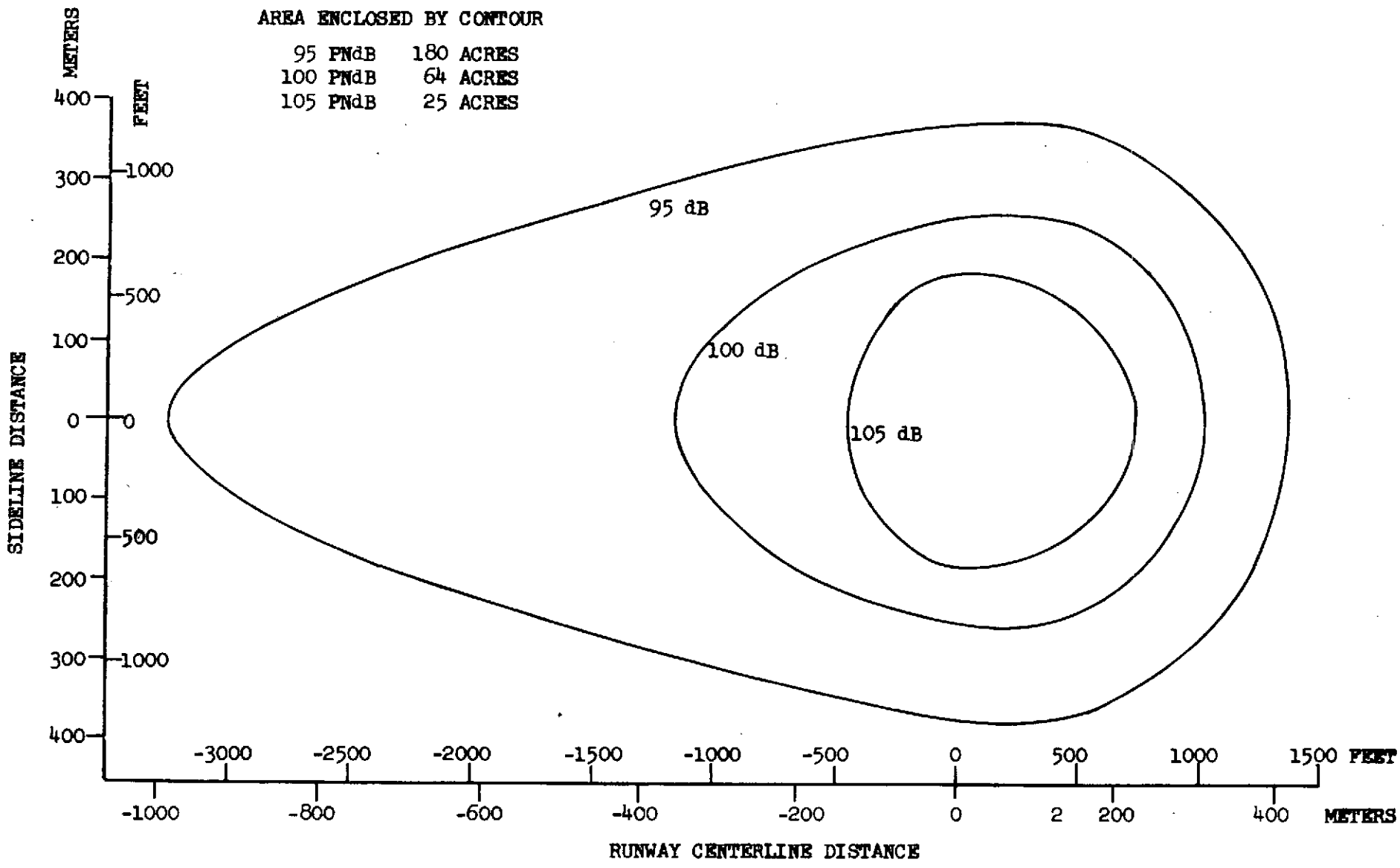

FIGURE 48 PHASE II AIRCRAFT APPROACH PNL CONTOUR

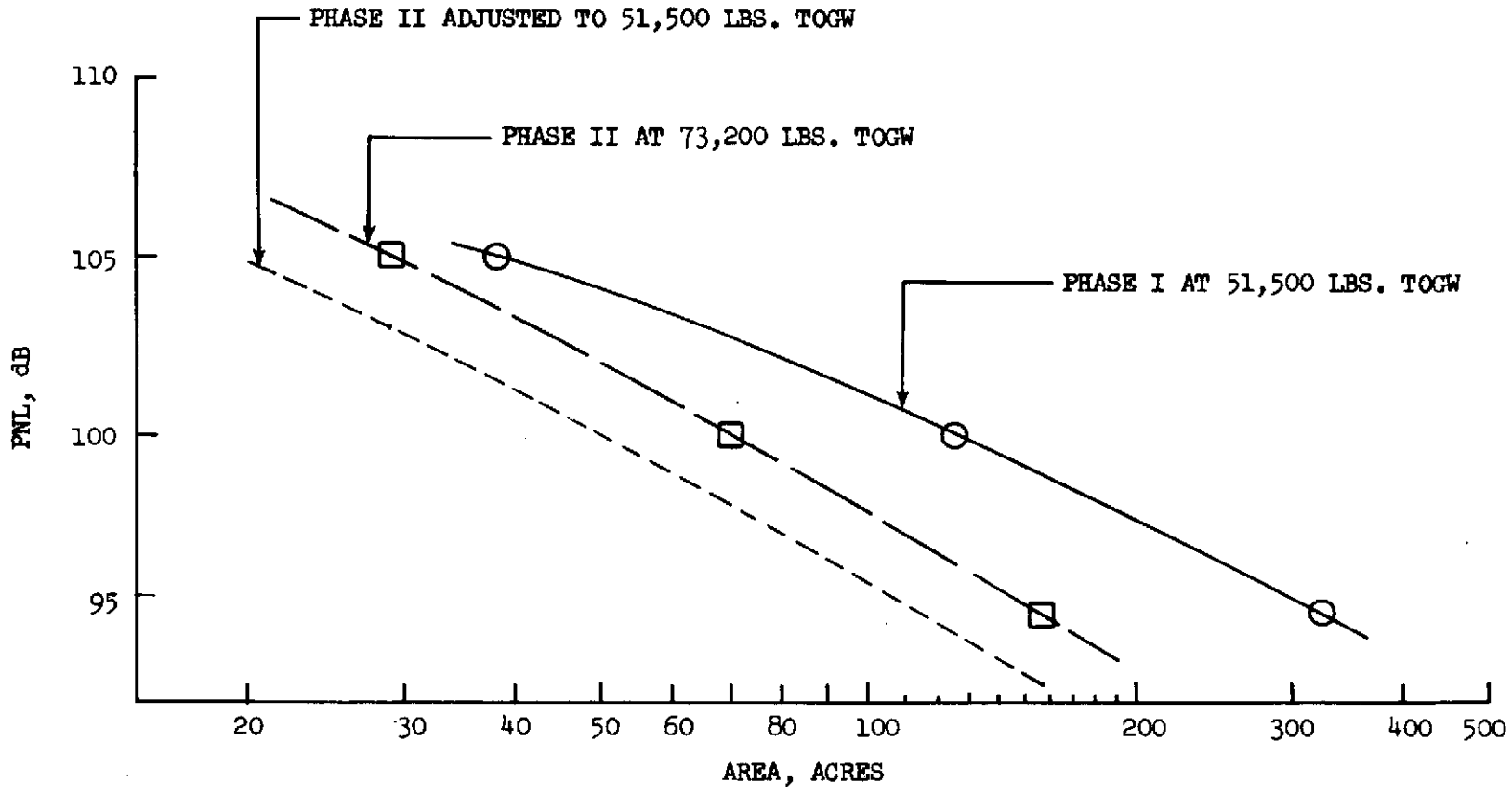

FIGURE 49 PNL CONTOUR AREA - TAKE-OFF OPERATION - COMPARISON PHASE I HIGH RISE AND PHASE II

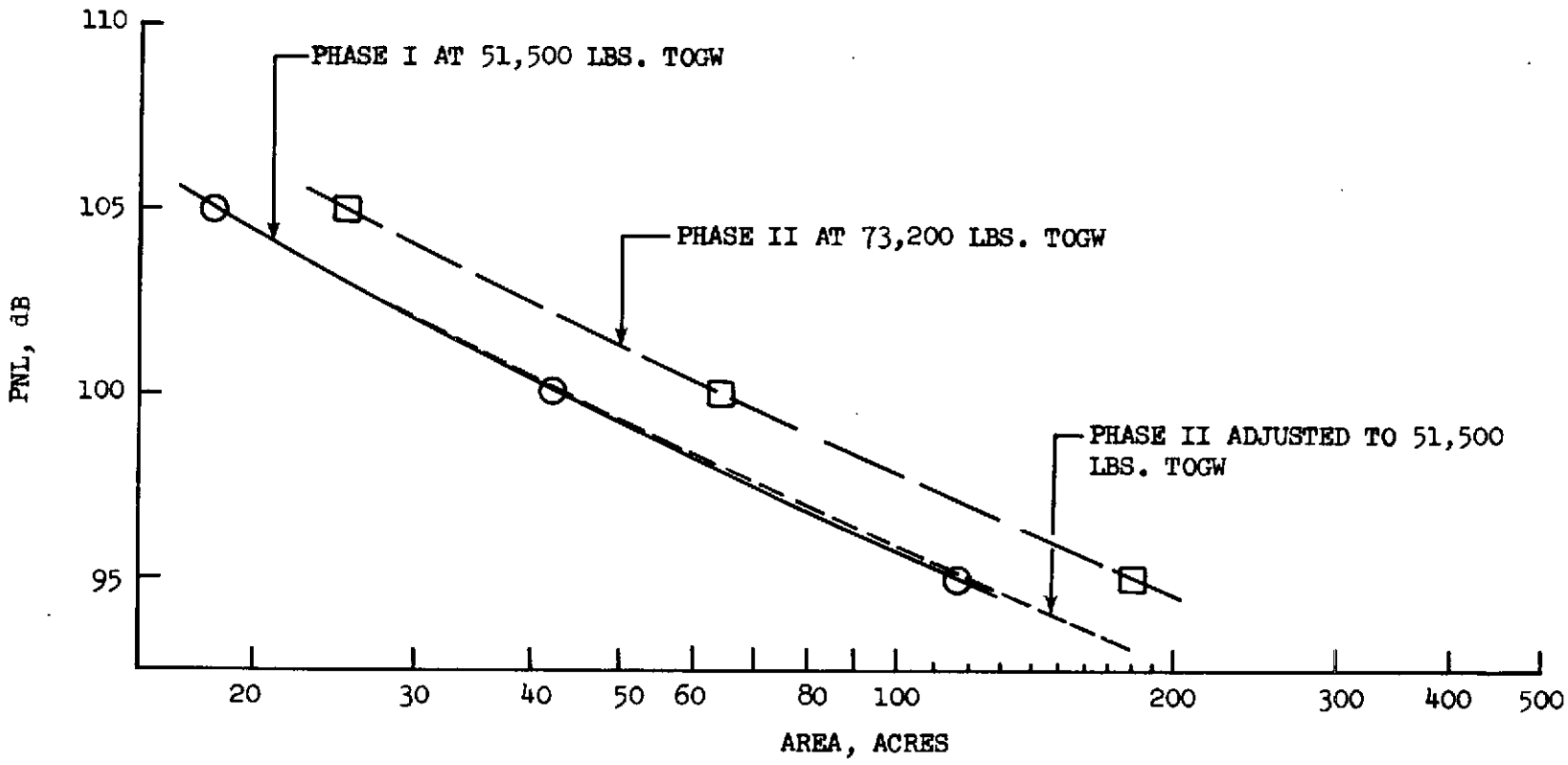

FIGURE 50 PNL CONTOUR AREA - APPROACH OPERATION - COMPARISON PHASE I HIGH DESCENT AND PHASE II

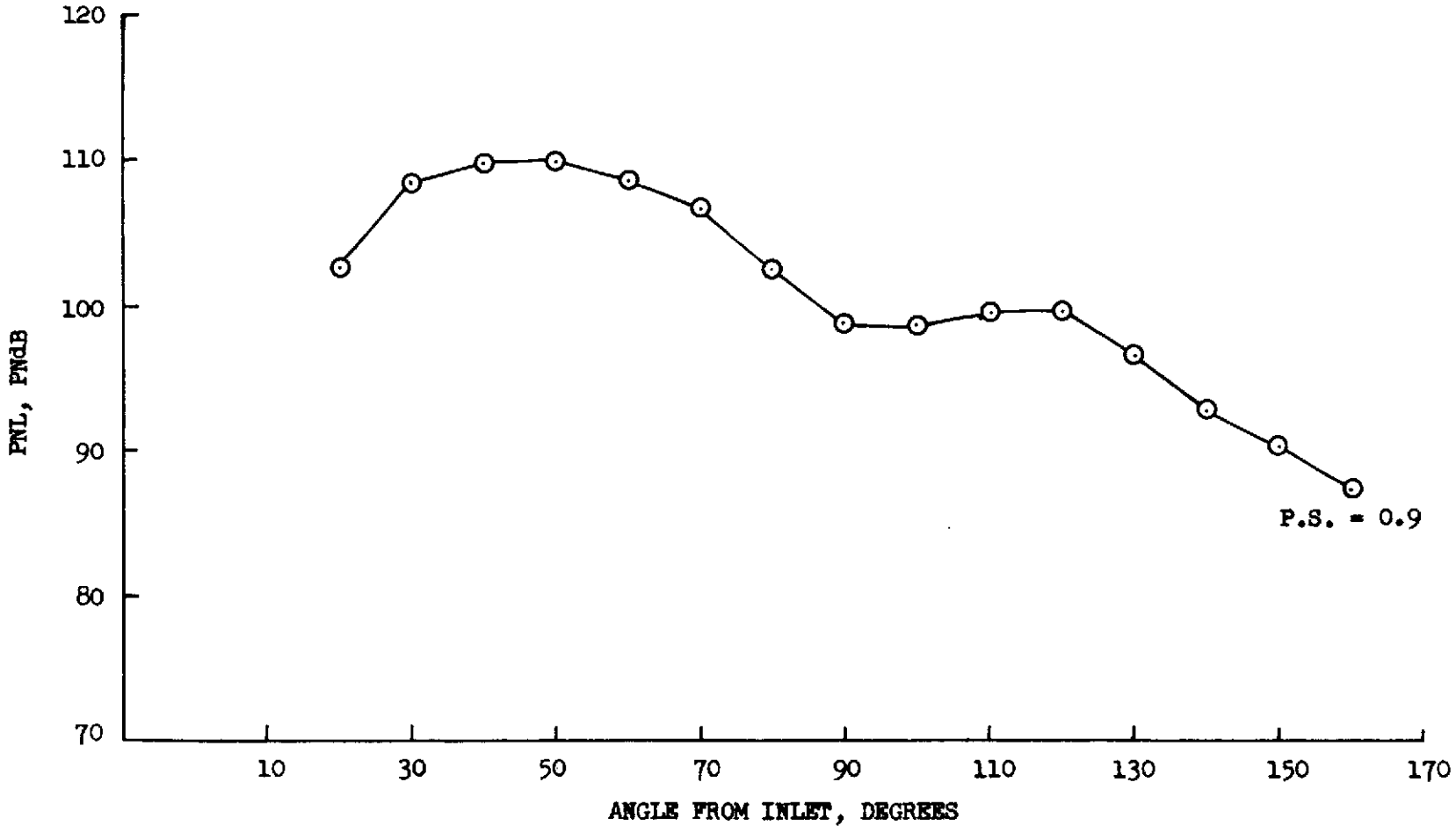

FIGURE 51 PHASE I AIRCRAFT COMPONENT NOISE - FAN INLET

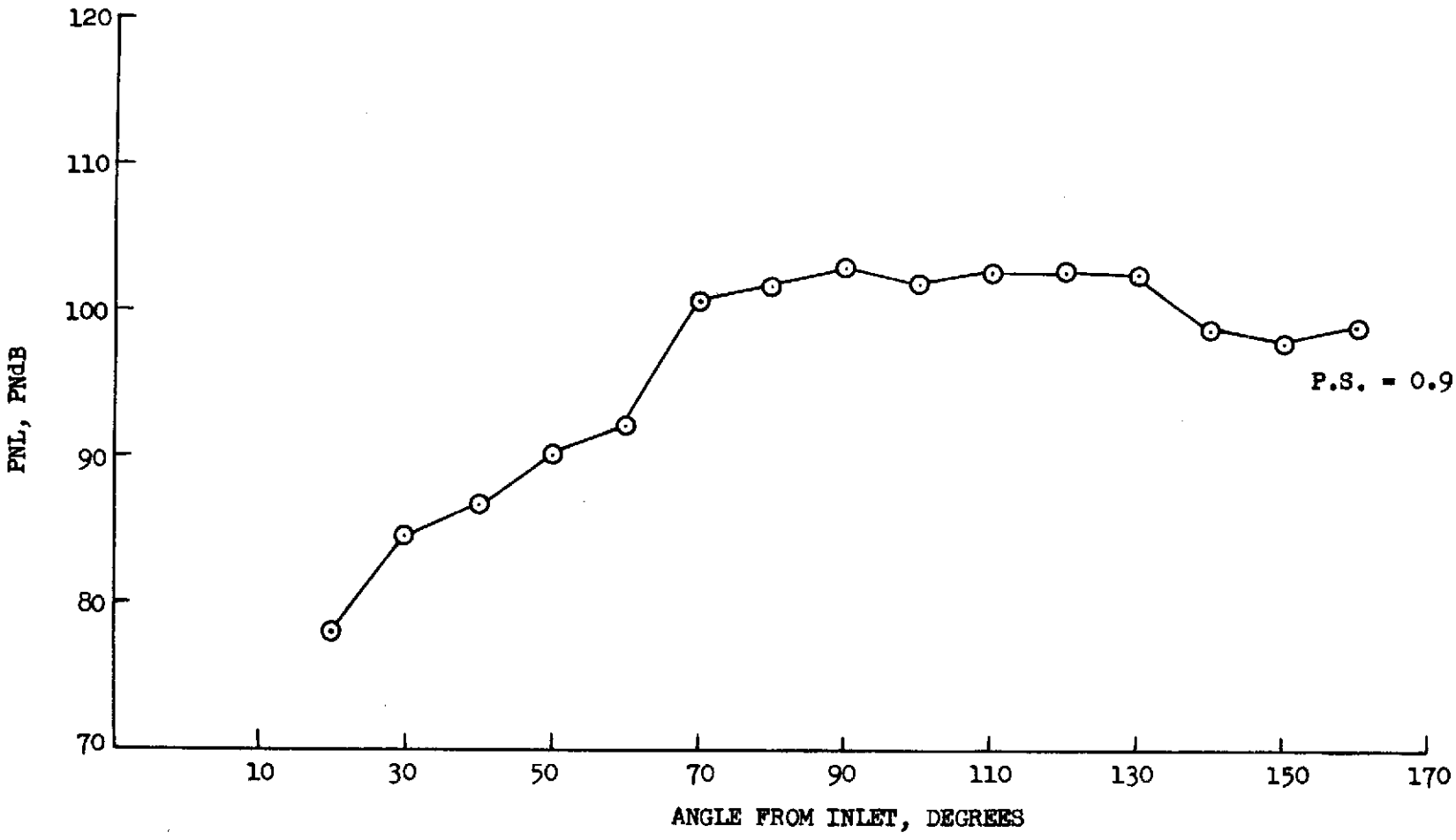

FIGURE 52 PHASE I AIRCRAFT COMPONENT NOISE - FAN EXHAUST

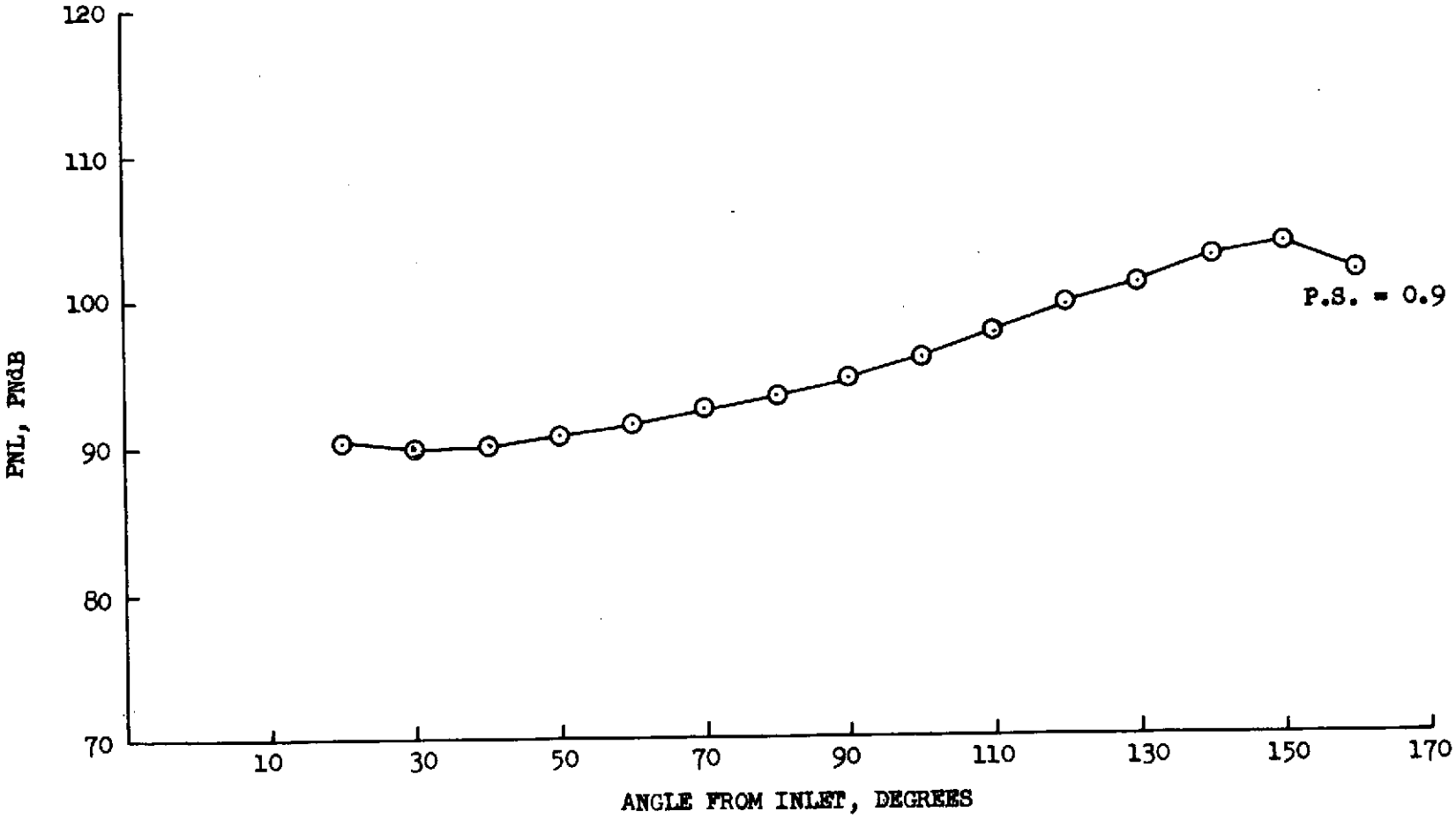

FIGURE 53 PHASE I AIRCRAFT COMPONENT NOISE - JET EXHAUST

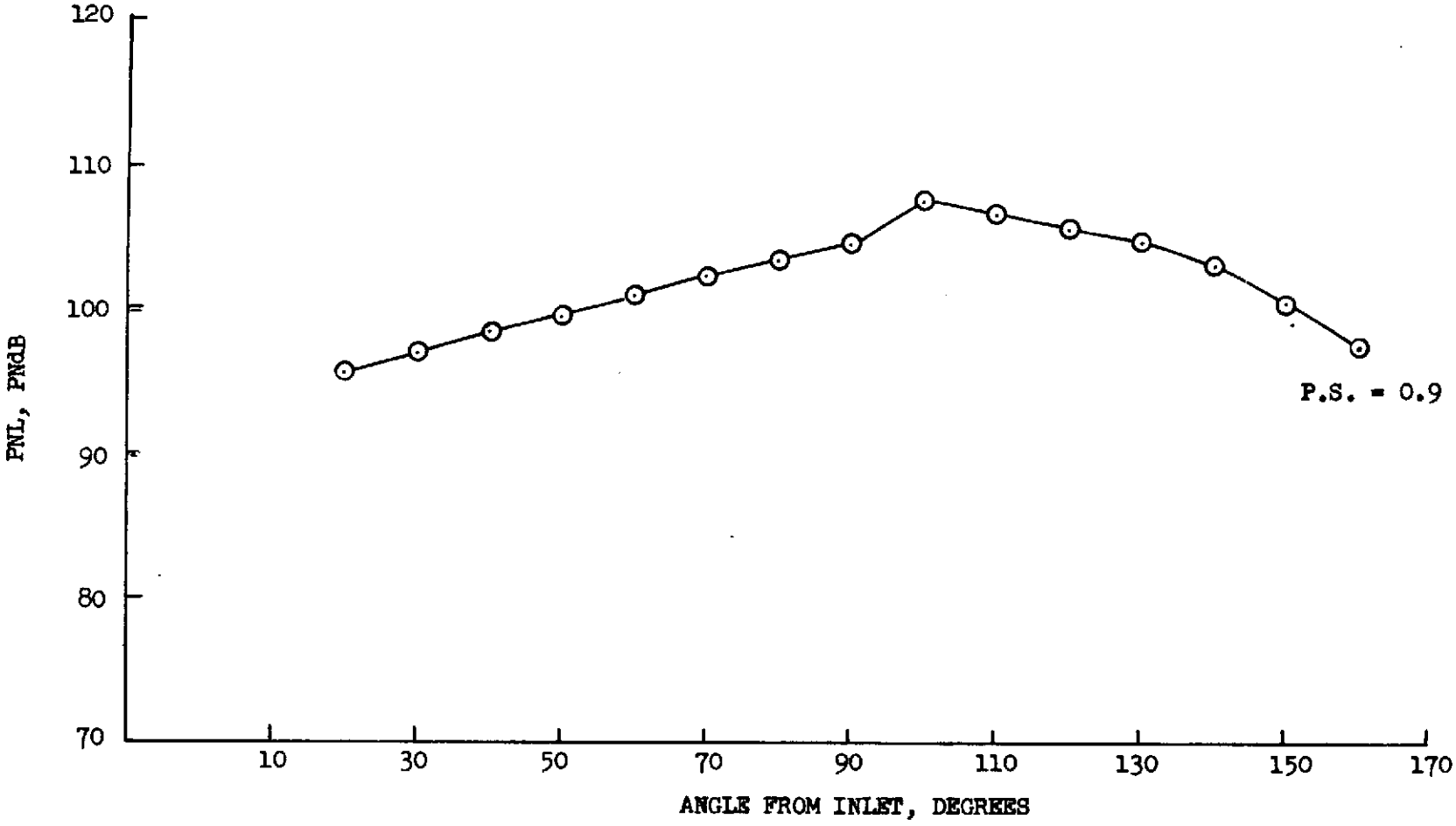

FIGURE 54 PHASE I AIRCRAFT COMPONENT NOISE - CORE TIRBINE

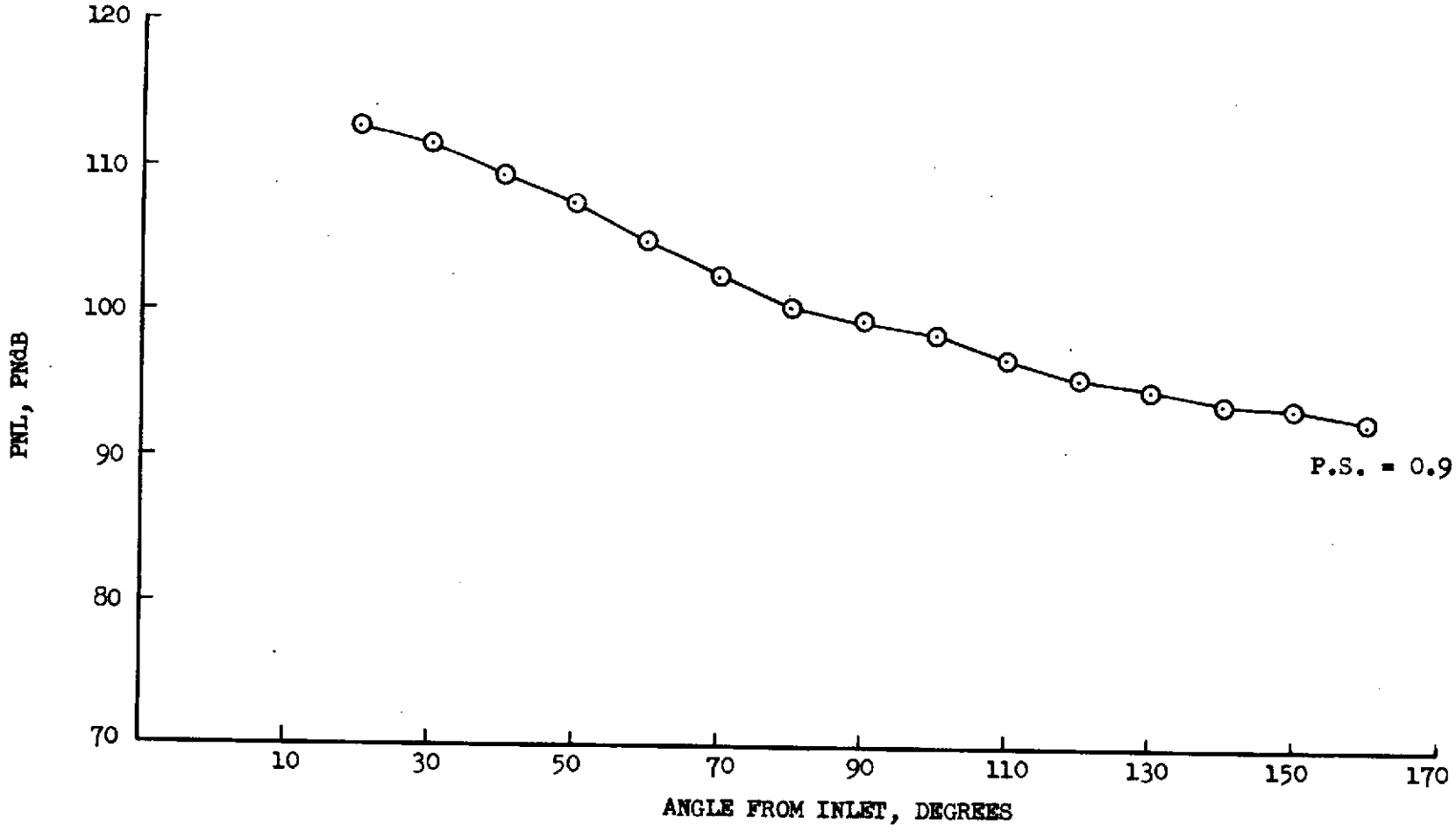

FIGURE 55 PHASE I AIRCRAFT COMPONENT NOISE - CORE COMPRESSOR

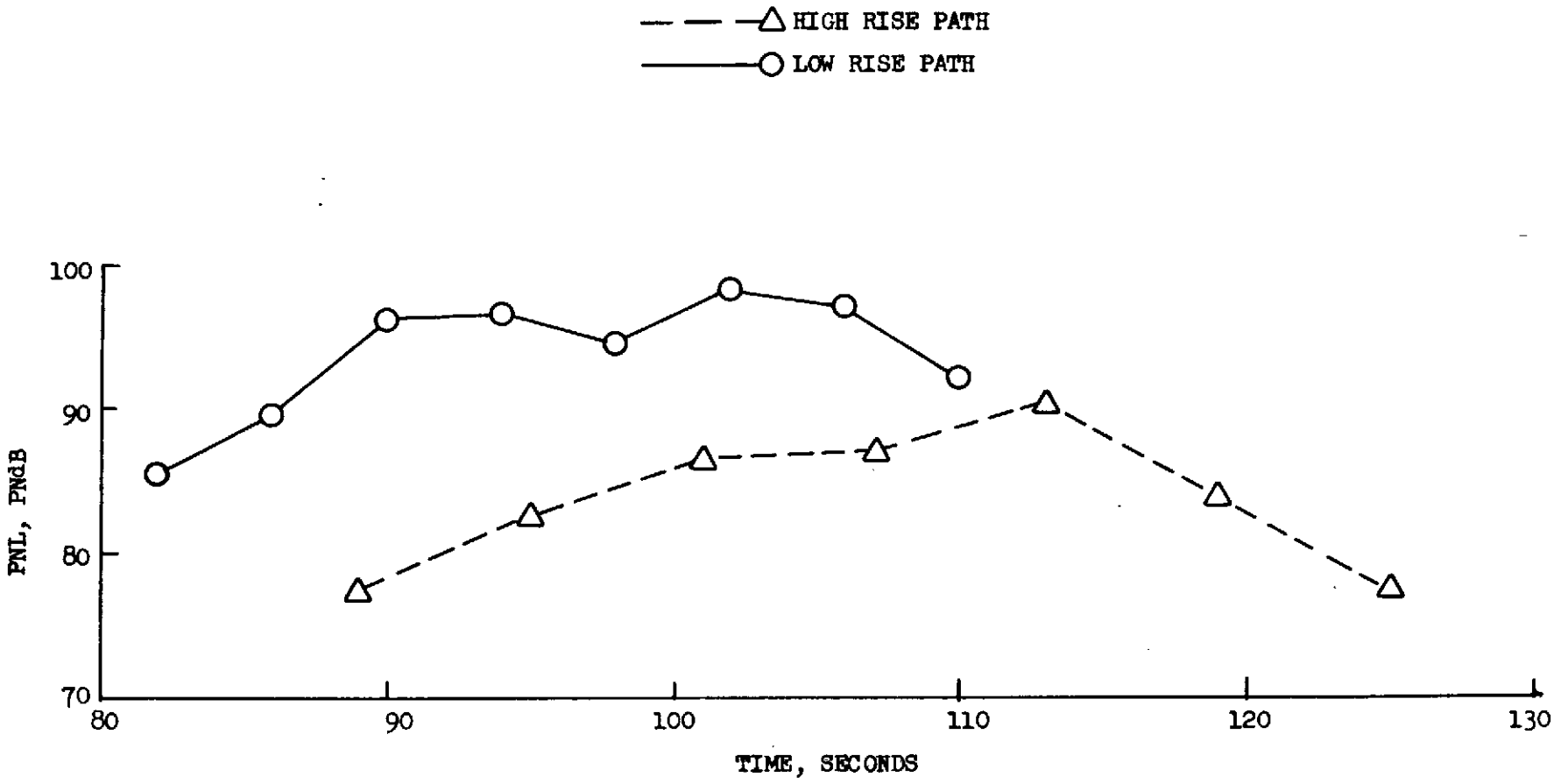

FIGURE 56 PHASE I AIRCRAFT TAKE-OFF FLYOVER PNL, FAN INLET COMPONENT, CENTERLINE MIKE

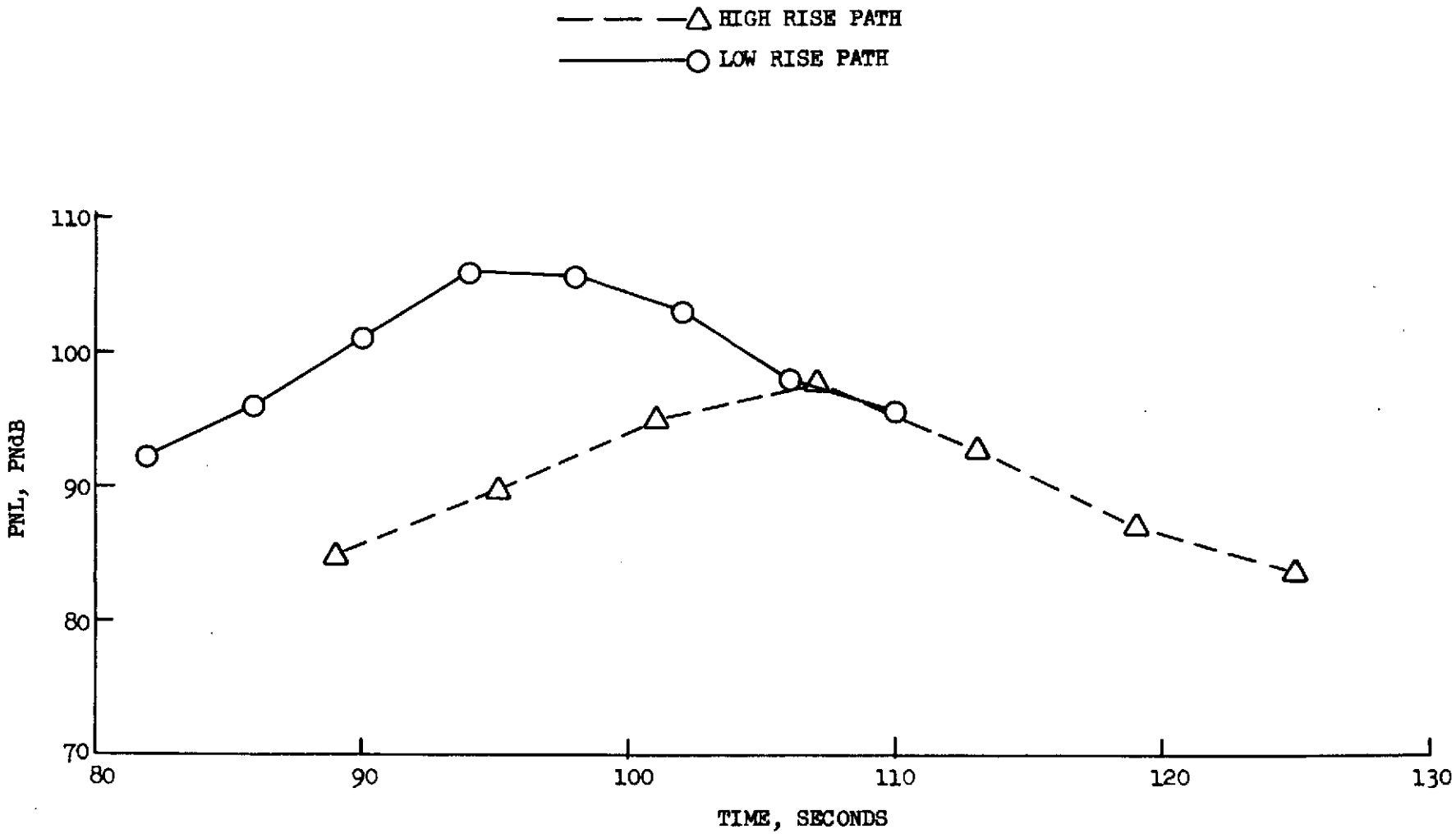

FIGURE 57 PHASE I AIRCRAFT TAKE-OFF FLYOVER PNL, FAN EXHAUST COMPONENT, CENTERLINE MIKE

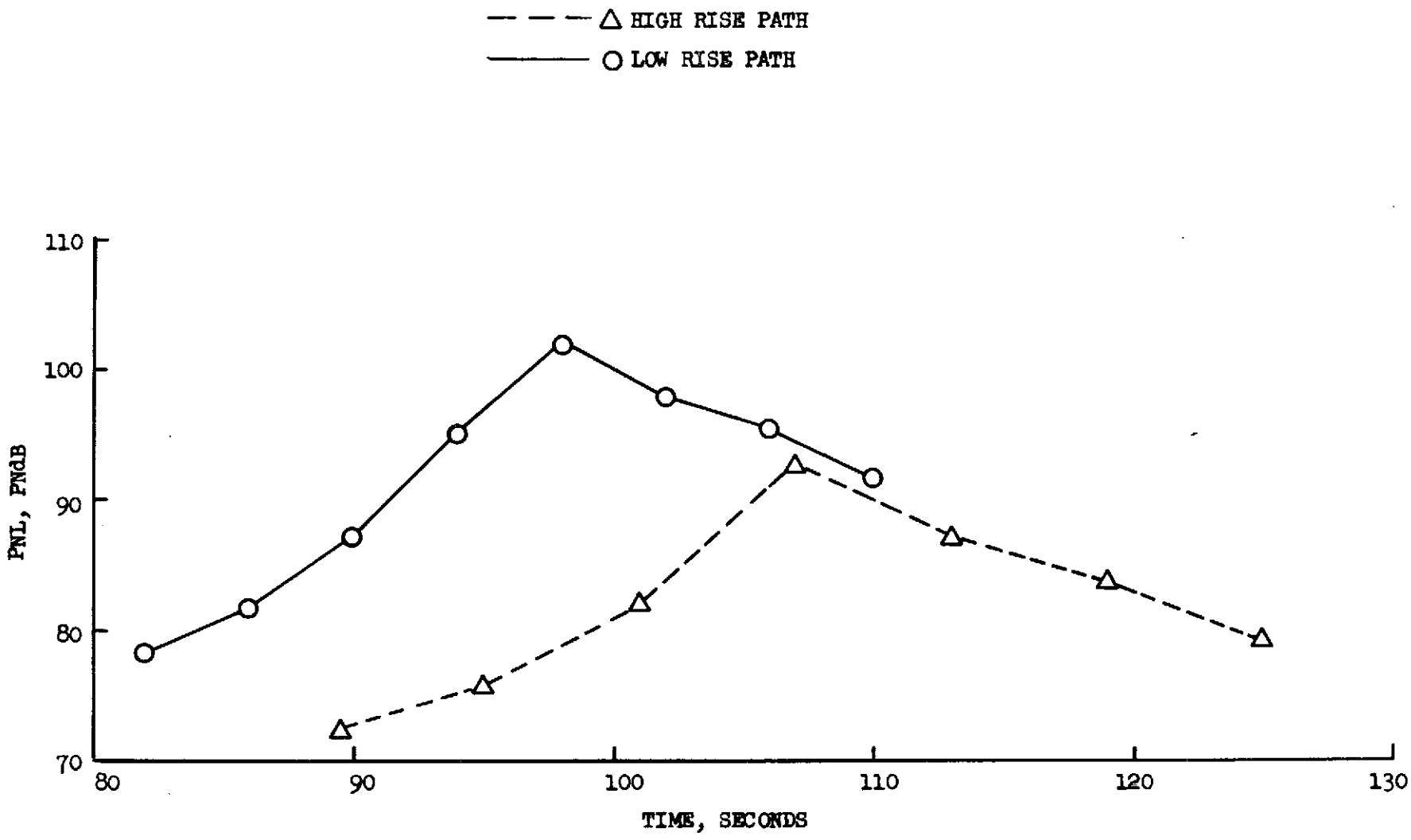

FIGURE 58 PHASE I AIRCRAFT TAKE-OFF FLYOVER PNL, COMBINED JET COMPONENT, CENTERLINE MIKE

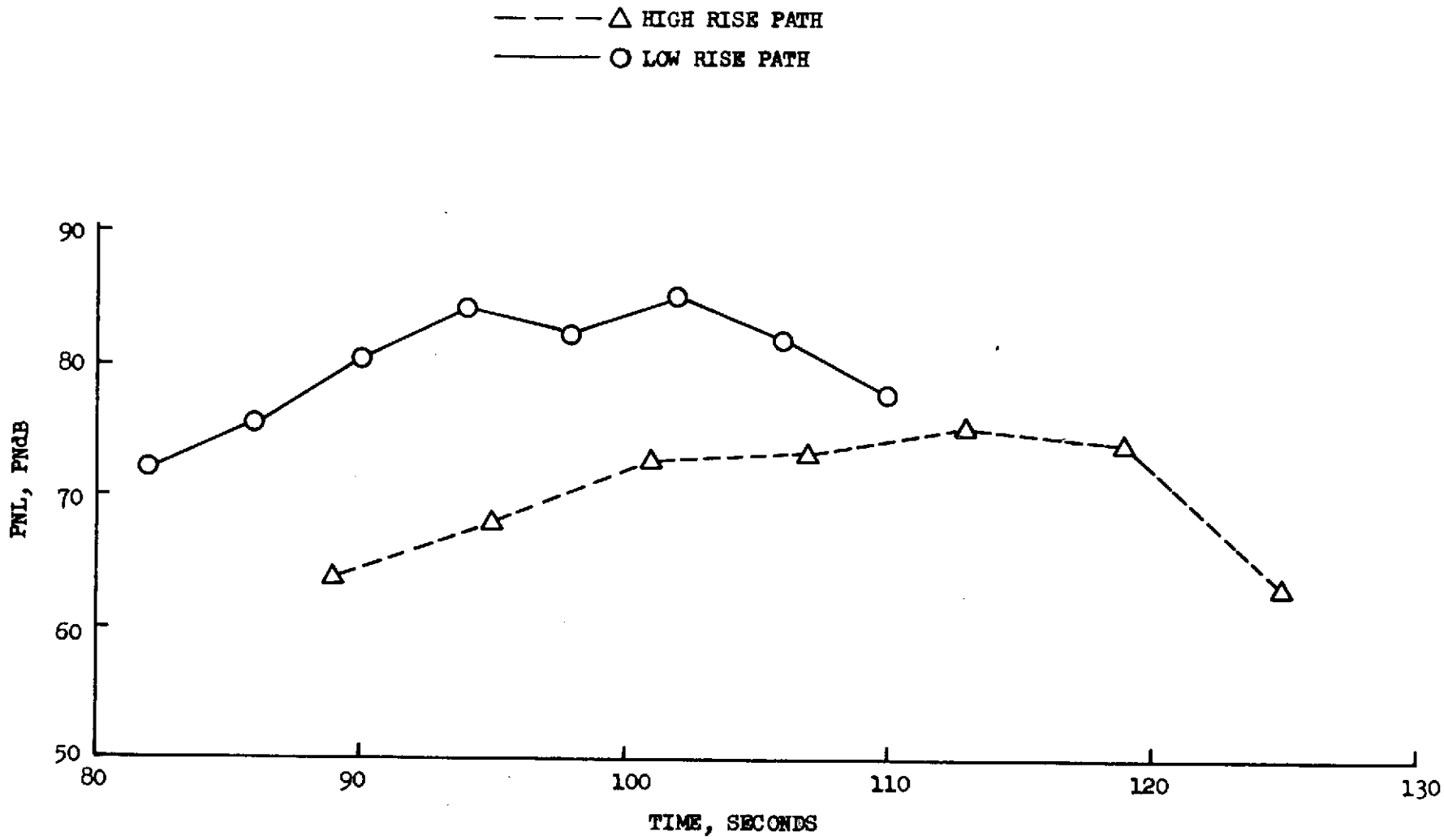

FIGURE 59 PHASE I AIRCRAFT TAKE-OFF FLYOVER PNL, TURBINE-TURBOMACHINERY COMPONENT, CENTERLINE MIKE

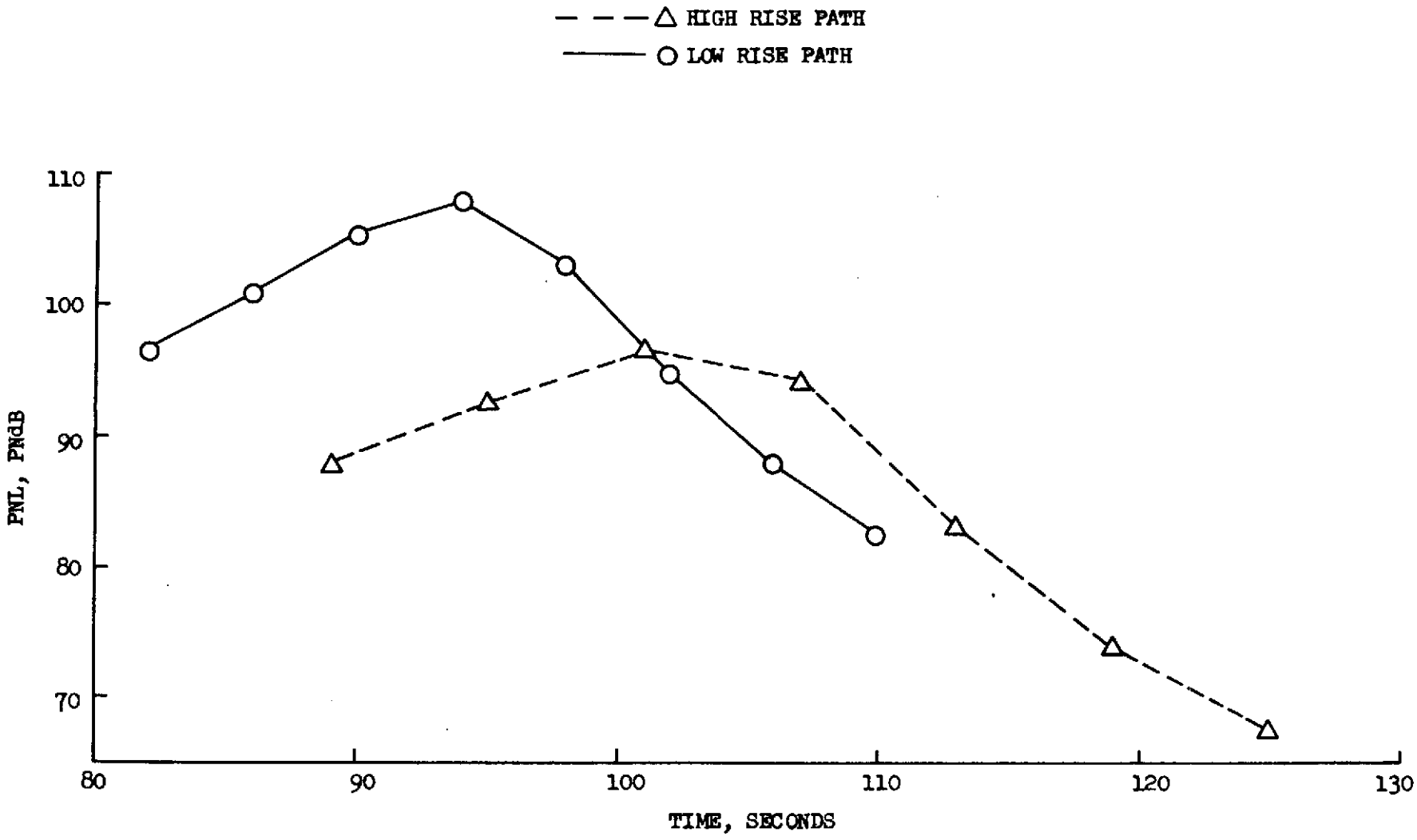

FIGURE 60 PHASE I AIRCRAFT TAKE-OFF FLYOVER PNL, COMPRESSOR INLET COMPONENT, CENTERLINE MIKE

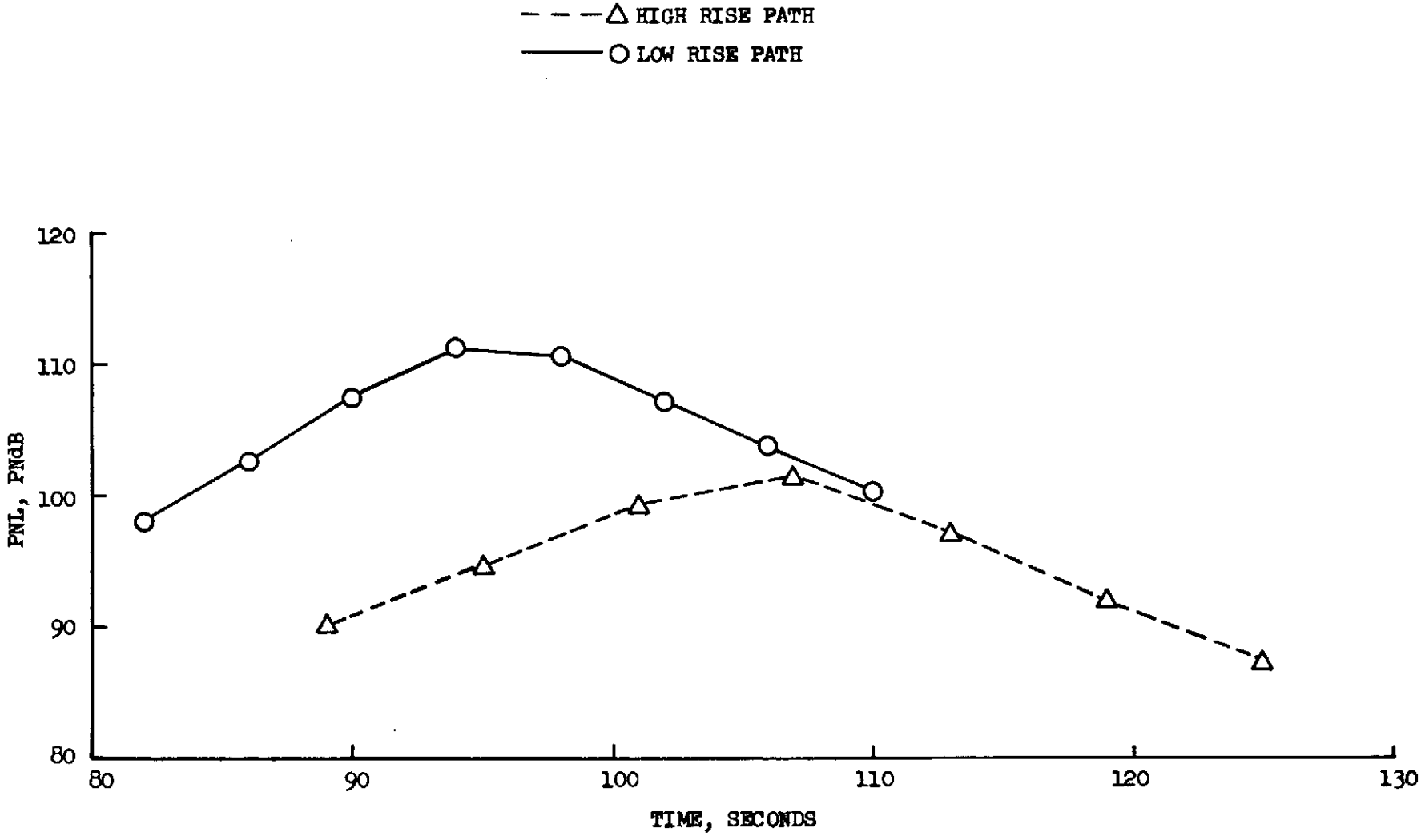

FIGURE 61 PHASE I AIRCRAFT TAKE-OFF FLYOVER PNL, COMBINED COMPONENTS, CENTERLINE MIKE

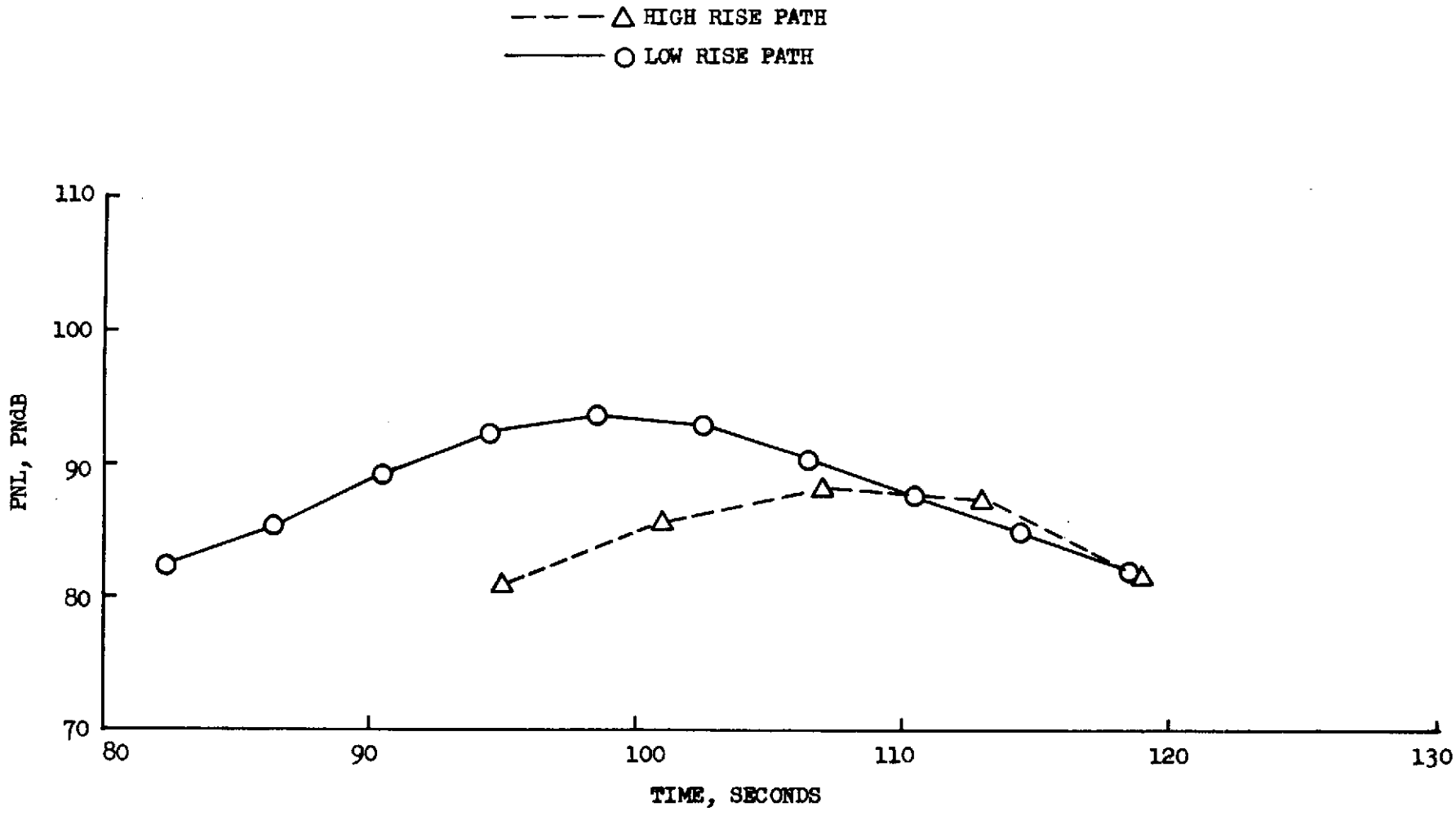

FIGURE 62 PHASE I AIRCRAFT TAKE-OFF FLYOVER PNL, FAN INLET COMPONENT, 740 FT. SIDELINE MIKE

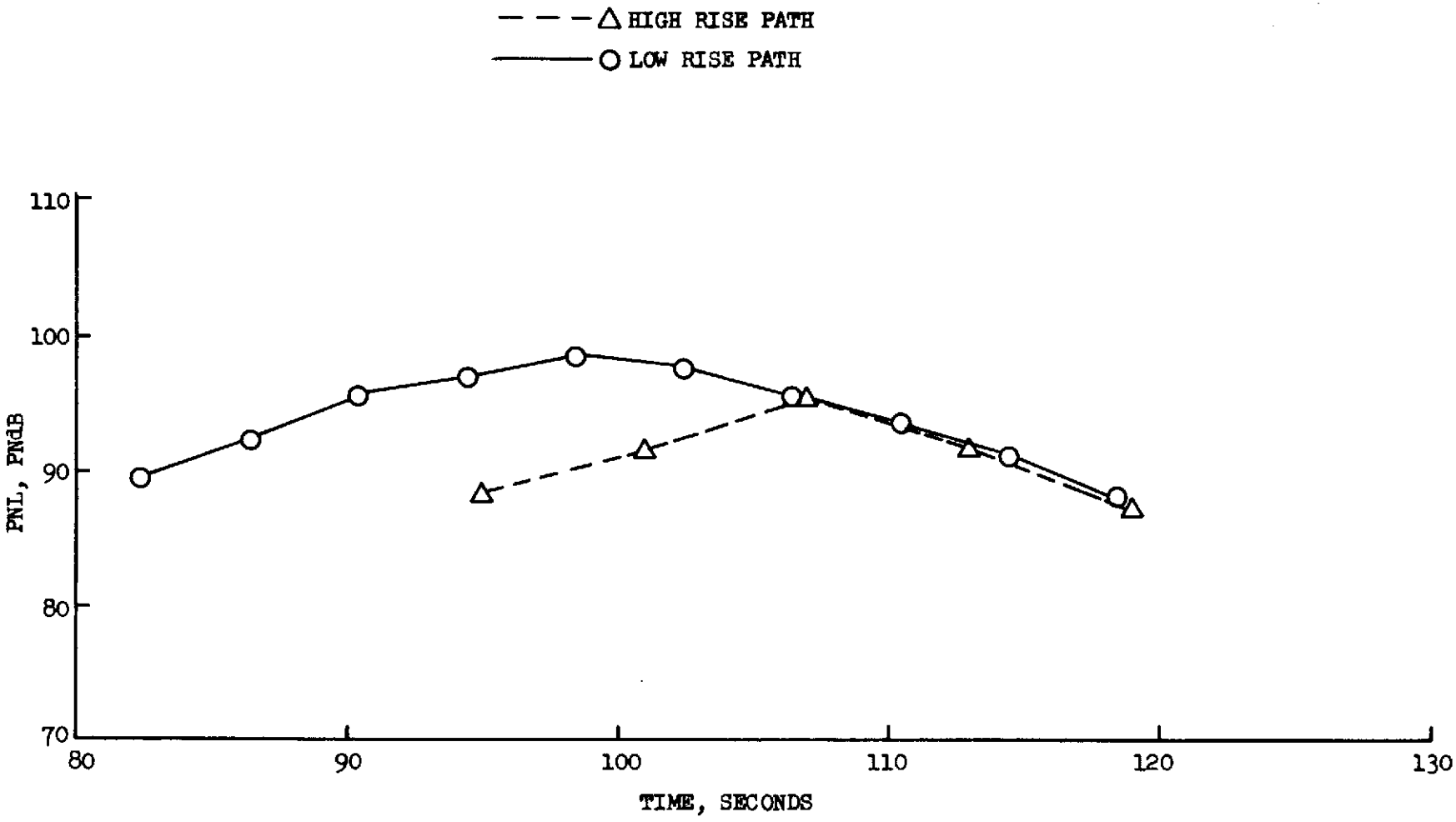

FIGURE 63 PHASE I AIRCRAFT TAKE-OFF FLYOVER PNL, FAN EXHAUST COMPONENT, 740 FT. SIDELINE MIKE

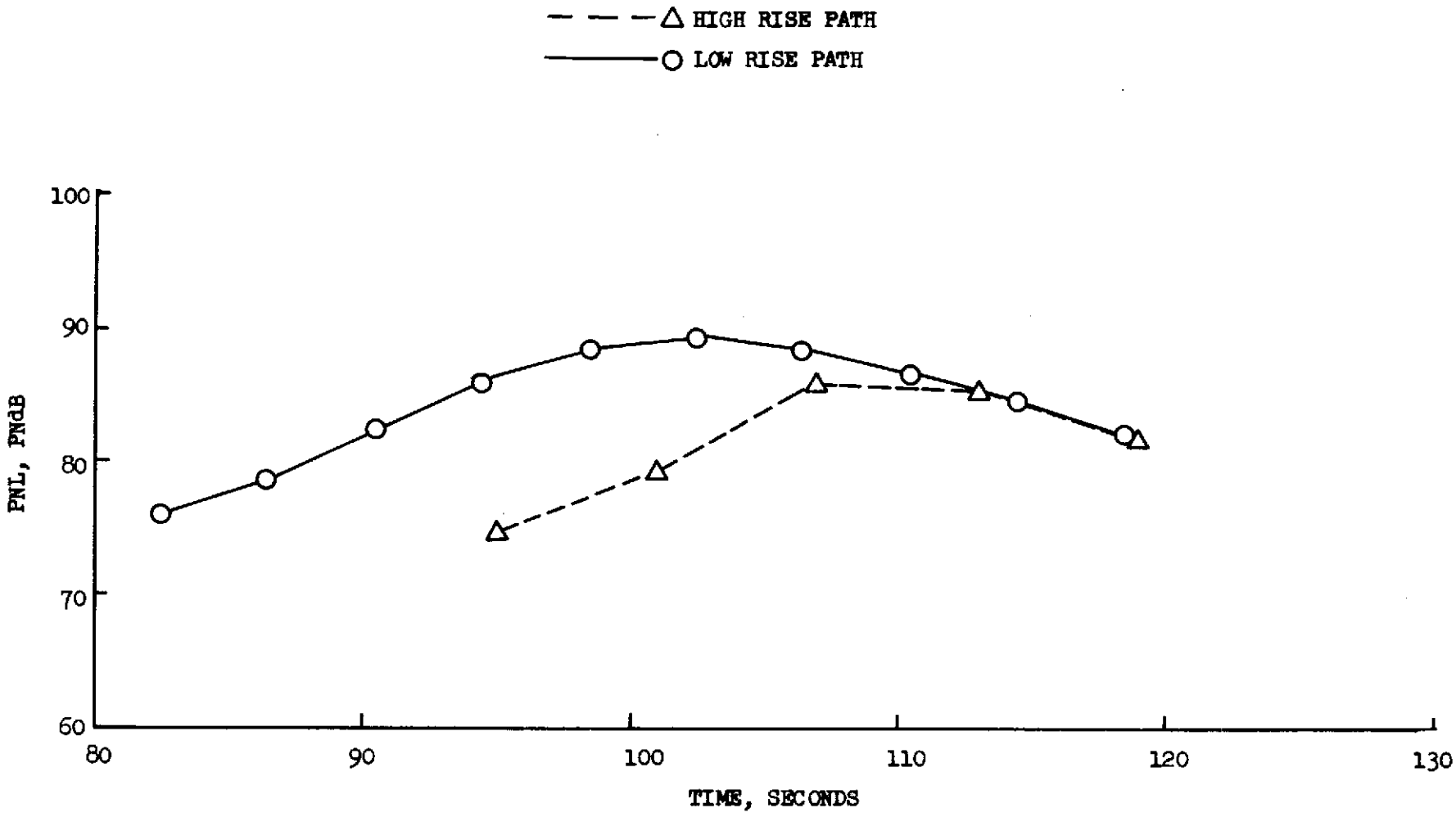

FIGURE 64 PHASE I AIRCRAFT TAKE-OFF FLYOVER PNL, COMBINED JET COMPONENT, 740 FT. SIDELINE MIKE

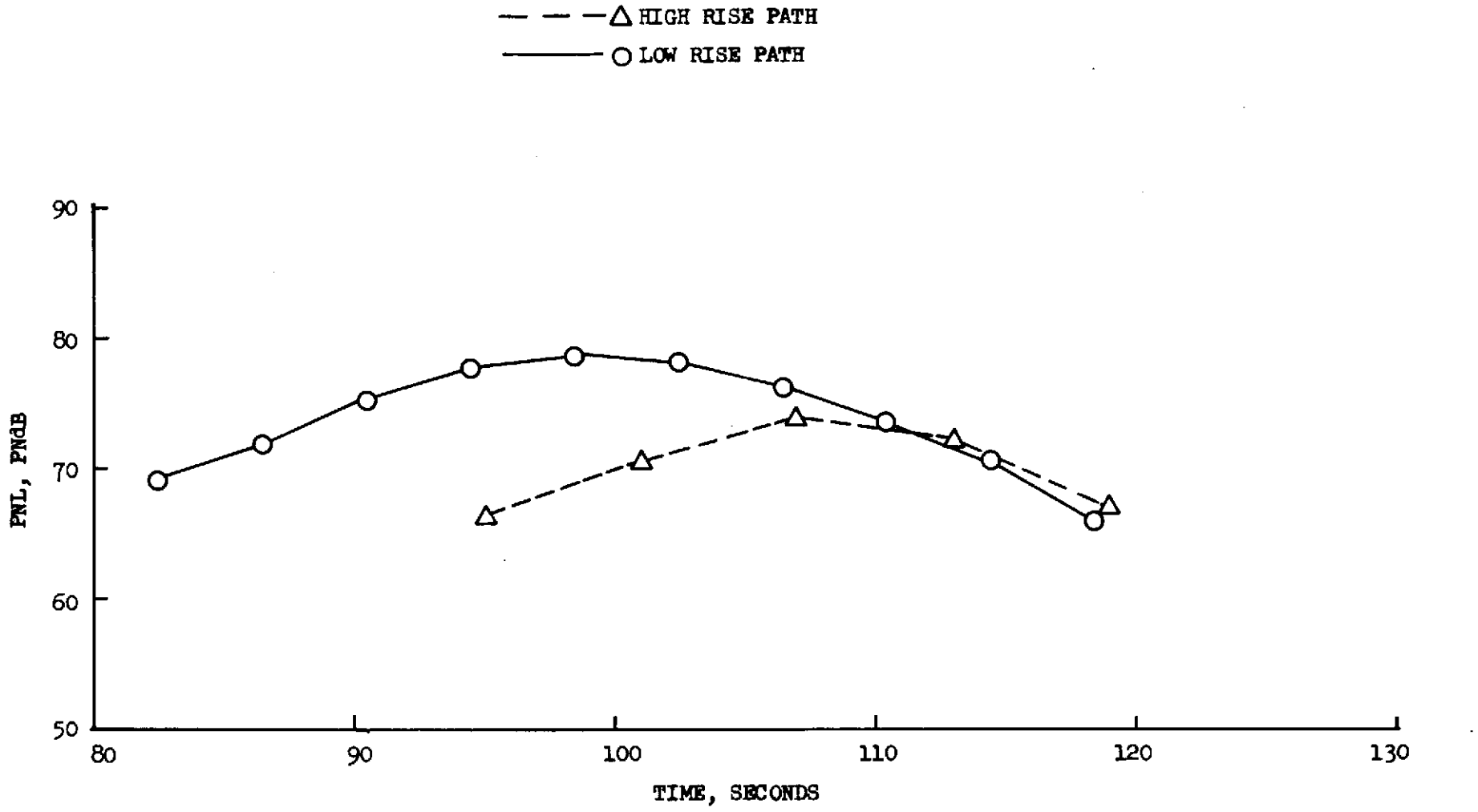

FIGURE 65 PHASE I AIRCRAFT TAKE-OFF FLYOVER PNL, TURBINE-TURBOMACHINERY COMPONENT, 740 FT. SIDELINE MIKE

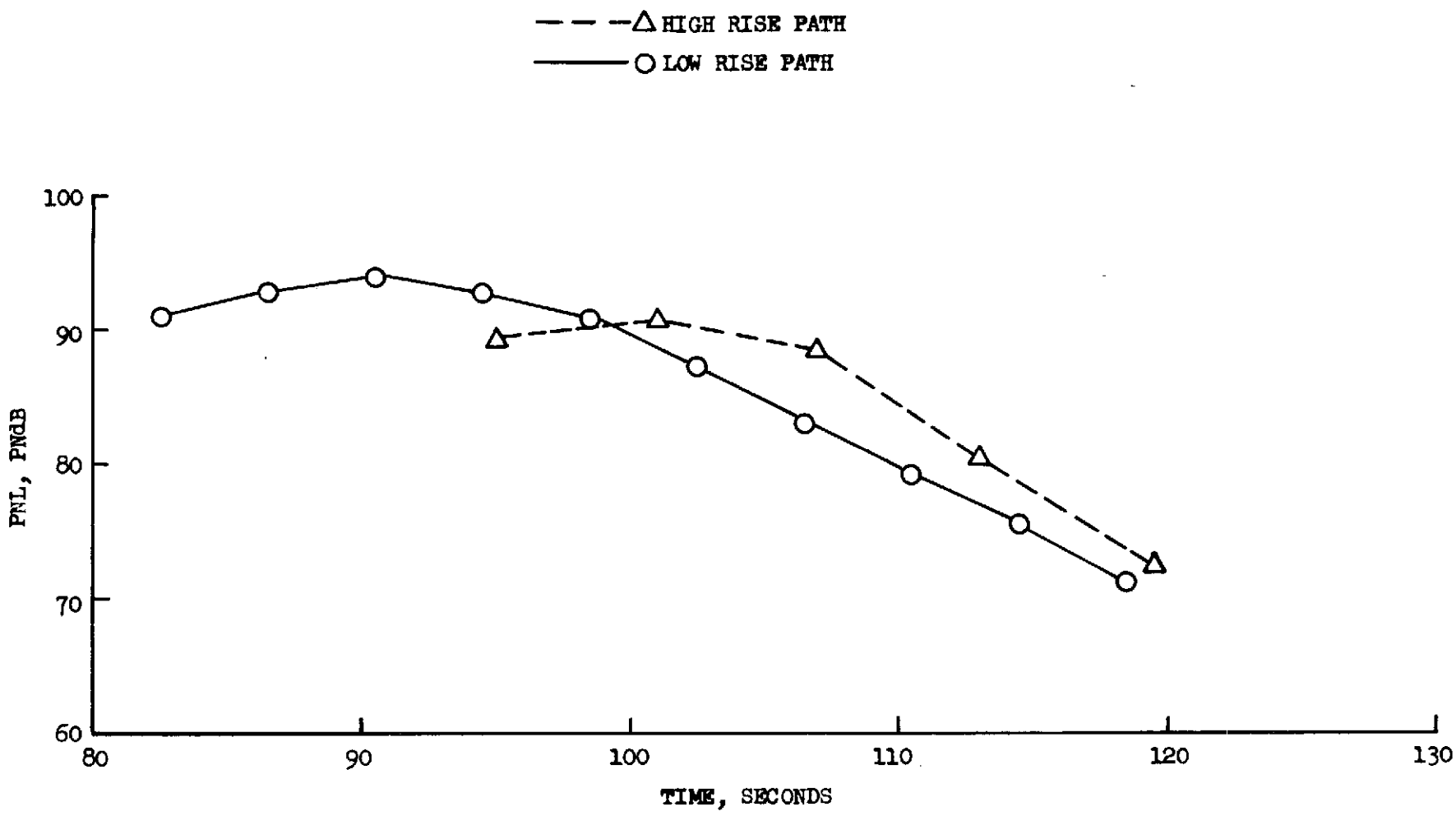

FIGURE 66 PHASE I AIRCRAFT TAKE-OFF FLYOVER PNL, COMPRESSOR INLET COMPONENT, 740 FT. SIDELINE MIKE

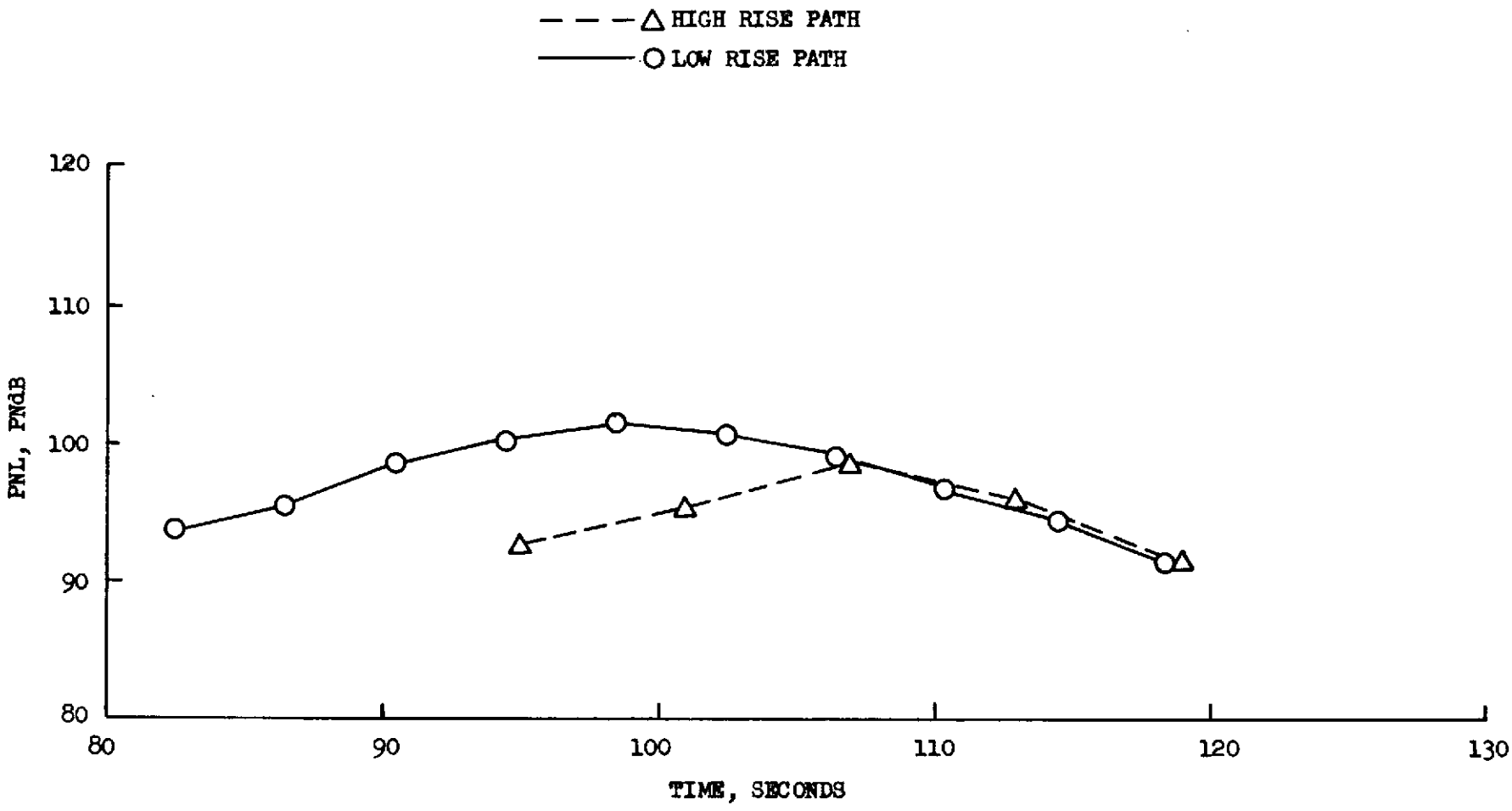

FIGURE 67 PHASE I AIRCRAFT TAKE-OFF FLYOVER PNL, COMBINED COMPONENTS, 740 FT. SIDELINE MIKE

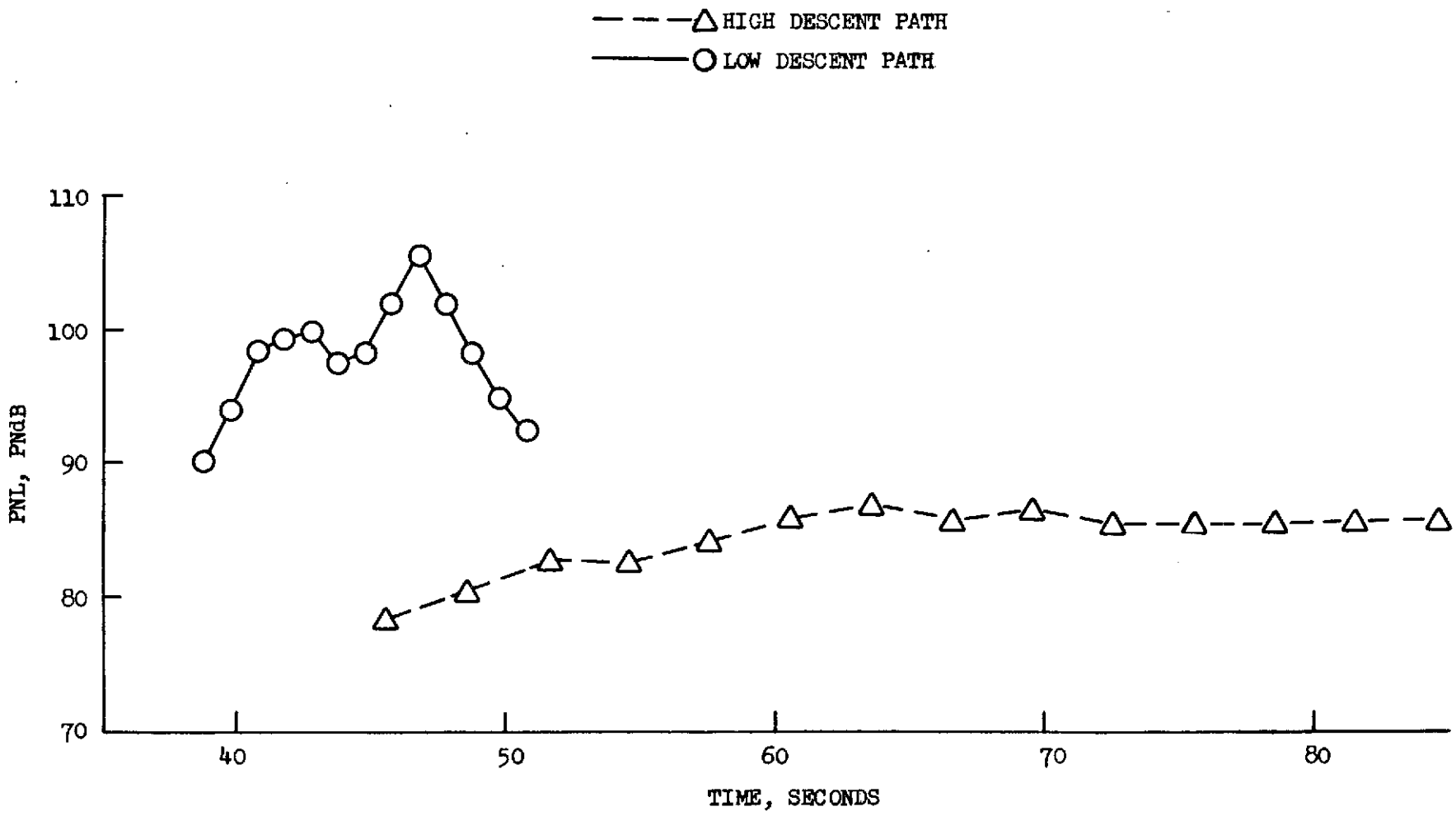

FIGURE 68 PHASE I AIRCRAFT APPROACH FLYOVER PNL, FAN INLET COMPONENT, CENTERLINE MIKE

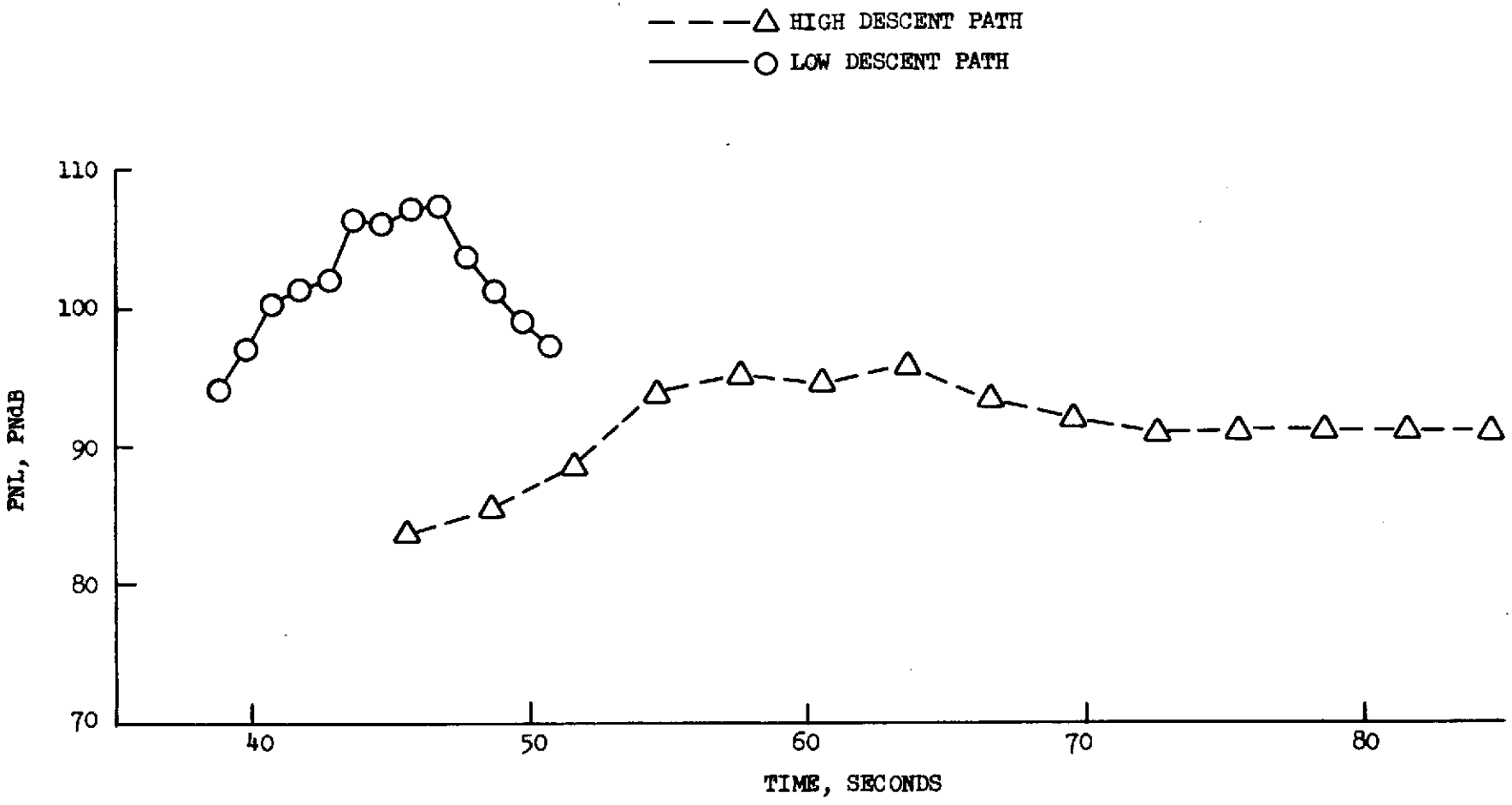

FIGURE 69 PHASE I AIRCRAFT APPROACH FLYOVER PNL, FAN EXHAUST COMPONENT, CENTERLINE MIKE

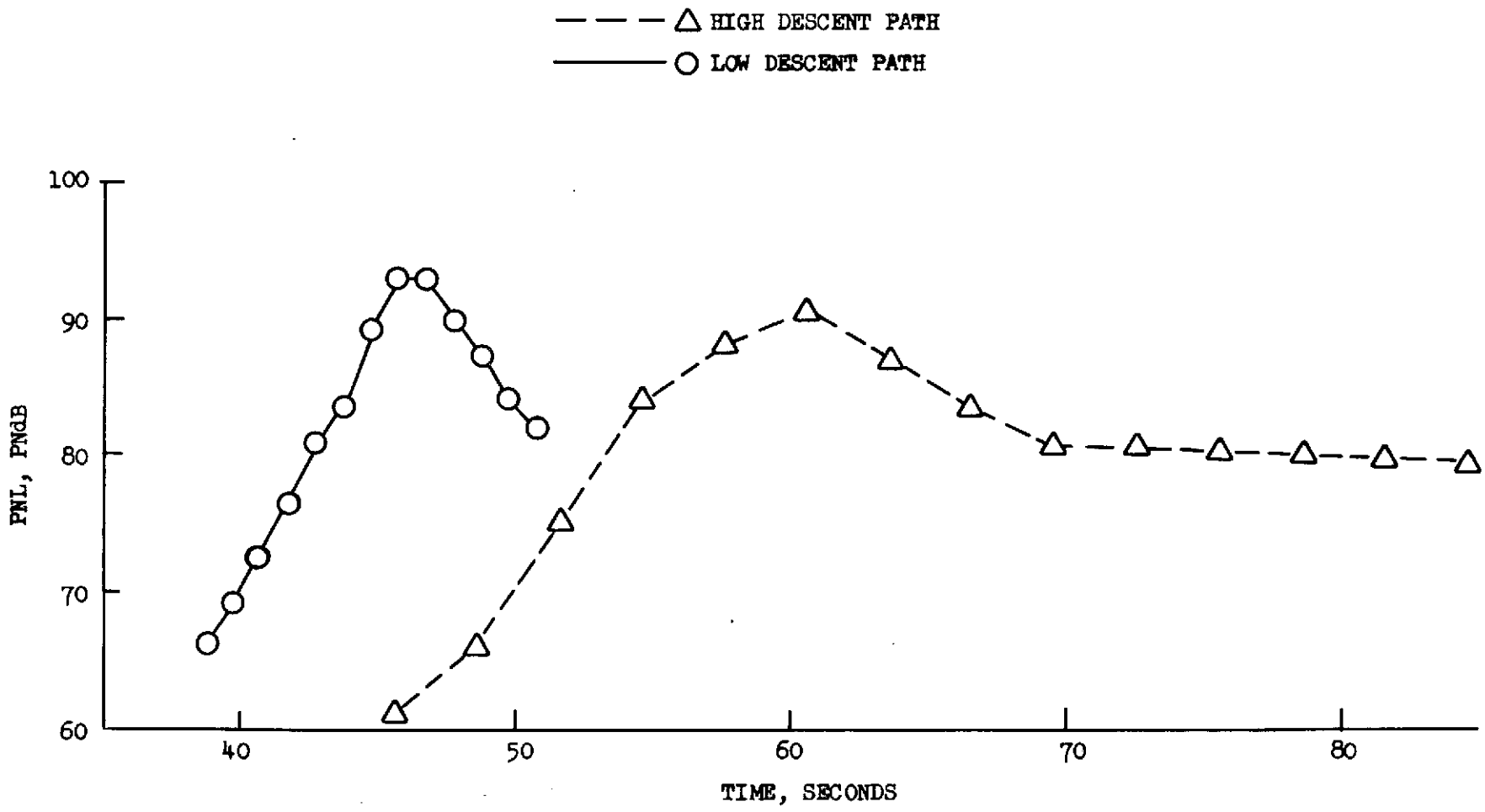

FIGURE 70 PHASE I APPROACH FLYOVER PNL, COMBINED JET COMPONENTS, CENTERLINE MIKE

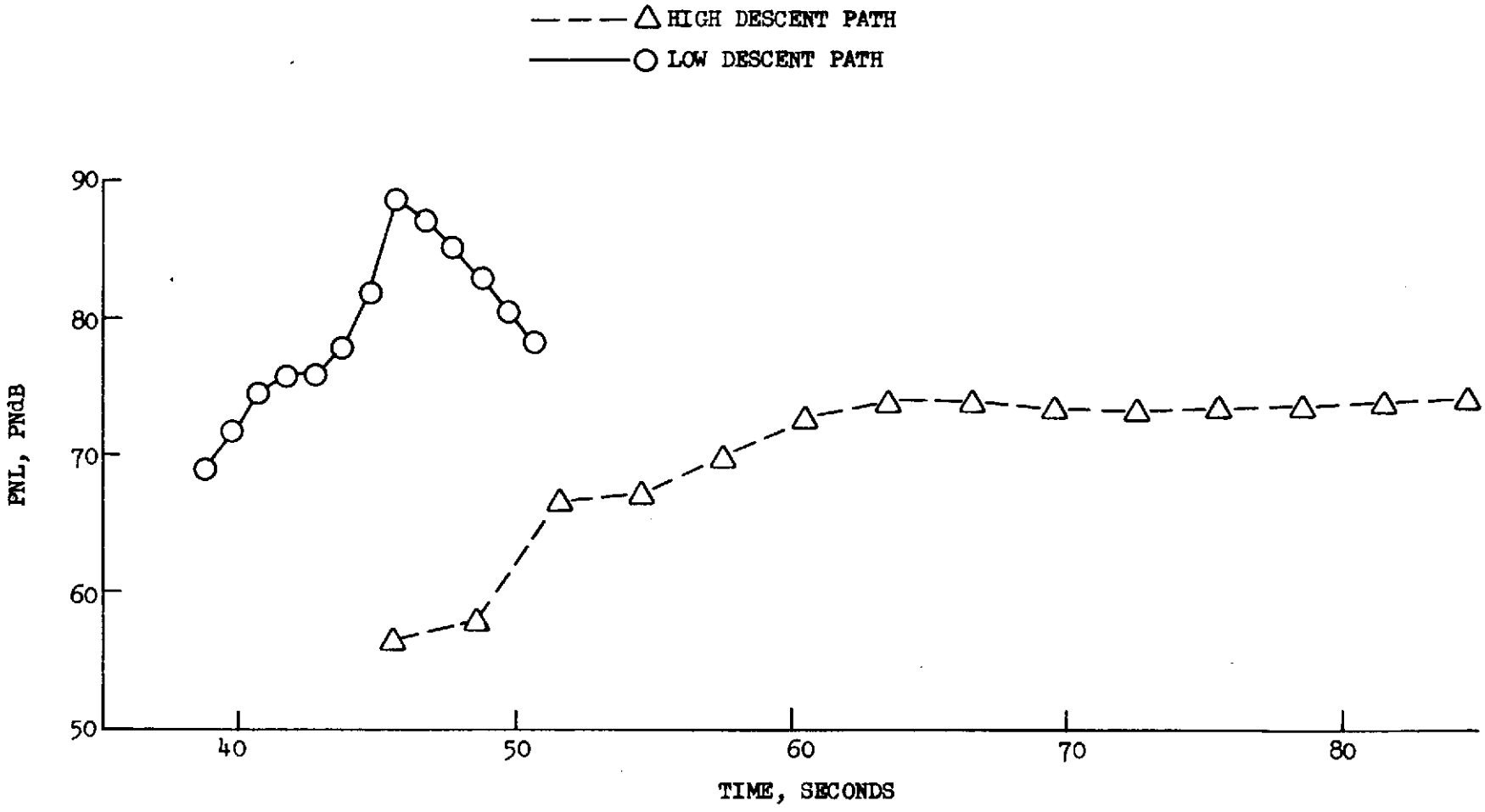

FIGURE 71 PHASE I AIRCRAFT APPROACH FLYOVER PNL, TURBINE-TURBOMACHINERY COMPONENT, CENTERLINE MIKE

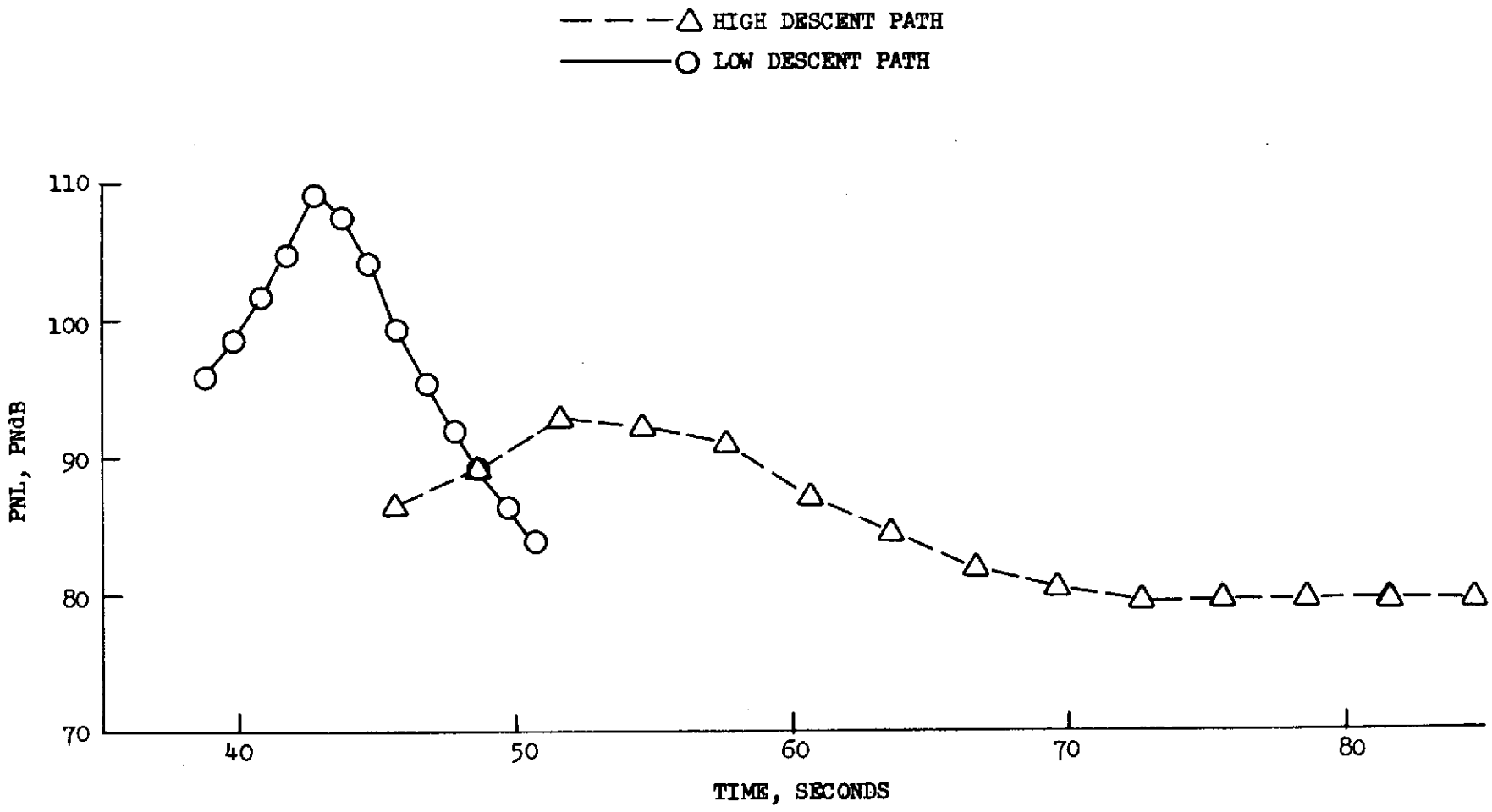

FIGURE 72 PHASE I AIRCRAFT APPROACH FLYOVER PNL, COMPRESSOR INLET COMPONENT, CENTERLINE MIKE

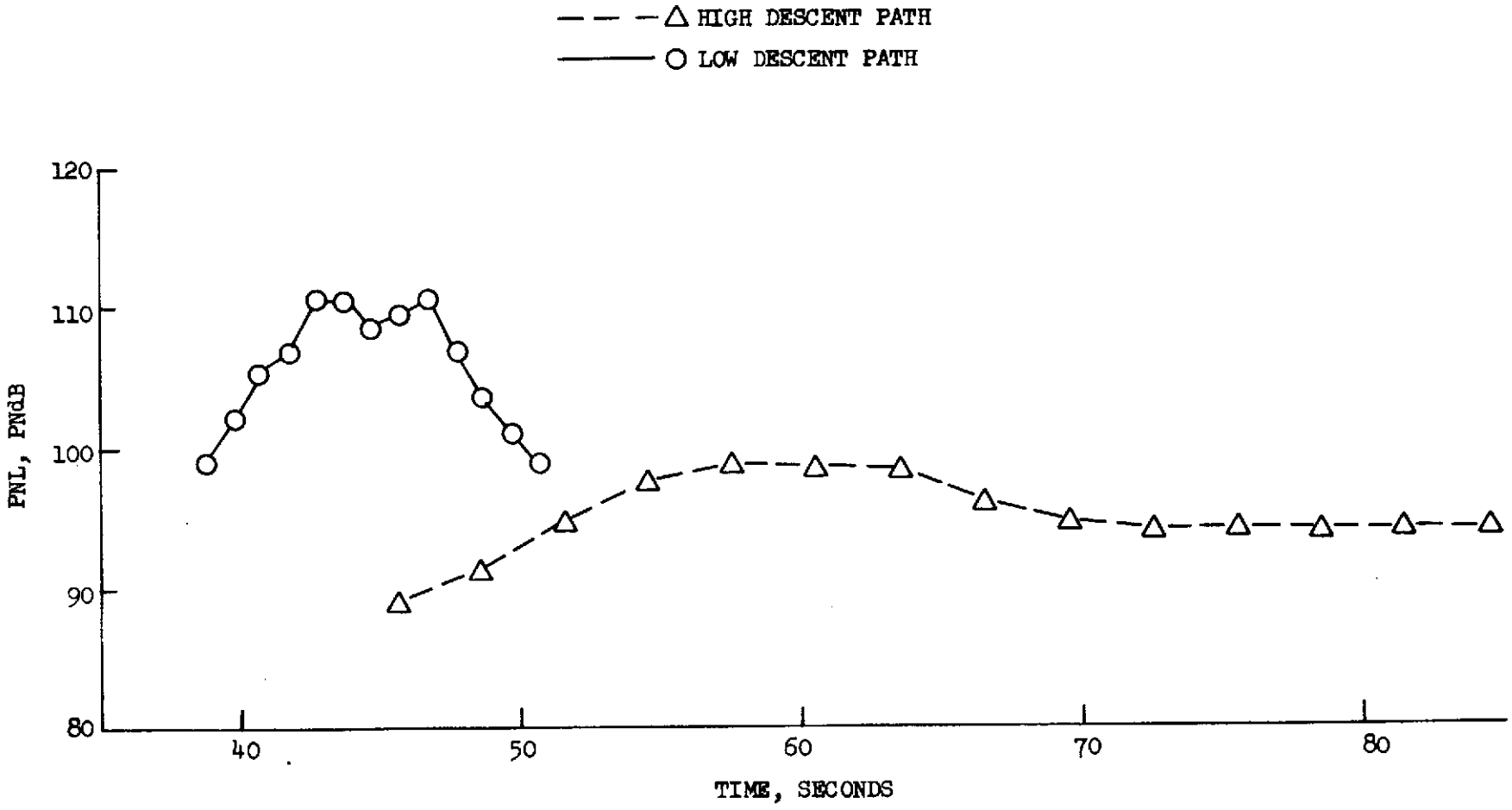

FIGURE 73 PHASE I AIRCRAFT APPROACH FLYOVER PNL, COMBINED COMPONENTS, CENTERLINE MIKE

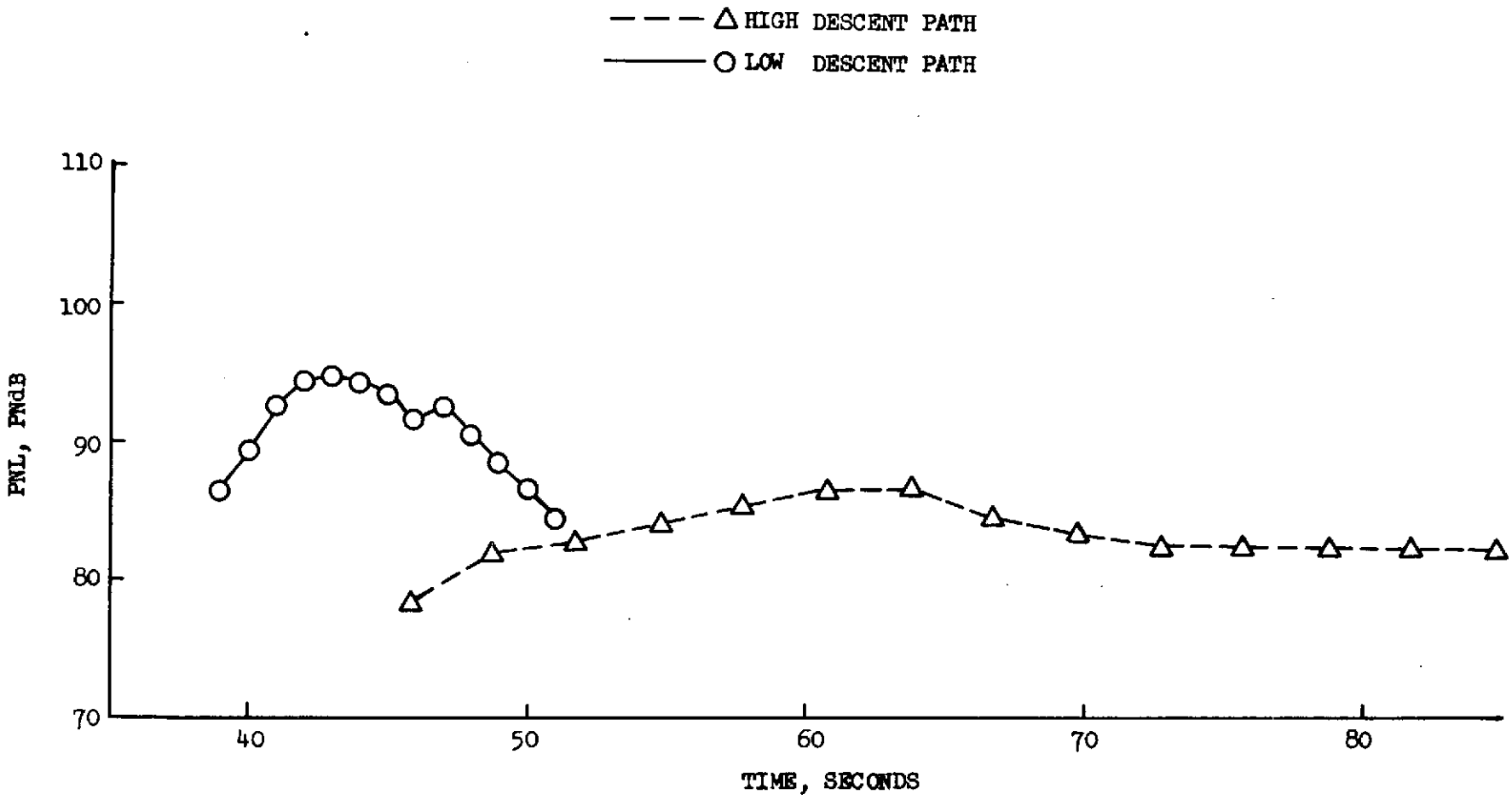

FIGURE 74 PHASE I AIRCRAFT APPROACH FLYOVER PNL, FAN INLET COMPONENT, 710 FT. SIDELINE MIKE

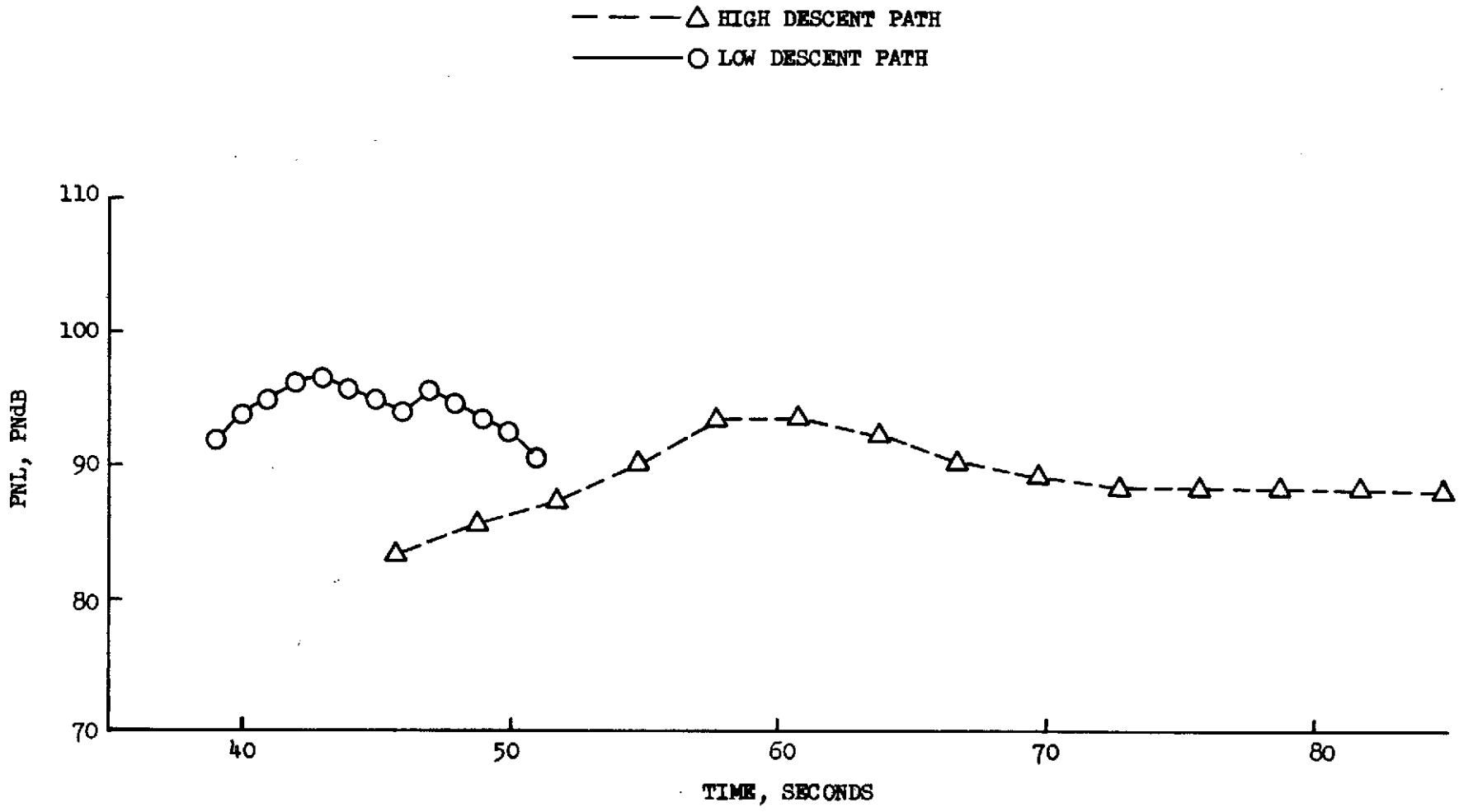

FIGURE 75 PHASE I AIRCRAFT APPROACH FLYOVER PNL, FAN EXHAUST COMPONENT, 710 FT. SIDELINE MIKE

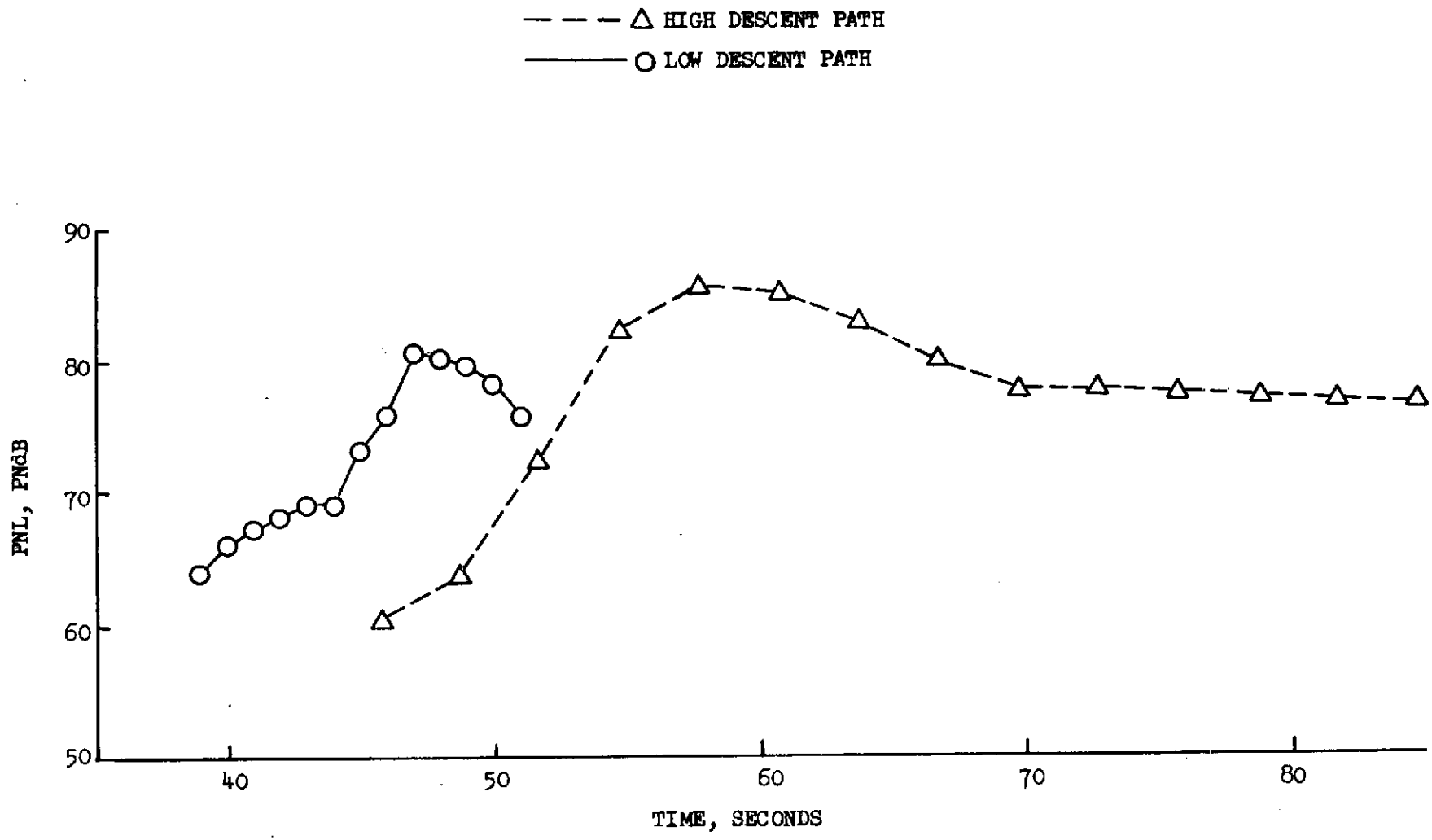

FIGURE 76 PHASE I AIRCRAFT APPROACH FLYOVER PNL, COMBINED JET COMPONENT, 710 FT. SIDELINE MIKE

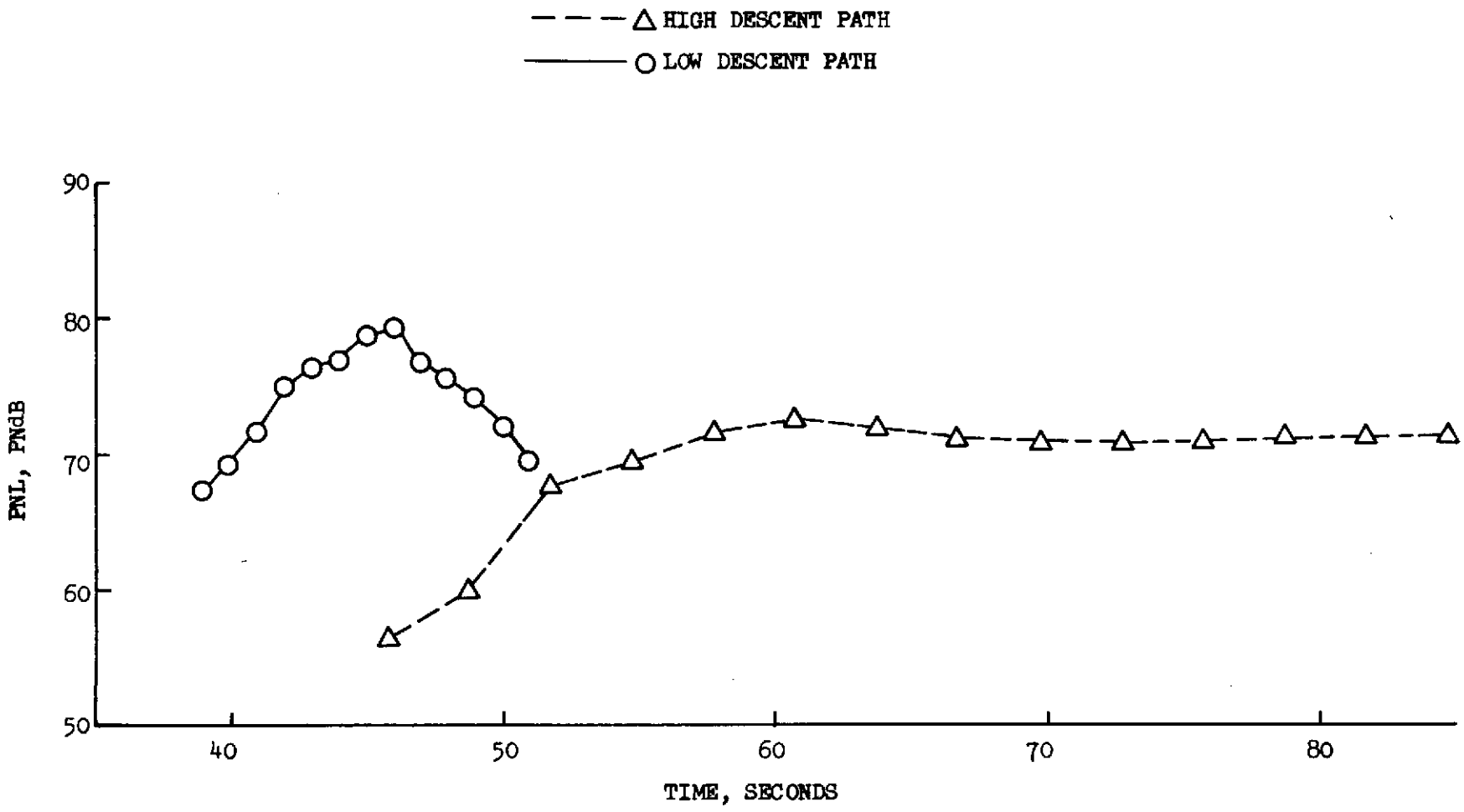

FIGURE 77 PHASE I AIRCRAFT APPROACH FLYOVER PNL, TURBINE-TURBOMACHINERY COMPONENT, 710 FT. SIDELINE MIKE

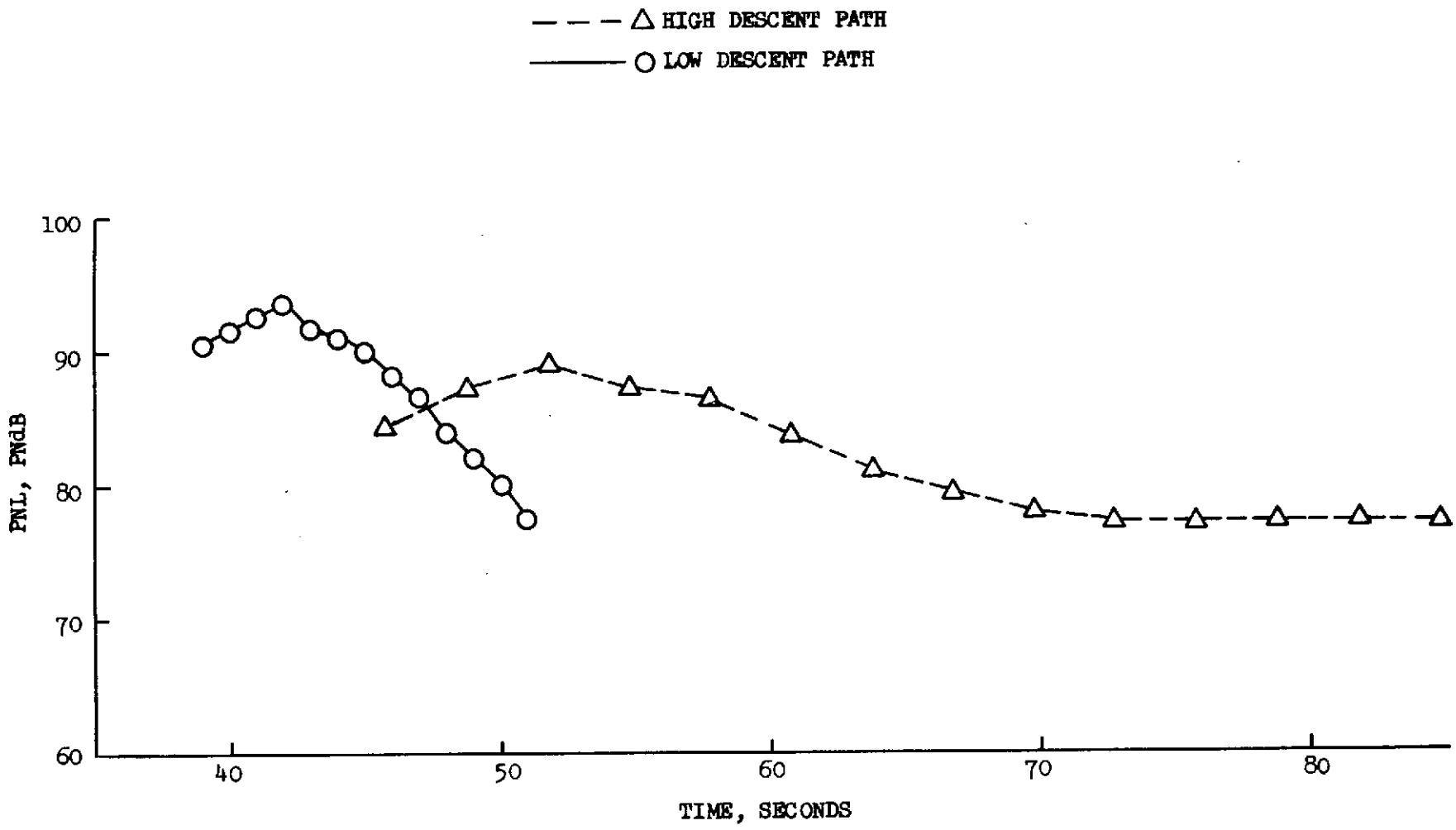

FIGURE 78 PHASE I AIRCRAFT APPROACH FLYOVER PNL, COMPRESSOR INLET COMPONENT, 710 FT. SIDELINE MIKE

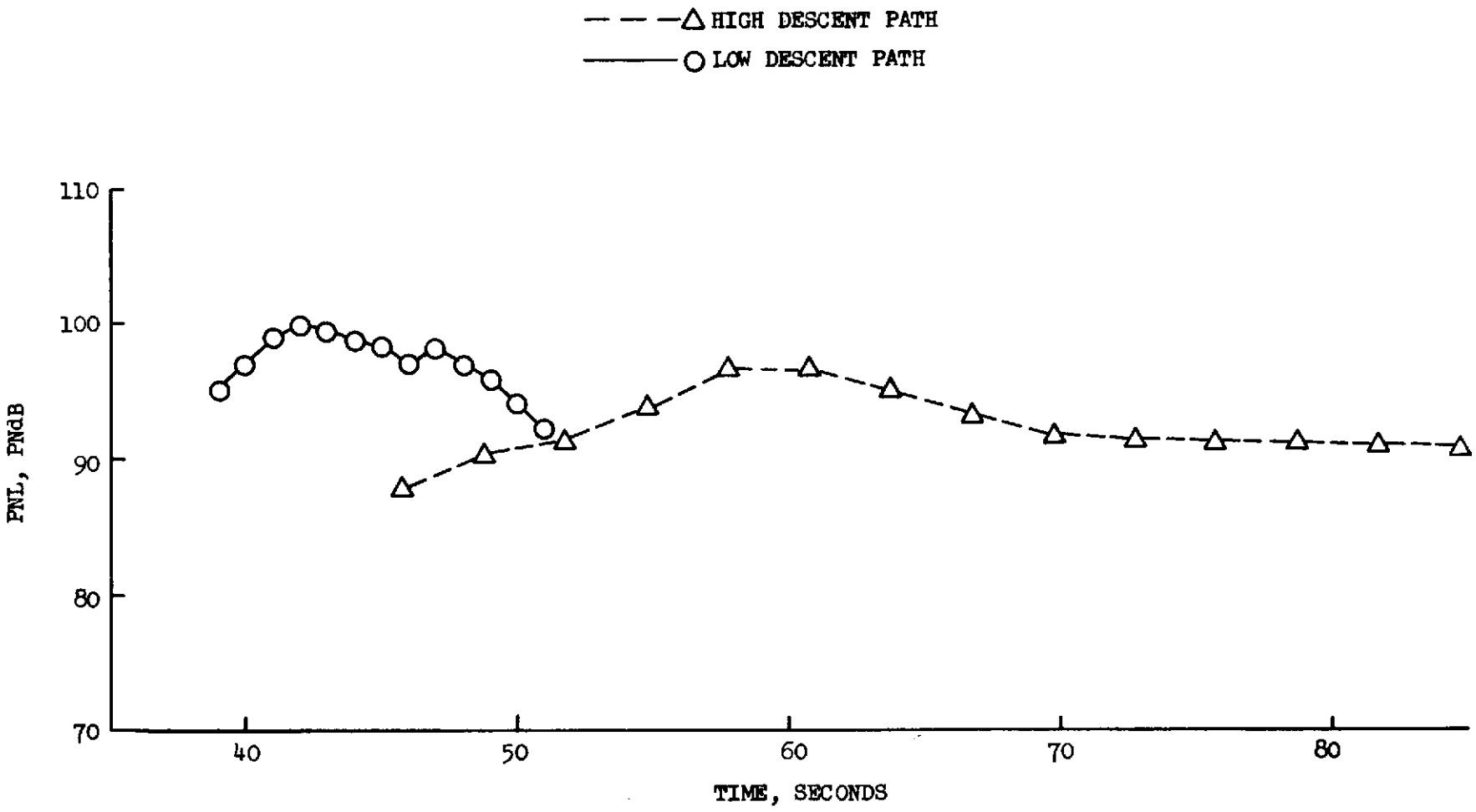

FIGURE 79 PHASE I AIRCRAFT APPROACH FLYOVER PNL, COMBINED COMPONENTS, 710 FT. SIDELINE MIKE

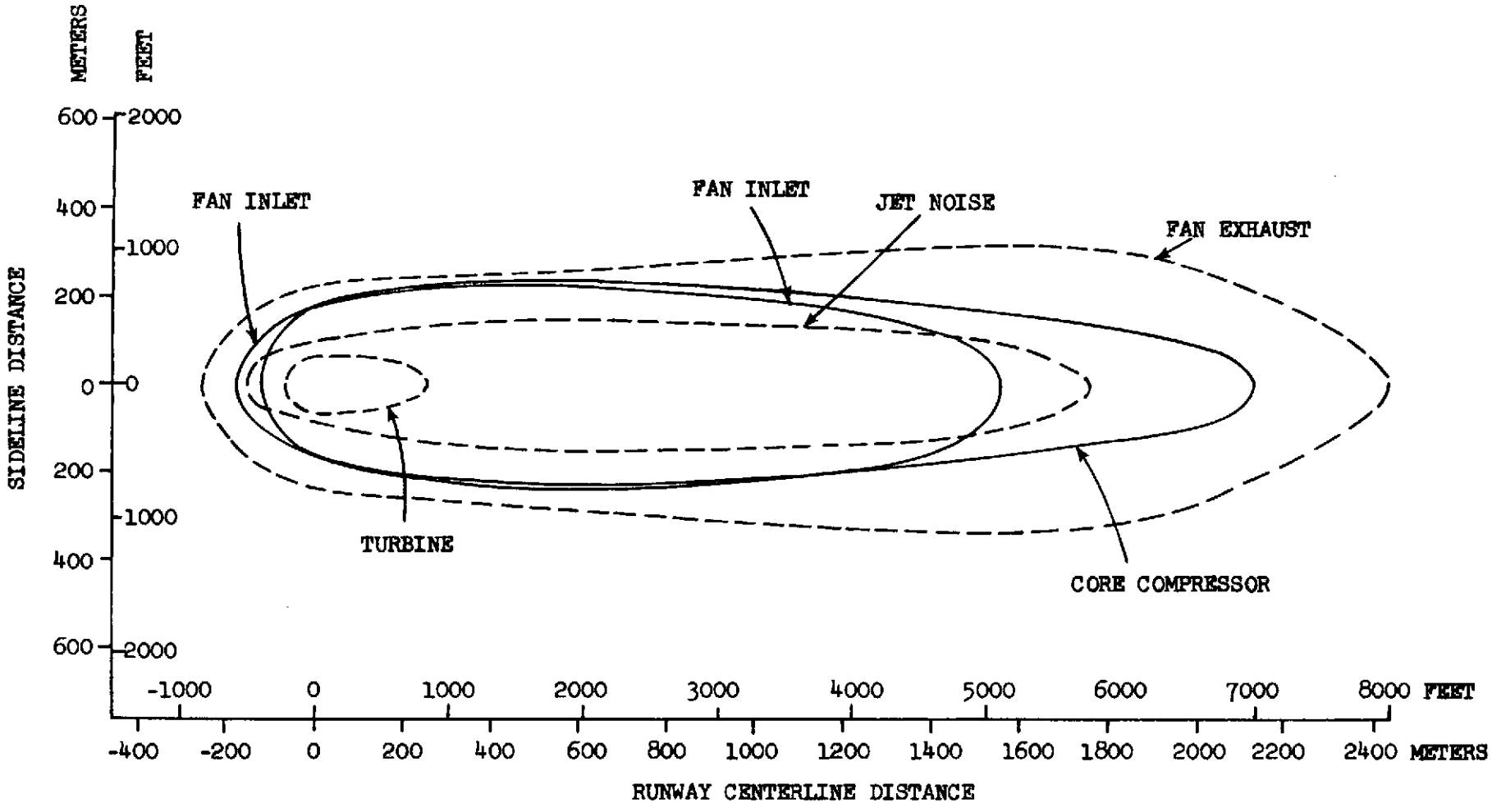

FIGURE 80 PHASE I AIRCRAFT 95 PNL COMPONENT CONTOURS, LOW RISE TAKEOFF

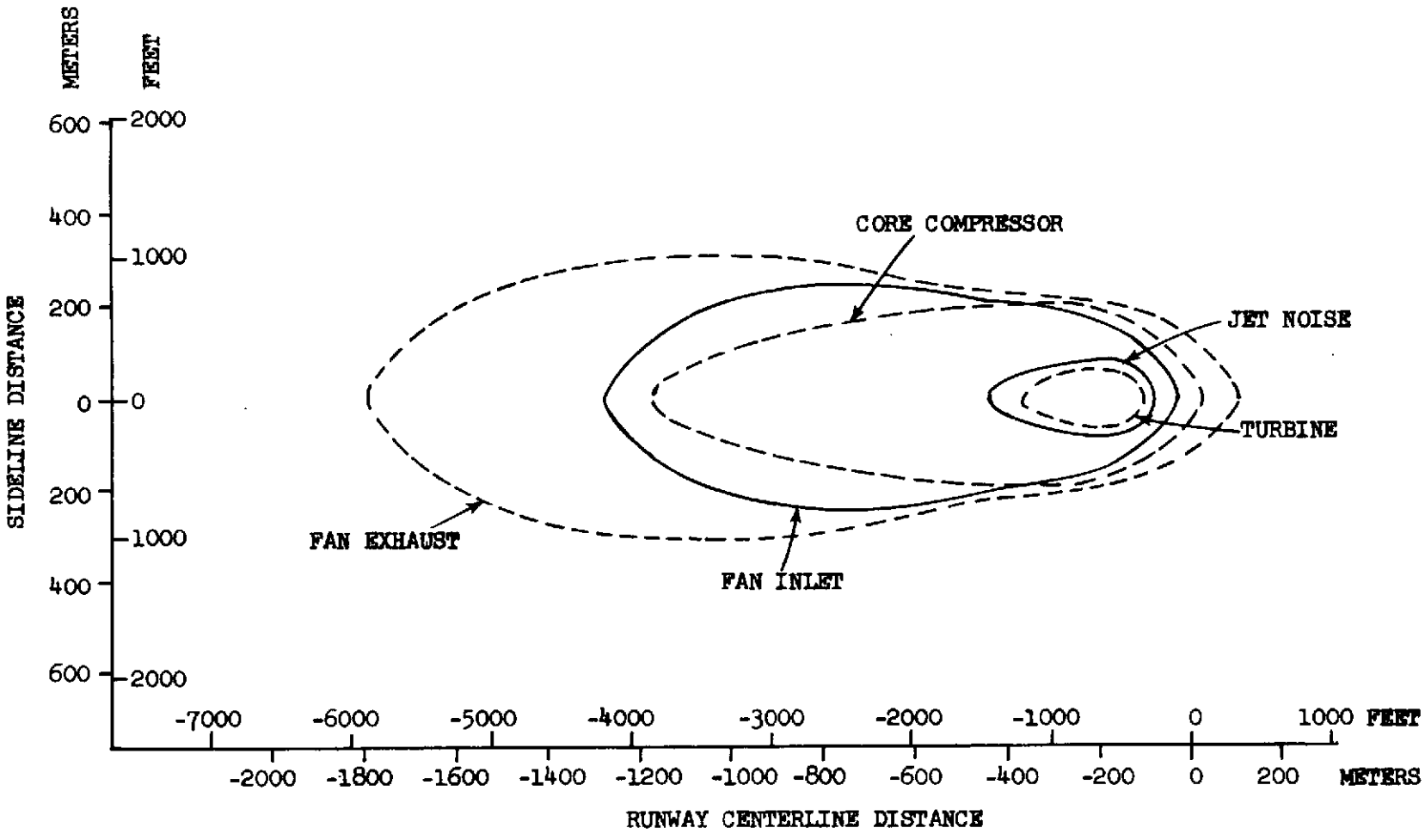

FIGURE 81 PHASE I AIRCRAFT 95 PNL COMPONENT CONTOURS, SHORT DESCENT APPROACH

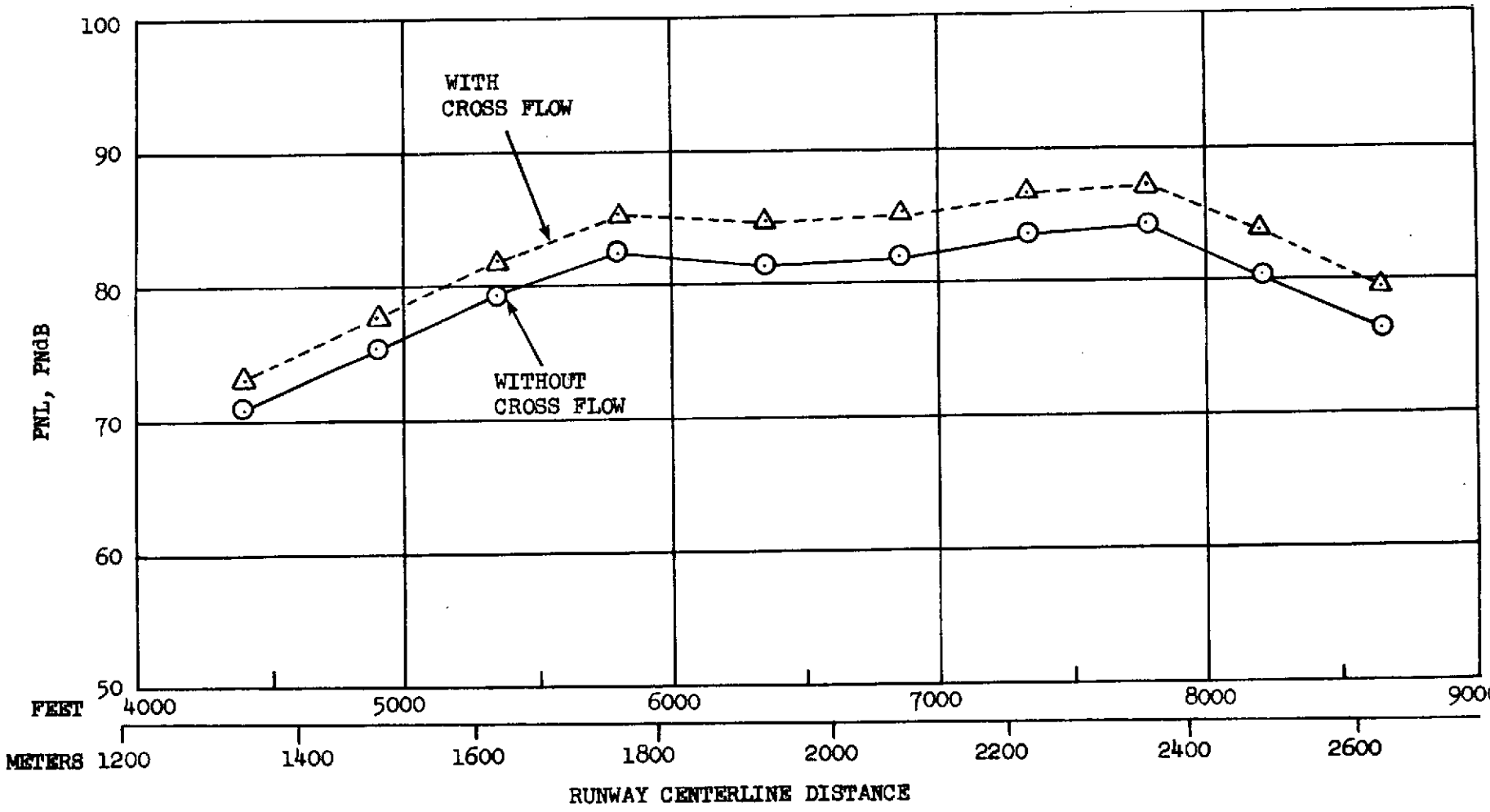

FIGURE 82 PHASE I AIRCRAFT CROSS FLOW EFFECT, LOW RISE TAKE-OFF, FAN INLET COMPONENT FLYOVER PNL

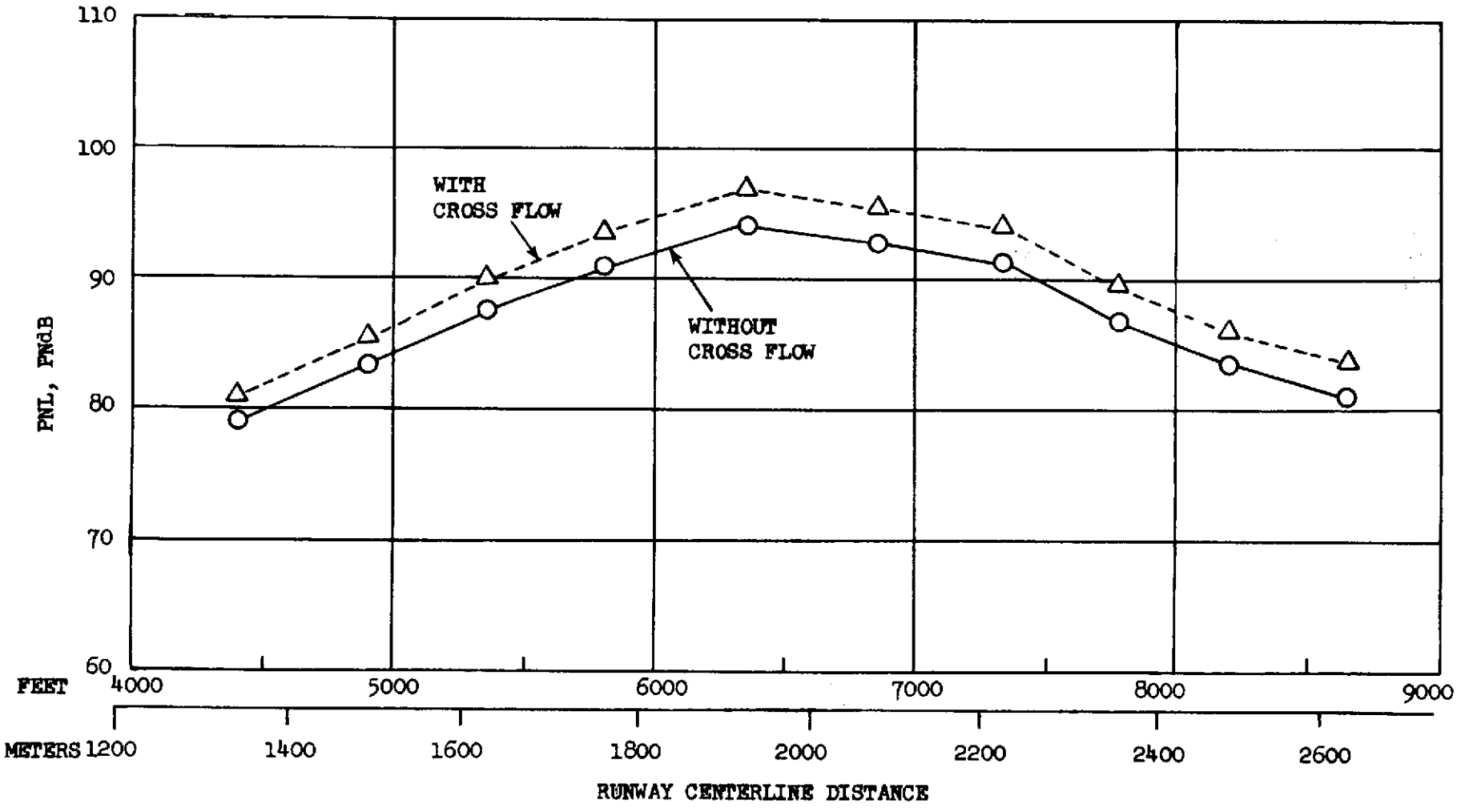

FIGURE 83 PHASE I AIRCRAFT CROSS FLOW EFFECT, LOW RISE TAKE-OFF, FAN EXHAUST COMPONENT FLYOVER PNL

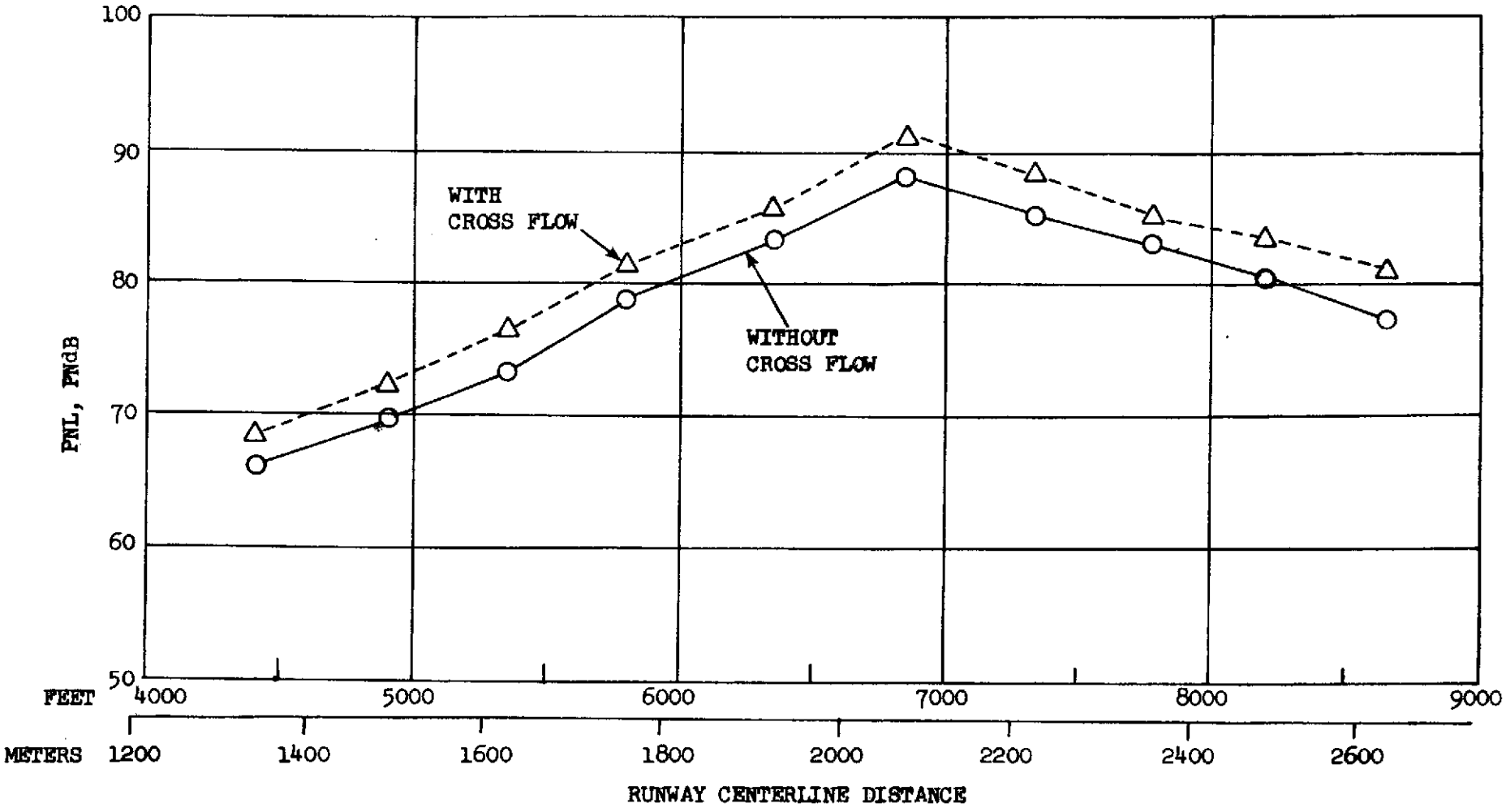

FIGURE 84 PHASE I AIRCRAFT CROSS FLOW EFFECT, LOW RISE TAKE-OFF, JET EXHAUST COMPONENT FLYOVER PNL

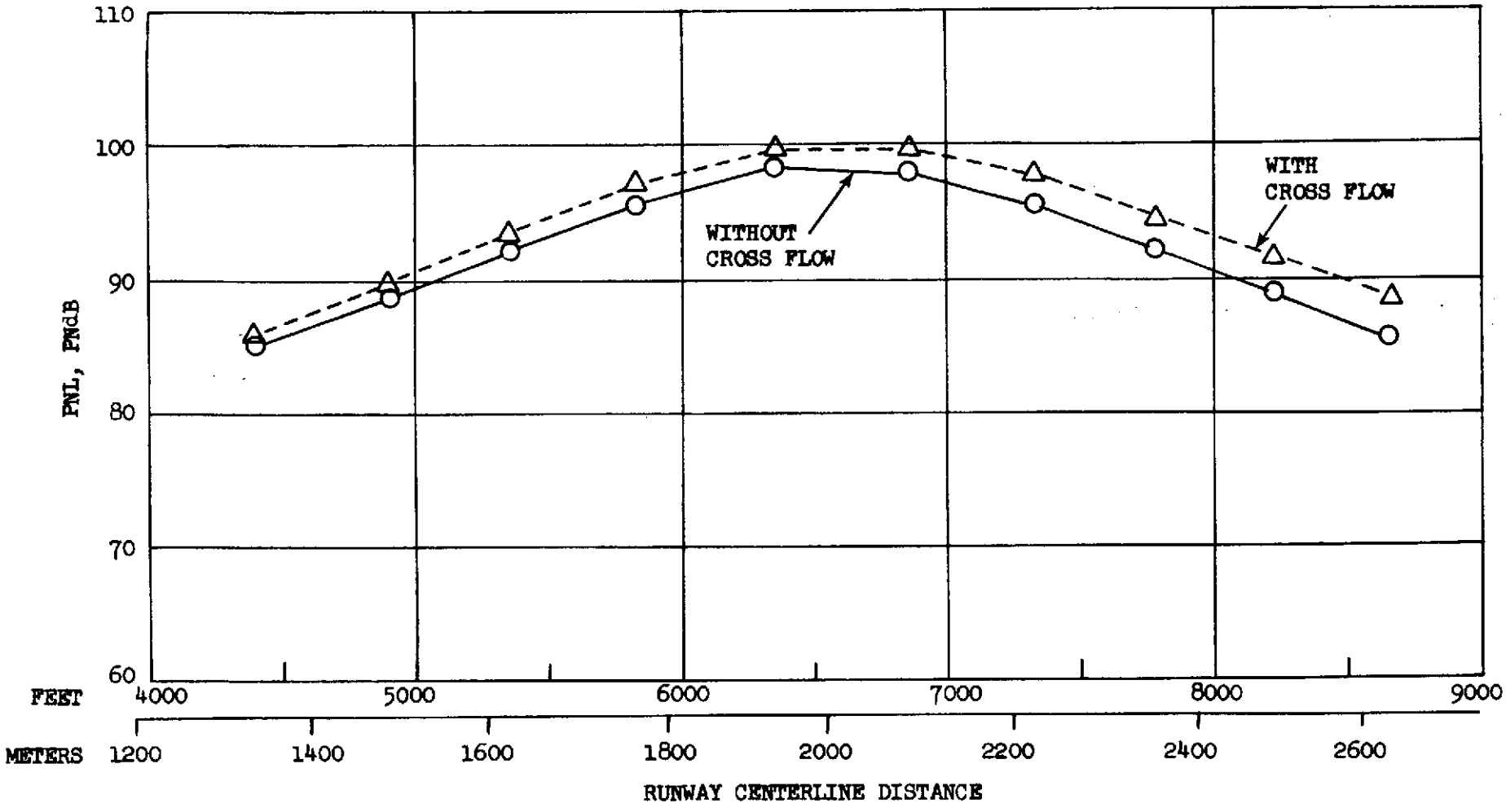

FIGURE 85 PHASE I AIRCRAFT CROSS FLOW EFFECT, LOW RISE TAKE-OFF, ALL COMPONENTS FLYOVER PNL

FIGURE 86 PHASE II AIRCRAFT COMPONENT COMPARISON FLYOVER PNL, REFERENCE CASE, FAN EXHAUST SUPPRESSION, NO NACELLE TREATMENT

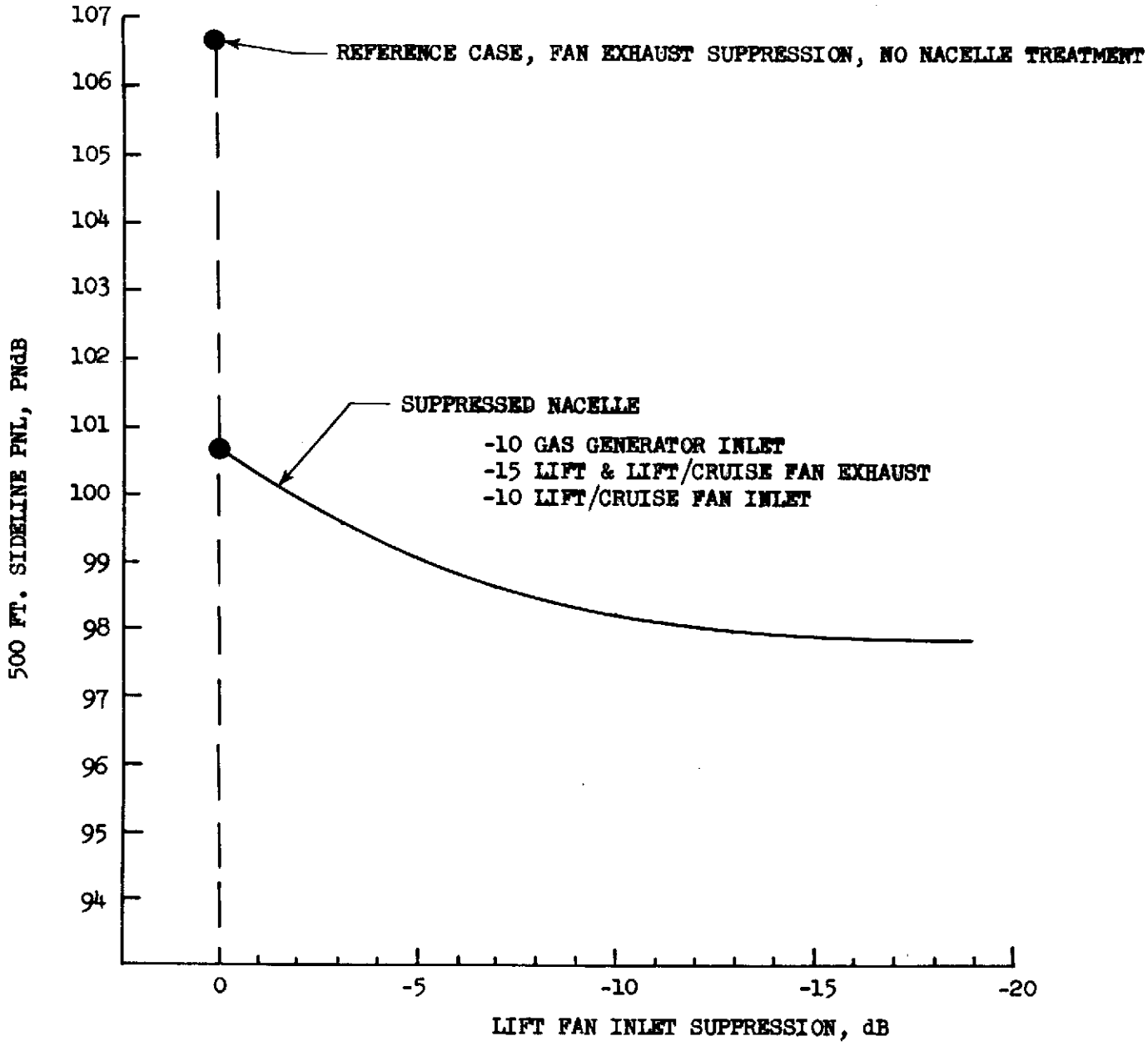

FIGURE 87 PHASE II AIRCRAFT FLYOVER PNL COMPARISON VARYING SUPPRESSION LEVEL ON LIFT FAN INLET